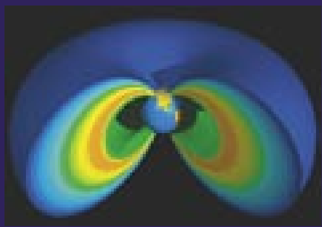
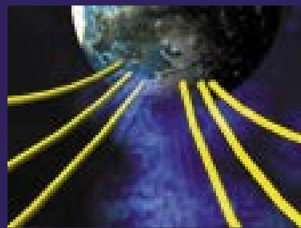
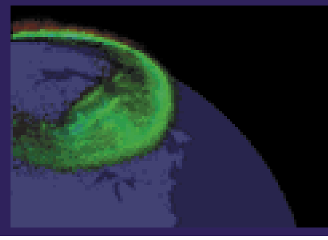
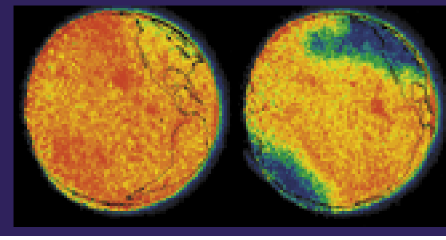
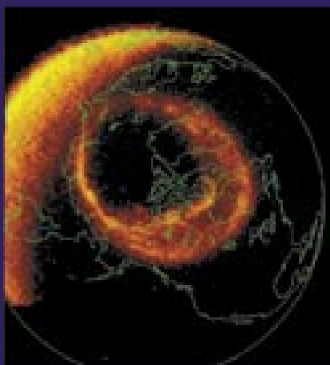
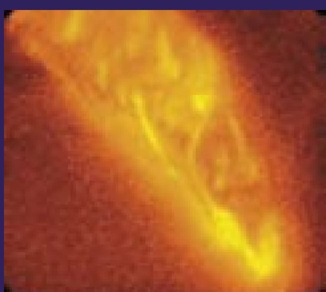
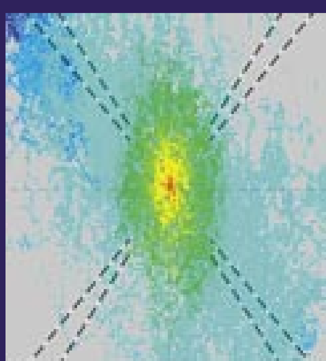

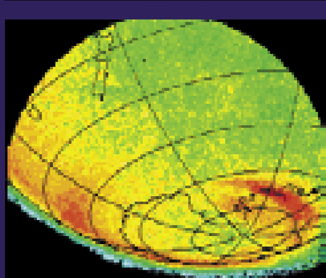

April 30, 2003

Polar

The Southern Hemisphere Campaign

Bernard Blake, CEPPAD, Aerospace Corporation
Louis Frank, VIS, University of Iowa
Theodore Fritz, CAMMICE, Boston University
Donald Gurnett, PWI, University of Iowa
Ching Meng, MDI, Johns Hopkins University
Thomas Moore, TIDE, NASA
Forrest Mozer, EFI, Univ. of California, Berkeley
George Parks, UVI, Univ. of California, Berkeley
William Peterson, TIMAS, Univ. of Colorado
Christopher Russell, MFE, Univ. of California, Los Angeles
Michael Schulz, PIXIE, Lockheed Martin
Jack Scudder, HYDRA, University of Iowa
Martin Walt, SEPS, Stanford University
Barbara Giles, Project Scientist, NASA
Robert Hoffman, Project Scientist Emeritus, NASA

National Aeronautics and
Space Administration

Goddard Space Flight Center
Greenbelt, Maryland 20771

Contents

Polar Facts:

Launch:	February, 1996
Current Orbit:	1.5 x 9.5 R_E, 82.4° inclination
	19° line of apsides precession/year
	18-hour period
Spacecraft:	all subsystems healthy
Instrumentation:	2 imagers (visible and UV), healthy
	3D electric and magnetic fields, healthy
	8 charged particle sensors, healthy
	(the wave experiment, 1 imager, and 2 charged particle sensors no longer fully operational)
Predicted EOM:	Spring, 2006

National Aeronautics and
Space Administration

Goddard Space Flight Center
Greenbelt, Maryland 20771

1. Executive Summary/Overview

Introduction to Objectives: Polar has played an integral part in the dramatic advancement of our understanding of energy and momentum transfer across the magnetopause and of electrodynamic coupling within the magnetosphere-ionosphere system. The Polar team has investigated large-scale structures and energy-transfer processes throughout the system. They have made critical contributions to understanding the micro-processes intrinsic to kinetic Alfvén waves and collisionless reconnection, delving into the details of the primary mechanisms by which energy and momentum are transferred within the system. Some of our more recent major accomplishments include:

- The determination that collisonless reconnection is “the” most important energy-transfer mechanism between the solar wind and magnetosphere;
- The discovery that intense, earthward-directed kinetic Alfvén waves are a major carrier of energy from the geomagnetic tail and coincide with the most intense aurora observed by our imagers;

and, in collaboration with other Sun-Earth Connections missions such as Cluster, IMAGE, Geotail, and FAST:

- The finding that magnetospheric substorms begin close to Earth rather than deep in the magnetotail;
- The discovery that terrestrial plasma mass-loads the outer magnetosphere very quickly after solar impulsive events and thereby may be a driver for, rather than a consequence of, magnetospheric dynamics.

Polar has well fulfilled its original science objectives and the specific objectives of its extended operations. However, recent discoveries, combined with the still remarkable capabilities of Polar’s instrumentation in its ever changing orbit, are opening new investigative paths that will yield even better understandings of how “mass, momentum, and energy flow through geospace.” Our new extended mission plan boldly envisions operational changes to pursue complementary themes that tie global processes to local physics and thereby address the most fundamental questions that Sun-Earth Connection (SEC) science can ask.

Our proposed activities will span the declining phase of the present solar activity cycle, a phase characterized by repeated encounters (hence long-lived) with high speed solar wind streams. Polar has not previously encountered the declining phase of a solar cycle. We will draw upon Polar’s unique complement of instruments, including fully 3D electric and magnetic fields, complete in-situ velocity distributions of both electrons and ions from ~0 eV to 60 MeV, and detailed global multi-spectral imaging at visible and ultraviolet wavelengths. A new opportunity to reallocate telemetry will provide significantly higher resolution measurements of electric and magnetic fields in situ, while precession of the orbit’s apogee through southern latitudes will provide new opportunities to study interhemispheric asymmetries of magnetospheric phenomena. We will continue our well-established collaborations with other missions and with ground observatories,

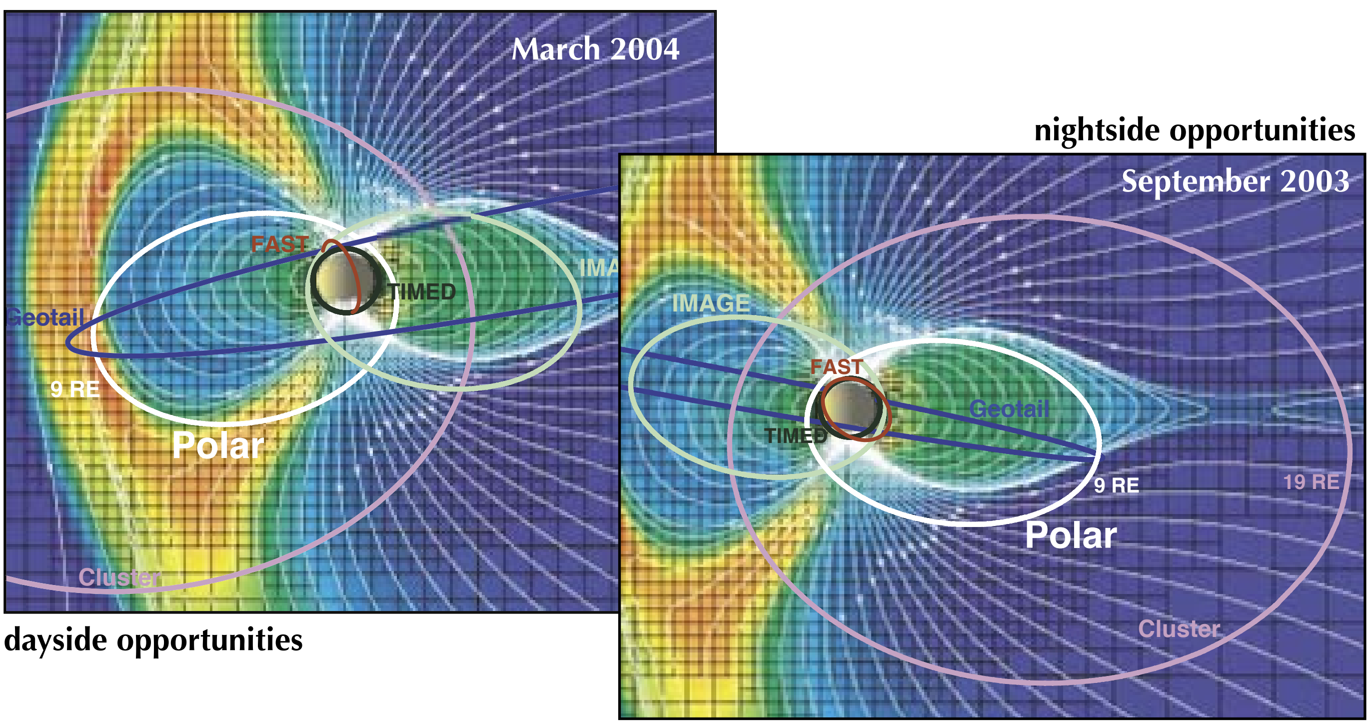

Figure 1: Polar’s apogee is now proceeding through the southern hemisphere providing increasingly good auroral imaging, opportunities for burst mode sampling of the magnetopause boundary layers, and successively deeper cuts into the inner magnetosphere at 9 to 5 R_E that are ideal for mapping substorm ignition within the near-Earth instability region and for diagnosing energetic particle injection and acceleration mechanisms.

while we continue to coordinate our measurements in space with mature modeling efforts. Our goal is to produce the best possible science at the lowest possible cost, and so we will seek to further streamline our operational procedures while meeting the community's standards for science-data integrity with full and open access to all of our data. With this approach we expect to achieve the new science objectives described in the boxes below.

Approach: The precession of Polar's apogee into the southern hemisphere (**Figure 2**) opens a wealth of new possibilities. Fundamental issues concerning the behavior of the magnetosphere can now be addressed in the context of our earlier northern hemisphere observations. This fresh perspective allows new analyses of interhemispheric asymmetries intrinsic to solarwind/magnetosphere and ionosphere/magnetosphere coupling processes.

While many of Polar's observations are made near apogee, valuable data are obtained around the entire orbit and especially near perigee. As apogee swings through the southern hemisphere, perigee will move over the highly instrumented northern land masses that feature extensive coherent (e.g., SuperDARN) radar coverage, dense magnetometer arrays (e.g., Canopus, Image), and optical instruments such as highspeed all-sky cameras and sensitive photometers.

The fuel supply that has previously allowed semi-annual attitude inversions to maintain Polar's spin axis normal to the orbit will be nearly exhausted by Fall 2003, at which time the spin axis will be permanently reoriented normal to the ecliptic. The new orientaton will not impair our ability to address the science objectives proposed. During March–September 2002 we operated Polar at an ecliptic-normal spin orientation, and from this experience we are confident of obtaining quality data (including our visible and ultraviolet images) in this mode. The main impact of operations at ecliptic-normal spin orientation will

Polar's Southern Hemisphere Campaign

Exploring Hemispherical Asymmetries

Identify important interhemispheric asymmetries and quantify the fundamental M-I coupling processes and parameters that influence and control them.

Problem:

- Great differences in the simultaneous behavior of the two hemispheres exist but a lack of observations force studies to assume symmetries of the system.

Opportunities and Unique Assets:

- Multispectral imaging of conjugate aurorals for acquisition of new information on substorm dynamics, inner magnetospheric current flows and ionospheric conductivities.
- Completion of extensive database by acquisition of southern hemisphere data to document interhemispherical effects.
- Field-aligned current and 3D electric field measurements.

Expected Results:

- How the solar wind interaction with the magnetosphere leads to hemispherical asymmetries.
- When solar wind and IMF induced asymmetries dominate over seasonal effects, such as ionospheric conductivity.
- Development of global MI interaction models at all activity levels by assimilation of southern hemisphere data into our already extensive set of statistical descriptions.

Lead Instruments: VIS, UVI, MFE, EFI
Contributing Instruments: TIDE, TIMAS, Hydra
Contributing Missions: IMAGE, FAST, DMSP, TIMED

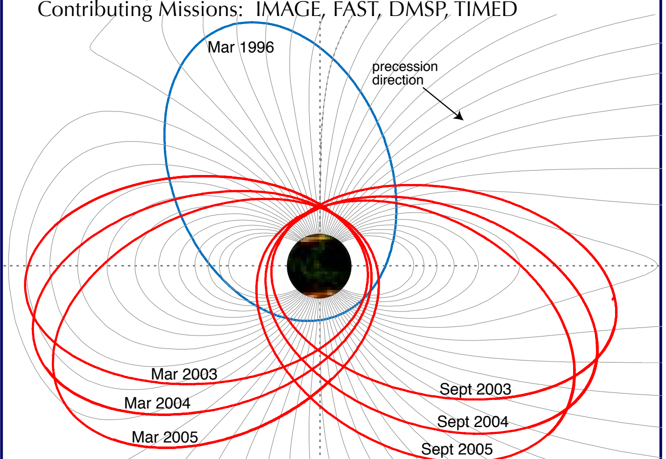

Figure 2: Precession of Polar's apogee providing magnetopause skimming, close tail observations, high latitude cusp, inner magnetosphere and low altitude northern auroral observations.

Transport Associated with High Speed Streams

Understand inner magnetospheric particle acceleration and circulation processes associated with high-speed solar wind streams prevalent during the approach to solar minimum.

Problem:

- The chain of causality and physical coupling mechanisms behind the energization, transport and loss processes of MeV particles in the magnetosphere remains a mystery.

Opportunities and Unique Assets:

- Approach to solar minimum is the most active time for the radiation belts.
- First measurements of the full pitch-angle and energy distribution of the radiation belts with 3D electric and magnetic fields during this phase of the solar cycle.

Expected Results:

- Why recurrent high speed solar wind streams are more effective in producing intense electron belts.
- Resolution of major outstanding questions as to the efficiency of various acceleration and loss processes to solar wind input, based on Polar's phase-space densities.
- Identification of acceleration and transport mechanisms responsible for sudden creation of new belts.

Lead Instruments: CEPPAD, CAMMICE, MFE, EFI
Contributing Instruments: TIDE, TIMAS, Hydra, PWI
Contributing Missions: SAMPEX, IMAGE, Cluster

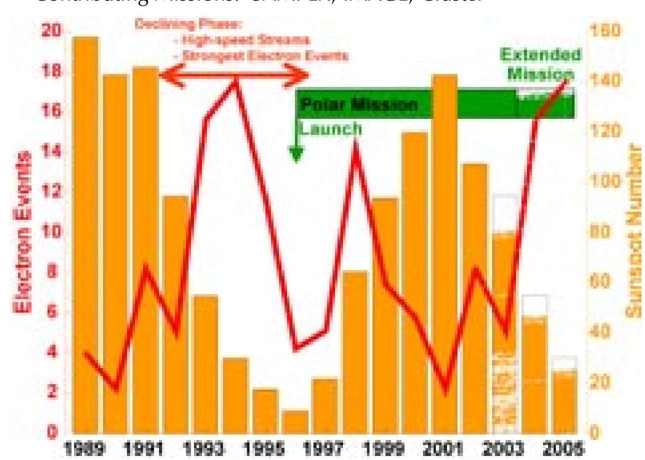

Figure 3: The pattern of magnetic storms producing MeV electron events at geosynchronous shows a clear concentration of electron events during the approach to solar minimum. [*O'Brien*, 2001].

be a reduced duty-cycle of Earth-viewing opportunities (4-6 hours per 18-hr orbit). Fortunately, we can (and will) reapportion the science-data telemetry when the imagers cannot see the Earth, so as to provide a higher sampling rate for selected in-situ measurements. This improved sampling will substantially benefit the study of kinetic processes, especially during magnetopause crossings.

Most of Polar's instruments remain healthy despite our radiation exposure (Section 3.1). Polar offers the only opportunity for an SEC mission to acquire inner-magnetospheric phase-space density measurements during the next few years, which will be characterized by recurrent high-speed solar-wind streams. Recurrent streams produce the strongest electron enhancement events (**Figure 3**), and the corresponding data will be of great value to the Living With a Star (LWS) Geospace program.

The Polar team has fulfilled the directions of the previous Senior Review team by emphasizing collaborations with the newer SEC missions such as IMAGE and Cluster. Moreover, we have developed new highly cost-efficient ways of operating the spacecraft and processing the data. Without loss of any capabilities, the data processing and distribution system has been re-engineered by automating the processing on new equipment, so as to achieve major operational cost savings. Further potential reductions in operations costs have been identified within the Polar and Wind Mission Operations Center, primarily in the implementation of unattended spacecraft contacts and data playbacks and these are being pursued. The practical effect of these cost savings has been (and will be) the maintenance of a robust science and data-analysis program despite declining budgets.

Finally, the Polar team has made critical and comprehensive contributions to public awareness of the science of Sun-Earth Connections, both with the development of products valuable to education and public outreach (E/PO) and with many direct contacts between its scientists and the public at formal and informal gatherings. We have identified a wide-ranging set of new E/PO objectives to be achieved over the next few years.

Understanding the Microphysics of Plasmas

Obtain new understandings of the ion and electron diffusion regions, solitary wave structures and the role of small-scale field structures

Problem:

- Reconnection is somehow enabled, but by unknown processes; insight is of fundamental importance throughout the Sun-Earth system.

Opportunities and Unique Assets:

- Skimming orbits through dayside boundary and the cusp
- Very high resolution burst mode across magnetopause
- Alfvén wave measurements in tail boundary region
- Doubling of the telemetry bandwidth for selected in-situ measurements through regions of interest
- Cusp campaigns with Cluster, a recent addition to the fleet

Expected results:

- Identification of the plasma parameters in the generalized Ohm's law important in controlling reconnection.
- How the bow shock and steady or transient reconnection over the dayside portions of the magnetosphere mediate and filter interplanetary input into the system.
- .How dominant a role Alfvén waves play in transferring energy from the magnetotail into the atmosphere.

Lead Instruments: Hydra, EFI, MFE, CEPPAD, CAMMICE
Contributing Instruments: TIDE, TIMAS, UVI, VIS, PWI
Contributing Missions: Cluster, Geotail, Wind

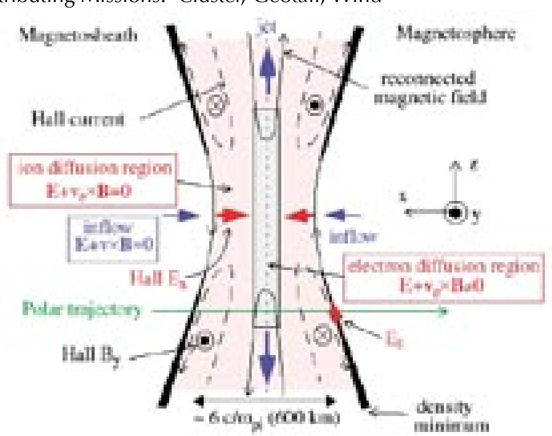

Figure 4: The geometry of the reconnection region. Ions are decoupled from the electrons and magnetic field in the ion diffusion region, creating Hall magnetic and electric field patterns.

Impact of the Ionosphere on Geospace Processes

Exploit Polar's new position in the SEC fleet to quantify the variable electromagnetic linkage between the solar wind and the ionosphere along with its reactive energy that introduces new dynamics into the system.

Problem:

- We now realize the extent to which ionospheric plasmas are distributed throughout the magnetosphere; their influence on system dynamics can no longer be taken as limited.

Opportunities and Unique Assets:

- Full pitch angle resolution of relevant particle populations
- Perigee auroral acceleration regions observations over northern array of ground observatories
- Constellation of spacecraft positioned to intercept relevant flows during the large field changes that occur.

Expected results:

- How ionospheric plasmas at the boundary layers impact reconnection processes.
- The role of terrestrial plasmas in the formation and dynamics of the near-Earth plasma sheet at onset of activity.
- Quantitative empirical and physical models of ionospheric outflow as a function of energy inflow.

Lead Instruments: TIDE, TIMAS, Hydra, EFI, PWI
Contributing Instruments: MFE, CEPPAD, CAMMICE, UVI, VIS
Contributing Missions: FAST, Cluster, Geotail, TIMED

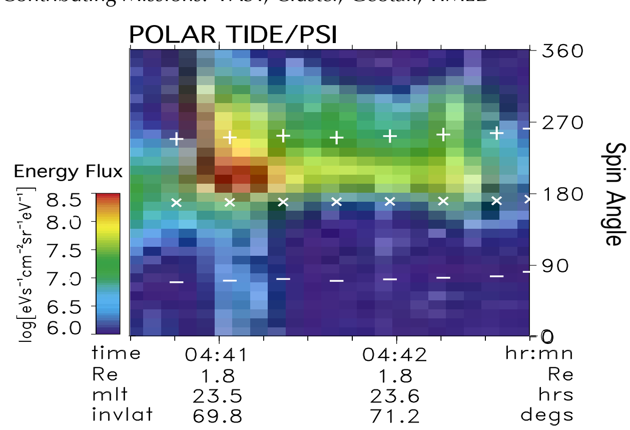

Figure 5: The ubiquitous nature of the terrestrial contribution to magnetospheric plasmas is demonstrated by the strong, escape velocity outflows that occur even during the benign conditions on the "day the solar wind disappeared".

2. Science Objectives

2.1. Exploring Interhemispherical Asymmetries: Quantify the fundamental magnetosphere-ionosphere coupling processes influenced and controlled by interhemispherical asymmetries.

General problem:

Because of incomplete observational data relevant to this topic, most studies of the solar wind-magnetosphere-ionosphere system have to assume north-south symmetry of the system. We know that great differences in the simultaneous behavior of the two hemispheres exist and it is now clear that what we thought we knew about north-south asymmetry is incorrect. Asymmetries show up over a variety of scale-lengths and are strong consequences of the solar wind driving the magnetosphere-ionosphere (MI) system. An understanding of the problem in sufficient detail to develop meaningful global models is not trivial and has been addressed only in specific areas. The extensive database being accumulated by Polar as it proceeds from the northern to the southern hemisphere, together with measurements from IMAGE, TIMED and from ground-based observatories, offers a unique opportunity to investigate the dynamics of interhemispherical behavior. This study is vital for advances in modeling the global behavior of the geospace plasma system.

How does the solar wind interaction with the magnetosphere lead to asymmetries in the MI-coupling processes?

When do solar wind and IMF induced asymmetries dominate over seasonal effects?

Which substorm onset behaviors are symmetric between northern and southern hemispheres?

Are the effects of asymmetric ionospheric conductivity local or global?

Recent Advances:

Auroras are the footprints of dynamics acting in more distant regions of the magnetosphere. They delineate the nature of the solar wind-geomagnetic field interaction mechanisms, how they affect MI-coupling, and the internal particle dynamics in the magnetosphere. The majority of auroral studies to date have relied on single spacecraft looking at one hemisphere (primarly the north). While a few conjugate observations have been made, a systematic analysis of the effects is needed. To date, advances in exploring interhemispheric asymmetries have been characterized more by recognition of the existence of asymmetries rather than in understanding *the reasons* for the asymmetries.

An important breakthrough in understanding the connection between outer magnetospheric processes and the aurora, and the possibilities for understanding the consequences of interhemispheric differences, came with the Polar observations of polarized electric field variations associated with strong magnetic field fluctuations within the outer boundary of the local midnight plasmasheet at 4-6 R_E [*Ober et al.,* 2001; *Wygant et al.,* 2000]. The associated Poynting flux was directed along the average magnetic field direction coinciding with intense auroral structures (~20-30 ergs/cm^{2}s). The energy flux in the Alfvenic structures, when mapped to ionospheric altitudes, provided sufficient power (~100 ergs/cm^{2}s) to drive all auroral processes, including acceleration of upward flowing ion beams, electron precipitation, AKR, and Joule heating of the ionosphere [*Wygant et al.,* 2000]. This was followed by the *Frank and Sigwarth* [2000a,b] study that determined that the auroral substorm onset occurred in the most equatorward auroral arc and that the magnetic field threading the auroral substorm onset region mapped to radial distances of 5 to 10 R_E in the magnetotail.

The power of simultaneous imaging of the auroral zones is shown with the unexpected auroral substorm onset finding by Polar/VIS (**Figure 6**). The onset of auroral brightening occurred about one minute earlier in the southern hemisphere relative to that in the north and significantly greater brightness of the southern aurora occured during the expansive phase of the substorm [*Frank and Sigwarth*, 2003]. This difference in time for coupling

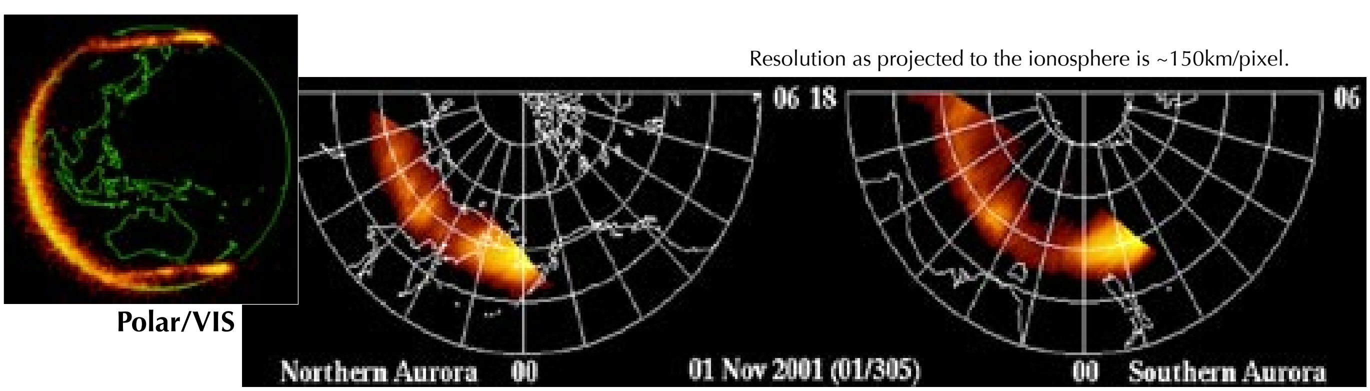

Figure 6: Auroras are the footprints of particle dynamics acting in more distant regions and are a prime tool for the identification and timing of substorm processes. Viewing both ovals allows latitudinal as well as longitudinal mechanisms to be identified. This image of the nighttime northern and southern auroral ovals is one of a series showing a substorm onset delayed in the North by about one minute, followed by greater intensities in the South during the expansive phase [*Frank and Sigwarth,* 2003].

of the magnetospheric plasma sheet with the ionosphere implies the presence of field-aligned currents, plasma waves, and/or particle scattering mechanisms that are not presently accounted for in treatments of auroral substorm dynamics. Careful mappings of simultaneous observations of both ovals as shown in **Figure 6** allow the event to be studied with resolutions of up to ~150 km. When these are taken with the same camera, no uncertainties are associated with luminosity or the timing of the signals.

Equally intriguing are Polar's statistical studies showing ionospheric conductivity differences associated with diurnal and seasonal illumination effects. A seasonal effect for the northern hemisphere is shown in **Figure 7**. Discrete auroras have been shown to favor winter conditions, and episodes of precipitated fluxes >5 erg/cm^{2}s occurred 3 times more often under conditions of local darkness [*Newell et al.,* 1996]. This implies that conditions for field-aligned electric fields associated with auroral arcs are more favorably hosted by the dark ionosphere. Because conductivities are often assumed to be symmetric in models, these and further studies with the new southern hemisphere observations have the potential to firmly establish the asymmetric behavior of substorm onset.

New Opportunities and Specific Goals:

We propose to obtain new information on MI-coupling by quantifying the similarities and differences of dynamical processes observed in the northern and southern hemispheres. The physics of MI-coupling is fundamental to our understanding of how mass, momentum and energy are transported from the solar wind and dissipated in the magnetosphere. The observations will be organized and related to varying solar wind and solar illumination parameters, including IMF orientation and clock angle, as well as for specific phases of storms and substorms. Specifically, we will:

- Clearly identify the effects of Earth's dipole tilt, season, IMF direction and magnitude, and solar wind density and speed on the conjugacy and nonconjugacy of features in the northern and southern hemispheres.
- Determine the relative motion of auroral features on minute time scales with respect to the above variables.
- Determine the conjugacy and nonconjugacy of auroral features as a function of substorm phases.
- Assess the role of solar illumination of Earth's ionosphere in MI coupling.
- Determine the asymmetry of the fields and particles between models based on observations completed in the northern hemisphere and the new observations to be made in the southern hemisphere.

Here, conjugate measurements are defined as those observed at the northern and southern ionospheric feet of their common magnetic field line. Conjugate auroral features are thus identified as symmetric features but can have different intensities. Asymmetric features are those appearing in one hemisphere but not the other and features displaced in longitude and/or latitude.

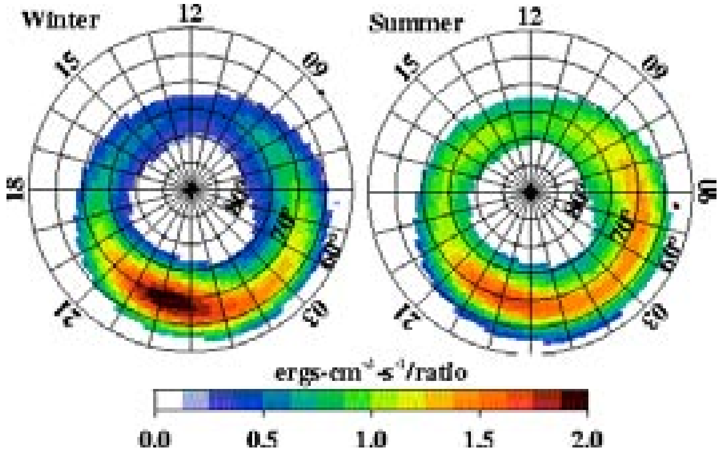

Figure 7: Extensive statistical analyses have been published for the northern hemisphere but little data exists for the southern. Shown here is the statistical summer/winter effect [*Liou et al.,* 2001]. We know that the northern substorm onset location shifts in local time with season, but given the observed IMF By effects in the closed magnetotail there is considerable doubt whether the southern onset location shifts in the same direction.

Approach:

Polar has already performed a complete survey of the northern magnetosphere and is now poised to carry this study into the southern hemisphere. The purposes of a southern hemisphere campaign are to deconvolve the important effects that stem from Earth's orbital motion, offset of the dipole axis, and the solar spin axis inclination angle from those stemming directly from variations in the IMF and solar wind dynamics.

Multispectral, simultaneous observations of the northern and southern auroral ovals from quiet to disturbed conditions as well as a full survey of the southern magnetosphere fields and particles will determine the nature, extent and dependencies of the asymmetries of conjugate and nonconjugate processes. Both types of data are needed to provide the guiding information for the improvement of effective MI coupling models. We will address the issues identified above with the following four types of investigations.

(1) Simultaneous observations of both the northern and southern auroral ovals for latitudes where the classical substorm occurs. See the cover, **Figure 6** and Section 3.1 for examples, some of which were acquired in "ecliptic normal" attitude, which is the orientation for future image acquisition. Even though such events are limited by the position of the spacecraft in its orbit, there is a period of about three months each fall season when there is continuous nighttime viewing of the two ovals for about two hours each orbit. This is sufficiently long to capture the auroral activity including the onsets and expansive phases of substorms. The first observing period in 2001 captured the dynamical behavior of 4 substorms. A similar yield can be expected for later observing periods. These types of images are a major advance in investigating the onset and expansive phase differences during substorms and the quiet-time auroral patterns that are fundamental to understanding the complex interactions of the magnetosphere with the ionosphere.

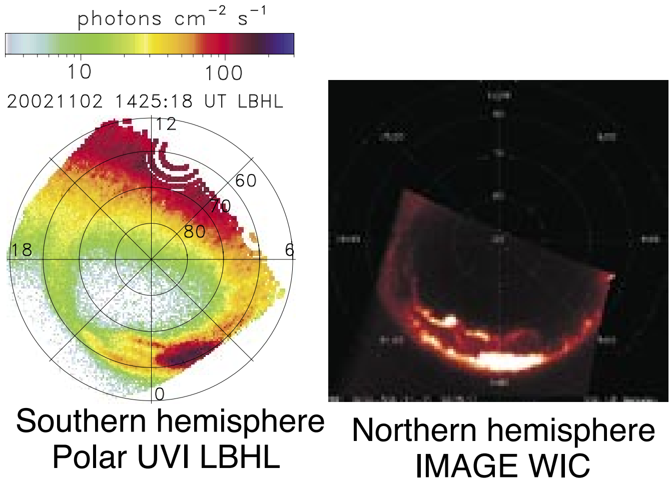

Figure 8: Simultaneous auroral images by Polar/UVI (left) and IMAGE (right). Taken within a few seconds of each other, and a few minutes after substorm onset, the center of activity is at local midnight in the north while it is toward dawn in the south. Also the northern poleward boundary activity is absent in the south. While acquisition is limited, such simultaneous viewings under varying conditions are invaluable as they reveal the important physics of solar wind-magnetosphere-ionosphere coupling.

(2) Simultaneous observations at more polar latitudes with the Polar spacecraft viewing the southern auroral oval and IMAGE viewing the northern oval. Again, though such events are limited by the positioning of each spacecraft (see section 3.1), acquisition will be extremely valuable in determining auroral oval and polar cap differences at latitudes exceeding the range of simultaneous oval viewing. Even allowing for instrumental variations, simultaneous viewing can discern key differences in the auroras for different seasons and geomagnetic conditions. **Figure 8** is from such a study and shows that the differences in emissions can be large. In the northern hemisphere the center of activity is at local midnight while it is toward dawn in the south. Also, intense activity is seen at the high-latitude boundary of the oval in the north which is not seen in the south. These analyses, both individually and statistically, offer a rich data source for studies of magnetospheric dynamics.

(3) Polar imaging of the southern auroral zone can be compared with simultaneous measurements by a host of ground-based and low-altitude orbiting observatories. These include radar, all-sky cameras, and magnetometer chains for the measurement of current systems and thermospheric/ionospheric flows. FAST and TIMED in particular provide high spatial resolution observations valuable for comparison to the more global Polar imaging. This is an important new arena for MI-coupling studies only in the initial stages of development.

(4) The assimilation of southern hemisphere data, both imaging and in situ, into our already extensive set of statistical descriptions will substantially contribute to the improvement of global MI interaction models for all substorm phases and all activity levels. For example, results from Polar/UVI in the northern hemisphere show a complex pattern of dependence on IMF clock angle [*Shue et al.,* 2001, 2002], with IMF By playing an unexpectedly important role. Which By effects are symmetric and which are antisymmetric between the two hemispheres is a matter for speculation. A good understanding of the Earth's interaction with the sun and its solar wind cannot be claimed while such basic issues are unresolved.

Similarly, a study by *Le et al.,* [2003] clearly shows a strong but unexpected day-night asymmetry in the equatorial ring current which increases with increasing disturbance levels (**Figure 9**). This survey of the magnetic field included sufficient redundancy such that statistics could be extracted as a function of geomagnetic conditions although the response had to be assumed independent of latitudinal effects because of insufficient southern hemisphere observations. It is fundamentally important to fill in the southern hemisphere so that the statistical representation of global currents can accurately reflect hemispherical asymmetries.

Expected Results:

The research proposed here will quantify and advance current understanding of the physics of solar wind interaction with the magnetosphere. At the end of this study, we will have made a great step forward by identifying and understanding what the various asymmetric effects are, the role of ionospheric conductivity, and how they affect auroral and magnetospheric dynamics.

The results we obtain will be compared to the predictions of existing models. Empirical models of the average ionospheric potential and field-aligned current patterns

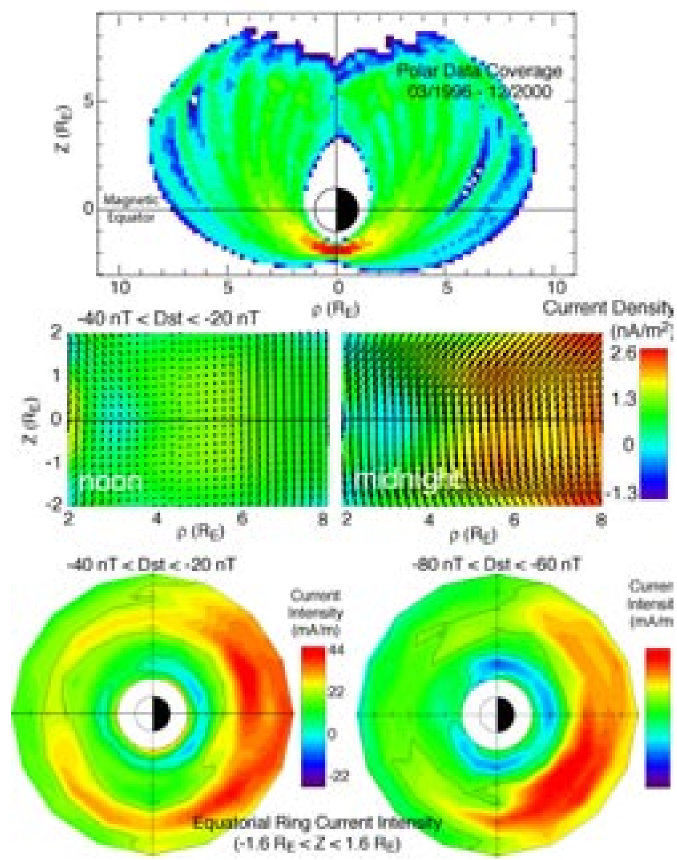

Figure 9: Magnetic field measurements obtained largely in the northern hemisphere showing dramatic ring current local time asymmetries. Southern hemisphere observations will remove the north-south symmetry assumption possibly revealing new patterns.

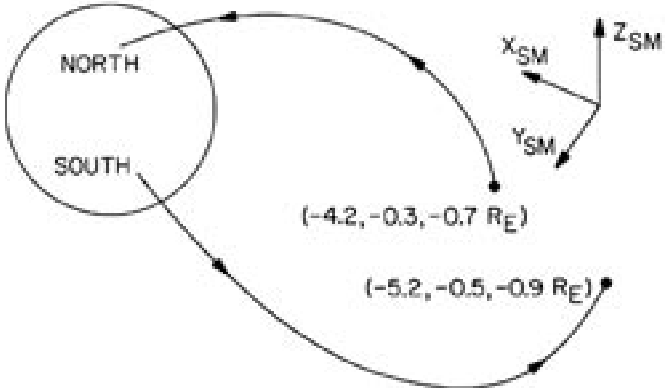

Figure 10: Mapping of conjugate auroral onset positions along the magnetic field to the equator. The mapped points miss by more than 1 R_E at a distance of ~5 R_E in the tail.

contain known asymmetries at high latitudes which evolve with clock angle changes in the IMF imposed on the system [*Weimer,* 2001]. However, asymmetries in dynamic patterns may be greater as evidenced by multi-satellite comparisons with MHD simulations of step changes in the IMF [*Maynard et al.,* 2001a,b]. In turn, we expect global MHD modeling to be significantly advanced by our work. MHD models are beginning to simulate substorm events [*Slinker et al.,* 2001; *Raeder et al.,* 2001] and are providing predictions of the evolution of ionospheric convection and field-aligned current patterns, which can be tested against global images and statistical patterns.

Global field models can also be expected to improve as a result of these supporting observations. In **Figure 10**, the current problems in mapping seemingly conjugate enhancements at substorm onset are demonstrated by mapping conjugate field lines from north and south onsets [*Frank and Sigwarth,* 2003]. A model consistent with the new observations would produce field lines that join but here they miss by more than 1 R_E at a distance of only 5 R_E in the magnetotail. Similarly, at the open-closed boundary on the dayside, *Siscoe et al.,* [2001] used MHD simulations for a 90° IMF clock angle to show that a field line can be found that extends from the northern hemisphere potential minimum at dusk to the southern hemisphere potential maximum at dawn. This line passes across the nose at a 45° angle, emphasizing that field lines do not follow the expectations of conjugacy. By testing where and how conjugacy breaks down, model and data comparisons will constrain interpretations, leading to better understanding of the physical processes involved.

2.2. Approach to Solar Minimum: Understand inner magnetosphere particle acceleration and transport associated with high-speed solar wind streams.

General problem

An understanding of the energization, transport and loss processes controlling MeV energetic particles throughout the magnetosphere is a central outstanding problem. Our understanding of these processes has already increased substantially with the use of complementary data sets from Polar, SAMPEX, IMAGE and ACE. The next few years promise an exciting opportunity to vastly increase this understanding. The solar cycle is beginning its approach to solar minimum ushering in a period of high-speed solar wind streams often producing intense magnetospheric energetic electron enhancements (**Figure 3 in Overview**). While the correlation with high-speed streams is well known, the chain of causality and physical coupling mechanisms remain a mystery. Polar is the only vehicle operating in the inner magnetosphere with a full complement of energetic particle and vector magnetic field measurements.

Why are recurrent highspeed solar wind streams more effective in producing intense radiation belts?

How can we relate the efficiency of various acceleration and loss processes to solar wind input?

What are the acceleration and transport mechanisms responsible for the sudden creation of new inner radiation belts?

Recent Advances:

Radiation belt science debates revolve around two sets of competing processes: acceleration versus loss and radial transport versus local acceleration. The importance of understanding the balance between acceleration and loss processes is illustrated in **Figure 11**. *Reeves et al.,* [2003] have shown that there is no typical radiation belt electron response to storm conditions. Only half of all storms produced elevated electron fluxes while fully one quarter produced permanent decreases.

There are two broad classes of mechanisms under examination as the cause of relativistic electron enhancements: 1) local acceleration that relies on VLF wave-particle interactions, and 2) ULF wave mechanisms or global electromagnetic fluctuations for diffusive inward transport from the plasma sheet. Recently, through theoretical and empirical means, great strides have been made toward resolving the relative importance of these two types of mechanisms [e.g., *Meredith et al.,* 2002; *O'Brien et al.* 2003; *Horne and Thorne*, 2003]. Circumstantially, both mechanisms occur during high-speed solar wind streams, particularly the long-lived recurrent streams associated trans-equatorial coronal holes at the sun, characteristic of the approach to solar minimum.

To distinguish between acceleration mechanisms, a key observation is electron phase-space density profiles versus magnetic L. The evolution of such a profile from a quiet-time outward gradient to a post-storm peak in the heart of the radiation belts would indicate local acceleration in addition to inward diffusive radial transport. *Green* [2002] has shown evidence for just such a peak (**Figure 12**), using Polar, the only spacecraft currently capable of making the required measurements in energy, pitch-angle, and L, accompanied by onboard magnetometry. The likely mechanism involved in the formation of this phase-space-density peak is VLF chorus heating of the electron distribution. Electric and magnetic field measurements from Polar/PWI have shown that the source of chorus is near the magnetic equator. The historical PWI database is invaluable in conjunction with new Cluster wave measurements because the Cluster wide band data does not provide simultaneous electric and magnetic field measurements. The predicted local-time asymmetry in MeV electron pitch-angle anisotropy has not been confidently confirmed. One to two more years of Polar observations are expected to provide sufficient additional examples to determine definitively whether the predicted anisotropy exists.

New Opportunities and Specific Goals:

The energization, transport and loss processes controlling MeV energetic particles as a result of the impact of high-speed solar wind streams on the magnetosphere need to be defined and quantified. By comparing theoretical predictions with Polar in situ data, we will determine which acceleration and loss processes combine to create the observed radiation belt structure and variability.

The Polar team will investigate why recurrent high-speed solar wind streams are more effective at pumping up the relativistic electron population in the radiation belts than are the geomagnetic storms that occur at as a result of CMEs. In concert with other ground-based and in situ measurements, the Polar team will determine what physical parameters associated with these streams produce the greatest difference in energetic particle response. Polar will assess the extent to which the variability in the electron response is a case of high geomagnetic activity driving greatly enhanced electron losses.

Polar measurements will quantify the relative importance of local heating as compared to the inward transport of magnetospheric energetic electrons. We will determine whether there is a sufficient source for these electrons in the mid-tail region (L=8-11) and if so, how particles of sufficient energy are produced there. With onboard magnetometry, the Polar team is able to establish the validity of dynamical phase space density gradients in the inner magnetosphere. Polar's excellent energy and pitch-angle resolution will help relate the efficiency of radial transport and pitch angle scattering processes to solar wind input and other magnetospheric parameters. This will permit the parameterization of these processes by solar wind speed, density, and IMF properties.

The Polar team will help identify the acceleration and transport mechanisms responsible for the sudden creation of new super-relativistic radiation belts deep in the inner magnetosphere.

Approach:

The approach to solar minimum promises new opportunities for scientific understanding of particle acceleration and loss processes. High-speed solar wind streams should appear throughout the 2003-2005 interval and are expected to cause numerous particle flux enhancement events for study. These events will be ideal for targeted detailed analysis because the magnetospheric environment will not be disrupted by the many complexities ensuing during solar maximum that can overwhelm clear understanding. The previous high-speed stream period was 1993-1994, prior to the launch of Polar when high-altitude energetic particle measurements were only available at geosynchronous orbit (Figure 3).

The orbit of Polar coupled with the locations of IMAGE, Geotail, Cluster, SAMPEX, and the LANL, GPS and HEO combination, give us an opportunity to monitor both the internal dynamics and the external source mechanisms as they respond differently to CME/magnetic cloud impact and to recurrent high-speed solar wind streams. In particular, the orbital precession of Polar allows sampling of the near-equatorial plane phase space density from the location of the peak electron fluxes around L=4 out past geosynchronous orbit to L=10. This moderate rate of orbital precession combined with Polar's array of particle instrumentation (see **Figure 26**) consistently enables important contributions to the understanding of energetic particle dynamics in the inner magnetosphere. It is currently the only mission that measures the 3D magnetic and electric fields along with the full range of energetic

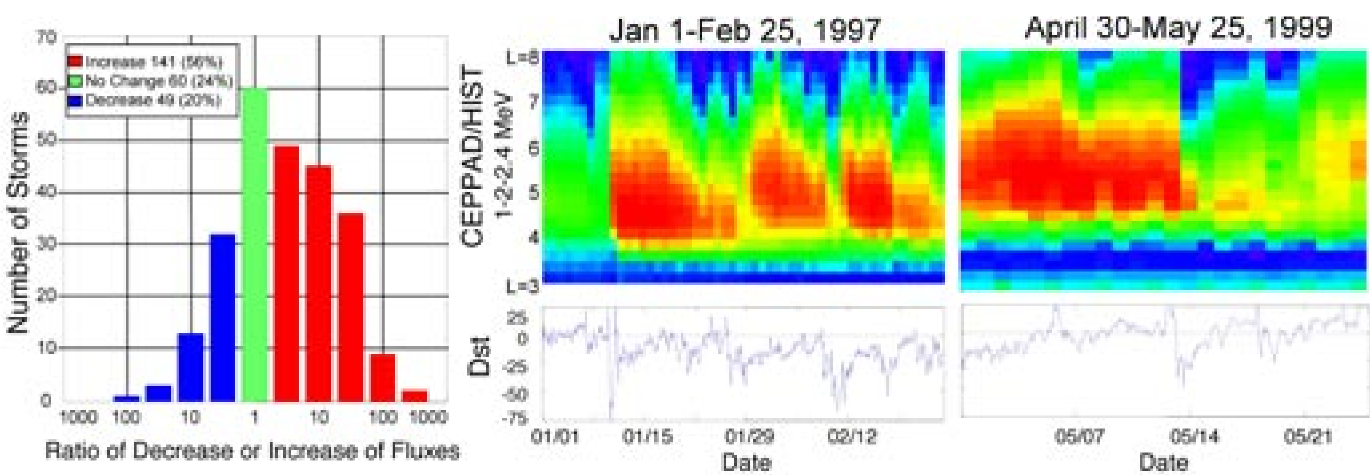

Figure 11: The MeV electron flux response to a magnetic storm is highly variable, with only a slight better than 50% chance of an increase [*Reeves et al.,* 2003].

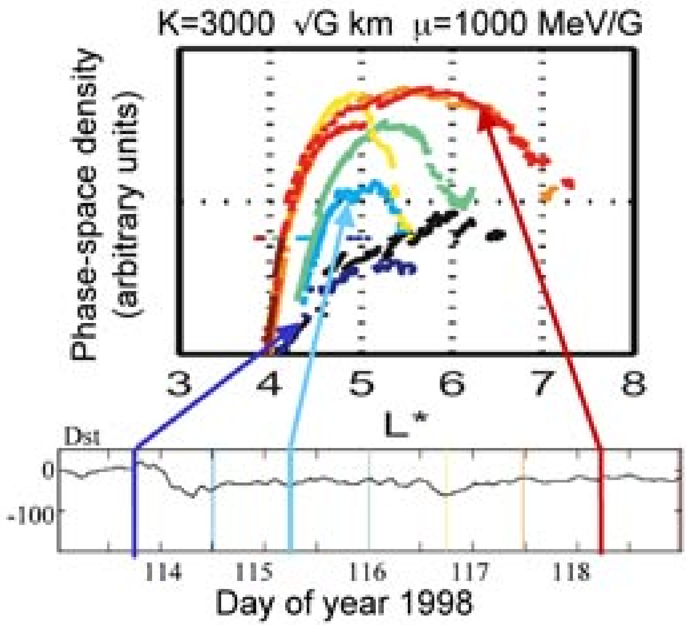

Figure 12: Polar electron phase-space density profiles during a magnetic storm show evidence of a growing peak in phase-space density near L~5-6. The evolution of such a peak is indicative of local acceleration [*Green*, 2002].

particles of interest. The data are also used in the interpretation of less sophisticated, off-equatorial observations on GPS and HEO spacecraft thereby expanding the range of coverage for phase space density statistical databases.

Polar crossings of the magnetic equator in the outer magnetosphere are excellent for observing strong low-frequency ULF waves. **Figure 13** shows an example when Polar/MFE observed EMIC wave activity in two distinct frequency bands modulated by Pc5 waves near the dusk equator. There are excellent opportunities to study the latitudinal characteristics of these waves. to compare with theoretical predictions, and to study their ability to heat radiation belt electrons.

Interplanetary shocks inject energetic heavy ions and super-relativistic electrons deep into the inner magnetosphere. Since the premature demise of CRRES, Polar has the only comprehensive set of measurements for specifying the initial conditions and validating models of the rapid formation of these intense, long-lived belts of these energetic heavy ions and super-relativistic electrons. Intense interplanetary shocks are not common at 1 AU, but Polar's continued operation during the approach to solar minimum will provide further opportunity for observing the unusual and highly geoeffective phenomena.

Finally, as the line of apsides of the Polar orbit precesses into the southern hemisphere the satellite will once again encounter the extended magnetospheric cusp and its population of energetic particles. The Cluster satellites also intersect this region in both the northern and southern hemispheres permitting this area to be studied in a manner that was not possible previously.

Expected Results:

There is renewed interest in isolating and understanding the mechanisms responsible for electron flux enhancements in the radiation belts that typically form during the recovery phase of geomagnetic storm periods. The interest in these events arises in part because of evidence that occurrence of these fluxes contributes to spacecraft operating anomalies or failures, especially at geosynchronous altitude.

During 2003-2005, Polar will be well-positioned to explore the critical mid- to high-L regions, both at and near the magnetic equator, where wave-particle interactions are expected to be an important contributor to energetic particle dynamics. As the Polar orbit evolves through southern latitudes, a follow-up to the *Green* [2002] observations of a dawn-dusk asymmetry in the pitch-angle anisotropy of MeV electrons will be pursued. This anisotropy is the hallmark of the leading VLF electron acceleration mechanism [*Summers et al.,* 1998]. The study established the asymmetry with an 83% confidence factor. A further study including another year or two of magnetic storms in the declining phase (2004-2005) is necessary to raise the confidence to a more satisfactory level of 95%.

The exact role of ULF waves in electron acceleration remains elusive, although important new mechanisms continue to be explored. A study of Polar electron flux observations as a function of L determined, in agreement with other studies, that sustained ULF power was a necessary criterion for relativistic electron enhancements at high L shells [*Green and Kivelson*, 2001]. For now, Polar has the only instrumentation that can measure the critical pitch-angle distribution and energy spectra at the resolution required to test and quantify the role of ULF waves in electron transport and acceleration.

Continued Polar and SAMPEX observations of electron precipitation into the upper atmosphere will be important to the determination of radiation belt lifetimes and the electron energy input to the atmosphere. The *Selesnick et al.* [2002] empirical model, maintained by the Polar/CEPPAD science team, is used to establish the global electron losses into the atmosphere both for studies involving the dynamics of the atmosphere and

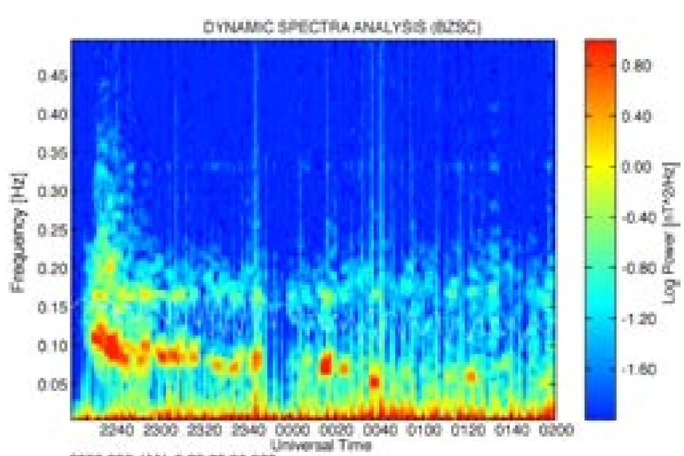

Figure 13: Polar/MFE EMIC wave activity in two frequency bands modulated by Pc5 waves near the dusk equator. Polar provides excellent opportunities to study the latitudinal characteristics of these waves and compare them with theoretical predictions.

of the radiation belts. The results show that the simple drift-diffusion model can account for the main features of the low-altitude radiation belt at L=3.5 during a period of steady decay. Low-altitude observations of electron precipitation, which are needed simultaneously with the high-altitude source observations, are not in the "core" observation plans for the Living with a Star Radiation Belt Storm Probe mission. Completion of this empirical modeling work during the Polar and SAMPEX years appears to be very important.

Polar's array of instrumentation, along with the SAMPEX, GPS and HEO missions, is able to sample the radial magnetic field–L-shell profile down to very low L. The Polar team has identified rapid energetic electron, proton and heavy ion flux enhancements at altitudes as low as L=2 [*Slocum et al.,* 2002]. These observations represent an entirely different class of radiation belt formation processes, likely related to the strong electric fields induced by interplanetary shocks [*Li et al*., 1993]. Such strong shock acceleration events are sufficiently rare that the last event of similar magnitude occurred during the CRRES mission 10 years ago. Polar fortuitously observed a second example of this kind of unusual, but highly geoeffective, magnetic storm in November, 2001. The similarities and differences will be investigated between the two events. We expect to determine whether this is a unique class of acceleration process or whether there is a relationship to more common, weaker shocks.

2.3. Understanding the Microphysics of Plasmas: Obtain new understanding of the ion and electron diffusion regions, solitary wave structures, and the role of small scale field structures.

General problem:

For many years evidence has been persuasively advanced that magnetic reconnection is somehow enabled, but by unknown processes. Understanding these processes is of fundamental importance to solar atmospheric processes, heliospheric processes, solar wind-magnetosphere and magnetosphere-ionosphere coupling, since reconnection is clearly the dominant mechanism by which magnetic energy is converted to plasma kinetic energy and thereby drives magnetospheric activity. The problem to be pursued is to provide in situ observational evidence for specific mechanisms that enable or control reconnection, thereby advancing its theoretical description. For example, the kinetic processes that demagnetize the electrons and issues regarding the role and topology of thin current sheets must be addressed. It is important for Polar to push the observational limits at reconnecting boundary layers now so that the soon-to-be-selected Magnetospheric Multiscale (MMS) experimenters have the best possible experience base for optimizing their multi-spacecraft experiments, which will fully explore the microscale layers involved in reconnecting regions.

What terms in the generalized Ohm's law are important in controlling reconnection and the physics of sharp boundaries?

Are solitary wave structures localized within the magnetopause layer?

How do the Earth's bow shock and magnetopause mediate and facilitate the transfer of energy from the solar wind to the magnetosphere?

What are the conditions that favor steady and pulsed reconnection?

Recent Advances:

In the past three years, the Polar team has made excellent progress delineating candidate reconnection layers and illustrating the importance of making explicit tests of the ways that collisionless magnetic reconnection occurs. *Mozer et al*. [2002] demonstrated the characteristic and opposed electric fields along the normal to reconnecting layers. [*Scudder et al*., 2002] provided evidence that Polar crossed the magnetic separator (**Figure 14**) numerous times and was able to resolve narrow spatial regions of very high electron beta (>600) localized about the magnetic separator on scales sizes, L, less than 1/20th the ion skin depth. Since the thermal electron gyroradius was shown to be on the order of 12L, the thermal electrons then are unmagnetized at the magnetic separator, identifying that site as a locale where the magnetic topology is changing. $E_{||}$ was measured for the first time within the

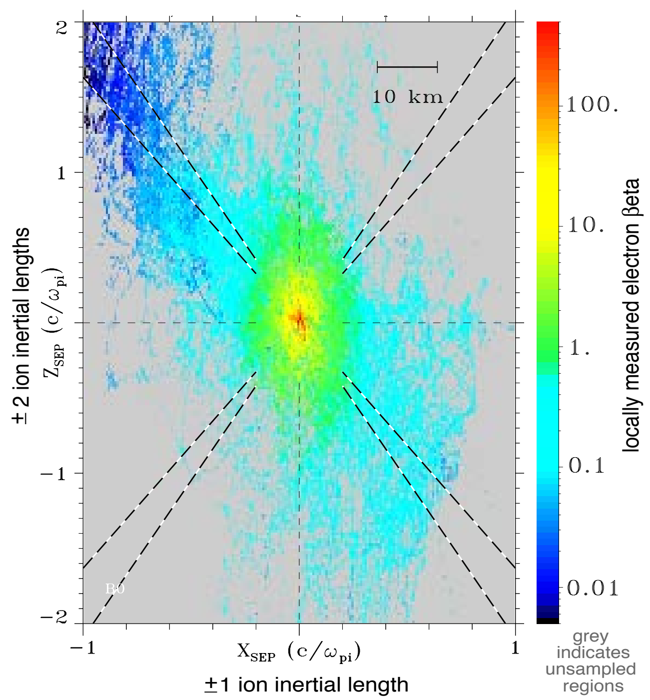

Figure 14: Superposed epoch map of electron beta, β_e, in the vicinity of a magnetic separator on May 29, 1996. Outward streaming and demagnetization of electrons, with β_e>>1, is shown within a narrow region synonymous with the "electron diffusion" region. Dashed lines reflect the separatrix, while color indexes the average value of β_e. The ratio of thermal electron gyroradius, α_e, to 1/42 ion inertial length is given by $\beta_e^{1/2}$. At the origin, α_e exceeds the scale of this structure by 25 times and the thermal electrons are not magnetizied. [*Scudder et al., in prep*].

magnetopause and shown to be supported by pressure divergence as predicted. These observations point to the importance of the $\nabla \bullet \mathbf{P}_e$ term in the generalized Ohm's law and to the pressure tensor being sufficiently deformed in the presence of agyrotropic electrons that it could be the principal controller of collisionless magnetic reconnection. Further examples and confirmations of these results are being actively pursued.

Other possible ways to enable collisionless magnetic reconnection are via electron inertial effects or wave particle momentum exchanges. Recent reports using Polar concerning the importance of these possibilities have conflicting conclusions (*Bale et al*. [2002] vs *Drake et al*. [2003] and *Cattell et al*. [2002]). The first group found that waves observed in a reconnecting layer were not an important contributor to the underlying physics. The second group identified large amplitude waves in boundary layers, which have visual similarities with "electron holes" seen in the auroral region. These observations were associated with the turbulence seen in 3D simulations of collisionless reconnection for layers with guide fields, concluding that the turbulence acts as the agent of collisionless magnetic reconnection. Several important questions remain to be answered, including where within the current layers, and under what conditions, electron holes and guide fields occur.

New Opportunities and Specific Goals:

The thin reconnecting boundary layers are traversed in times comparable to the reporting cadences of most scientific instruments currently in flight through these regions (**Table 1**). Polar is now in a position to more than double the telemetry allocations of the EFI, MFE, and Hydra sensors on a time-shared basis (see section 3.1, Science2 mode). Doing so will increase the electric field sampling to 80 Hz, the magnetic field sampling to 25 Hz, and via Hydra, even higher sampling of the full magnetic field vector at 54 Hz. With the 3D ion and electron distributions sampled every 2.3 seconds, this will provide new insights into the diffusion regions, solitary wave structures, and small scale field structures. Our specific measurement goals are to:

Table 1: Reporting rates for current SEC space assets and relevant scale sizes. With its new Science2 burst mode, Polar has the opportunity to provide the highest resolution, 3D particle and fields ever taken through these regions from a single platform.

Diffusion Region	approx scale size	transit time
Electron, magnetopause	1 to few km	0.01 to 1 second
Electron, tail	10-50 km	0.1 to 5 seconds
Ion, magnetopause	30-100km	0.5-20 seconds
Ion, tail	400-2000km	6-400 seconds
Platform (mode)	**B** report rate	**E** report rate
Polar (nominal)	8.3 Hz (MFE) 27 Hz (Hydra)	40 Hz
Polar (nominal burst)	8.3 Hz (MFE) 27 Hz (Hydra)	1600 Hz for 25 sec* twice per orbit
Polar (Science2 nominal)	25 Hz (MFE), 54 Hz (Hydra)	80 Hz
Polar (Science2 burst)	25 Hz (MFE), 54 Hz (Hydra)	1600 Hz for 50 sec* twice per orbit
Cluster (nominal/burst)	22 Hz/67 Hz	25 Hz / 50 Hz
Wind (nominal/near Earth)	10 Hz/20 Hz	n/a
Geotail (nominal/burst)	16 Hz	32 Hz / 64 Hz

*EFI burst mode rate is programmable (e.g., Figure 16)

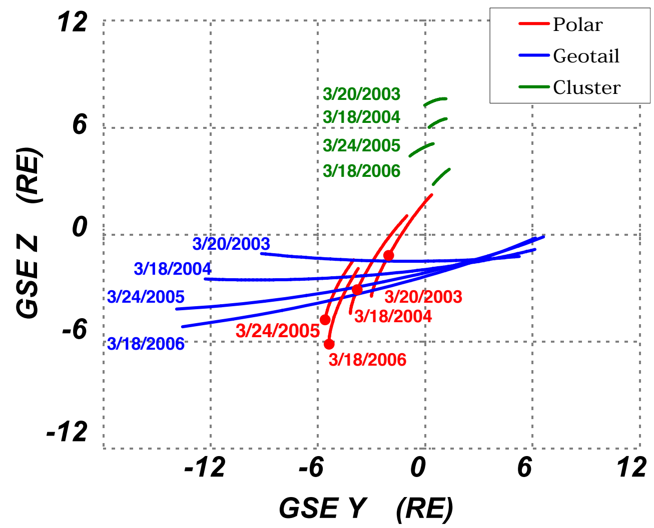

Figure 15: Modest magnetopause compressions place Polar within the low latitude boundary layers where reconnection is taking place and its direct dynamical consequences detected. Near simultaneous Geotail cross cuts through the equatorial plane and Cluster high-latitude reconnection measurements will help document the extent and stability of dayside neutral lines.

1. Obtain a better understanding of the ion and electron diffusion regions in the dayside magnetopause and tail.

2. Determine the distribution of solitary wave structures in reconnecting boundary layers.

In addition to Polar's high-resolution data, the combination of Polar, Cluster, FAST and Geotail covering complementary parts of the global interaction area (**Figure 15**) will make it possible to systematically investigate large-scale dynamics and make estimates of the global influx of solar wind plasma under varying conditions. Goals in this area are to:

3. Determine the extent that less than anti-parallel magnetic shear supports reconnection.

4. Isolate, for varying conditions, as many reconnection events as possible to statistically determine the preference for steady versus pulsed reconnection.

Approach:

The physics of reconnection cannot be adequately understood via simplified magnetohydrodynamics because the ideal MHD approximation neglects key terms in the generalized Ohm's law, which may be written as

$$\mathbf{E} + \mathbf{U}_e \times \mathbf{B}/c \equiv -(1/en)\nabla\bullet(\mathbf{P}_e + m_e n \mathbf{U}_e \mathbf{U}_e)$$
$$-(1/en)\partial(m_e n \mathbf{U}_e)/\partial t + EMF_{drag}$$

where, **E** and **B** are the vector electric and magnetic fields, $\mathbf{U}_e$ is the electron fluid velocity, $\mathbf{P}_e$ is the plasma pressure tensor, and EMF_{drag} is the net EMF resulting from wave-mediated momentum exchange between all ions and the electron fluid (i.e, anomalous resistivity). The terms on the RHS of the equation are arranged in their likely order of importance. How the ordering may change in the presence of abrupt spatial or temporal variations must be investigated along with explicit tests to demonstrate conditions when EMF_{drag} becomes important. Particularly exciting experimentally is the quest to identify which of the terms in the equation above contribute to the curl E which must be non-zero to enable magnetic reconnection. *Vasyliunas* [1975] foresaw that an electron pressure tensor with 3 distinct eigenvalues would provide an important source term for such a curl. For a strongly magnetized gyrotropic electron fluid at least 2 eigenvalues of $\mathbf{P}_e$ are equal, while a plasma with three distinct eigenvalues implies the plasma is agyrotropic. When the thermal electrons are demonstrated to be agyrotropic, then no sub-population of the plasma remains to define the "field line" velocity and collisionless magnetic reconnection is shown to be underway.

Pursuing these objectives requires in-situ measurements of the electron distributions and the magnetic and electric fields in the ion and electron diffusion regions. The exact size of these regions is not known but depends on the dominant diffusive processes. **Table 1** summarizes the expected scale sizes and reporting cadences of the instrumentation currently flying through the diffusion regions. Better definition of the electromagnetic field through the boundary layers by increasing key Polar reporting cadences will significantly increase the understanding of these regions, and the processes within.

In a particular example, Polar/EFI captured ~5 sec of high data rate waveforms (up to 8000 samples/s) in its burst mode configuration (**Figure 16**). The figure shows

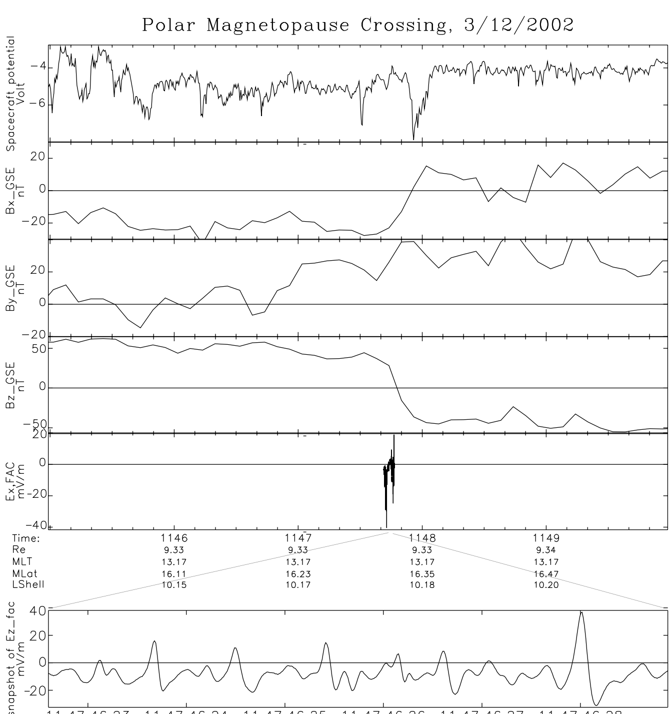

Figure 16: Polar EFI and MFE burst mode waveform captured at the magnetopause. Shown is the spacecraft potential, the spin averaged magnetic field, the x-component of the electric field, and an expanded plot of the parallel electric field that shows solitary waves structures. No other spacecraft has had the capability to resolve these field structures.

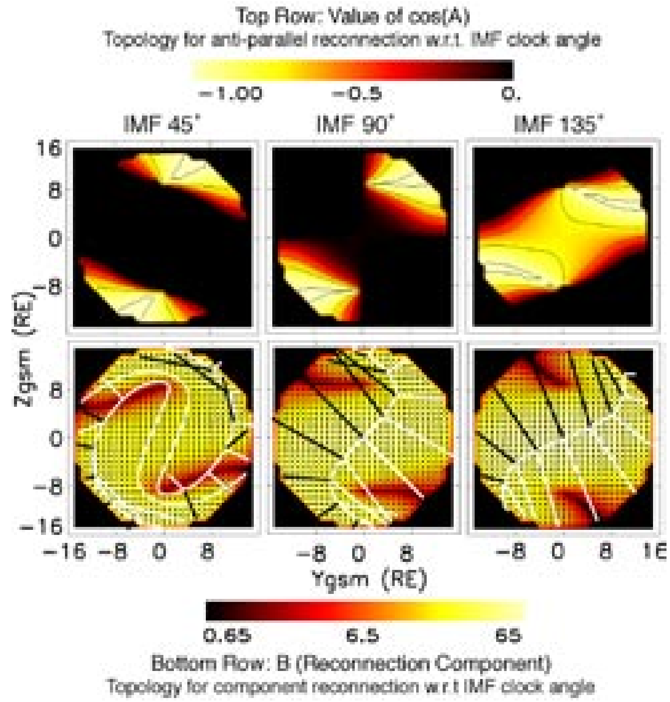

Figure 17: Simulations comparing predictions of the reconnecting topology for the extremes of purely antiparallel and for component reconnection [*Moore et al.,* 2002]. Computed X-line (white curve) and the local boundary layer flow on either side of the X-line (black and white vectors) are superposed.

a magnetopause crossing for which the burst data were obtained on the magnetospheric side of the current sheet and clearly shows solitary wave structures in the bottom parallel electric field panel. *Drake et al*. [2003] have shown, through simulation, that solitary waves should generally be observed on the magnetospheric side of the current sheet boundary. With additional burst mode operations, the waveform observations in these events will cover the entire magnetopause crossing and determine where and under what conditions, in the magnetopause current layer, solitary waves are most likely to appear. In addition, early in the mission, Polar/PWI provided near continuous sampling (up to 32,000 samples/sec) of lower hybrid waves, whistler mode waves, electrostatic electron cyclotron waves, and impulsive solitary wave structures at the magnetosheath/magnetopause boundary. These were observed at and near probable sites of reconnection and are a resource for more detailed study.

In the next three years, the SEC fleet will provide many opportunities to investigate how changes in the large-scale magnetic topology influence where and how reconnection occurs. There are two competing views of the spatial and temporal extent of solar wind plasma entry, steady-state [*Crooker,* 1979] and impulsive injection [*Smith and Lockwood,* 1990]. Quasi-steady reconnection on a boundary surface should be constrained topologically as well as by local magnetic shear. If so, neutral line configurations under varying IMF clock angles should occur as illustrated in **Figure 17.** Impulsive injection suggests that solar wind enters in spatially and temporally isolated locations and has a fundamental period near 8 minutes.

Polar observations have shown that both views are somewhat valid. In a series of studies, *Fuselier et al.* [1999, 2000a,b, 2001, 2002], *Avanov et al.* [2001], *Topliss et al.* [2000] and *Trattner et al.* [1999, 2002a,b] used particle observations to establish the stability of the reconnection location during intervals of steady IMF, and that it occurs over long X lines. [*Trattner et al.,* 1999] also demonstrated quantifiable intervals of pulsed plasma entry. It is anticipated that merging may be intermittent in regions where the tangential magnetosheath velocity exceeds the Alfvén speed [*Rodger et al.,* 2000]. As Polar transitions to higher Southern Hemisphere latitudes, Cluster/Polar conjunctions offer a unique opportunity to monitor the cusps at multiple sites to separate spatial and temporal variations.

Recently it has been shown that 557.7nm all-sky imagers provide a "television" picture of the merging processes at the magnetopause [*Maynard*, 2003]. The Japanese 557.7nm imager at South Pole along with the Southern Hemisphere SuperDARN network can be used to record the temporal and spatial response in the ionosphere to merging while Polar and Cluster provide in situ details of the electrodynamics of the process. Variations with IMF (including the tilt with B_X [see *Weimer et al.,* 2002]), dipole tilt, and activity level will be separated.

Expected Results:

With better resolution of reconnecting boundary layers, better understanding of the applicable geometry and spatial scales should be forthcoming. With the enhanced E and B recording and the Faraday Residue technique [*Terasawa et al.,* 1996], many more boundary layers will be resolved and their substructure and their scales catalogued. During magnetopause skimming orbits, magnetic and plasma structures propagating relative to the boundary layer will be identified along with the shape and size of observed boundary waves. The observations will be compared with models that can then be improved to better represent the primary influences giving rise to reconnection and to the entry of solar wind plasma into the terrestrial system. Polar's progress in this area will be of immediate benefit to Magnetosphere Multiscale Mission investigators as they optimize their experiments, data analysis, data assimilation and modeling tools for flight.

2.4. Impact of the Ionosphere on Geospace Processes: Exploit Polar's new position in the SEC fleet to quantify the variable electromagnetic linkage between the solar and the ionosphere along with its reactive energy that introduces new dynamics into the system

General problem:

The ionosphere and upper atmosphere are the loads on the Sun-Earth Connection system. The magnetosphere acts as an electromagnetic linkage system between the solar wind and the ionosphere, with reactive energy and plasma storage that introduces new and unique dynamics into the system, depending on the amount of ionospheric plasma supply. We have known that the ionosphere responds to solar photon and energetic particle energy inputs, as well as electromagnetic energy inputs from the solar wind, in ways that influence its load properties and feedback to overall system energetics. But now we have come to realize the extent to which ionospheric plasmas are distributed throughout the magnetosphere and are lost into the solar wind. Thus ionospheric influences on system dynamics can no longer be taken as limited to the ionosphere and thermosphere. Instead they influence the entire space weather system in substantial ways that must be included in our system descriptions (global simulations) if they are to predict the overall system dynamics.

How do ionospheric plasmas interacting at dayside boundary layers impact reconnecting processes?

Do terrestrial plasmas play a significant role in the formation and dynamics of the near-Earth plasma sheet during substorm dipolarizations and storms?

What is the linkage between solitary and kinetic Alfvén waves and dynamic plasma acceleration processes?

What are the UV and SEP effects on upper atmosphere - ionosphere coupling and the subsequent outflow of plasma?

Recent Advances:

Most striking is the discovery that the geopause – the boundary inside of which terrestrial plasmas dominate – is often present just inside the magnetopause. Cold but anisotropic plasmas are routinely present just inside the magnetopause, and not only when the magnetopause is compressed [*Su et al.,* 2001; *Chandler et al.,* 2003]. The composition is distinctly plasmaspheric, with H^+, He^+, and O^+ in descending order of importance (**Figure 18**). The density varies from a fraction to a few tens per cc, evidently in response to inner magnetospheric convection and the formation of plasmaspheric drainage plumes such as those seen by IMAGE [*Sandel et al.,* 2001]. Substantial densities of cold plasma at the magnetopause means that ionospheric plasma permeates the entire magnetosphere and participates in all magnetospheric processes, even at its outermost boundaries.

The impact of ionospheric plasmas on substorm processes has only begun to be explored. Because the downtail distance at which ionospheric plasma interacts with the plasmasheet varies with source energy, mass and activity conditions, advances in understanding the midnight auroral zone, plasmasheet, and high-altitude 7-9 R_E transition region must all be evaluated as to how particle source variations affect the dynamics. Especially relevant to this is Polar's determination that a significant part of the power for the substorm aurora comes in the form of Alfvén waves propagating from a high altitude source [*Keiling et al.,* 2003; *Toivanen et al.* 2001; *Wygant et al.,* 2000; *Peterson*, 2002]. Heating results which increases ion outflow. Also important is the detailed chronology of events surrounding substorm onset [*Newell et al.,* 2001 and *Liou et al.* 2001a, 2002a]. Events in the near Earth plasma

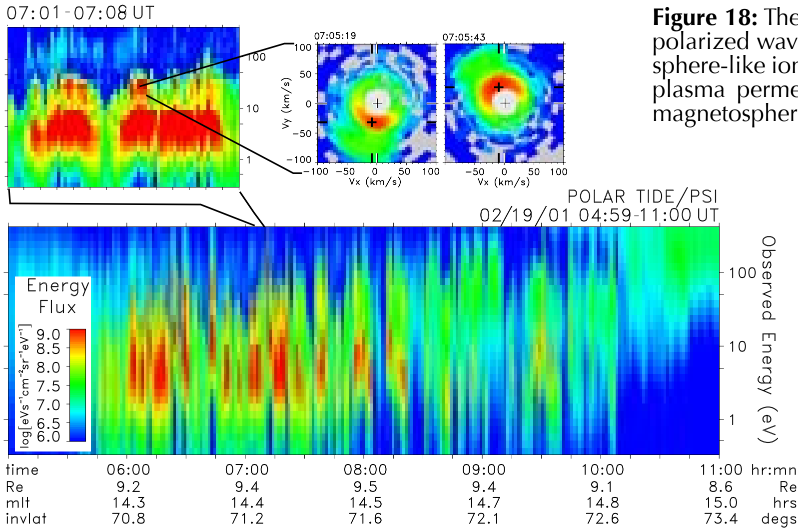

Figure 18: Thermal ion spectrograms and distrubtions show circularly polarized waves near the dayside magnetopuase accelerating plasmasphere-like ions to 30-40 km/s [*Chandler and Moore,* 2003]. Ionospheric plasma permeates the entire magnetosphere and participates in all magnetospheric processes.

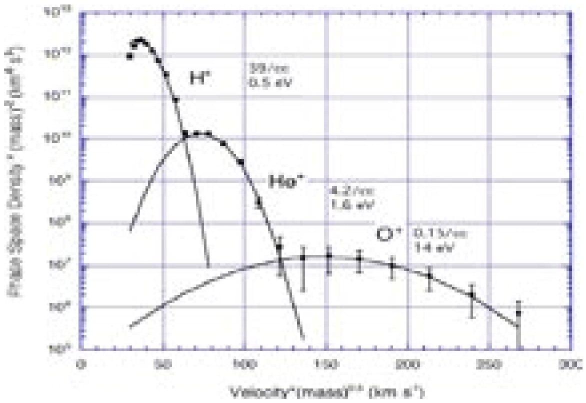

sheet and the initial brightening of the aurora are found to occur before reconnection is initiated in the plasmasheet. This supports theories and observations that substorm onset occurs relatively close to Earth in regions richly supplied with ionospheric plasmas [*Lui et al.,*1998; *Maynard et al.,*1996; *Erickson et al.,*2000; *Frank et al.,* 2000a,b].

A 3D model of the auroral plasma fountain is in development. *Valek et al.,* [2002] found that dayside auroral heating extends equatorward of the cusp, consistent with precipitating electrons and/or electromagnetic energy flux as drivers of the heating. Specific statisical descriptions have contributed to understanding auroral energy deposition, ionospheric heating and outflow, and their dependence on the state of the ionosphere [*Su et al.,1998; Elliott et al.*, 2001; *Peterson et al.*,2001; *Olsson, et al.,* 2002].

New Opportunities and Specific Goals:

Skimming orbits of the magnetopause (Figure 1, dayside opportunities) enable extensive studies of the character and global distribution of ionospheric plasmas over a greater portion of the dayside magnetopause including any hemispheric effects on the supply and transport.

A scientifically powerful constellation of spacecraft for the study of magnetospheric substorms forms each fall when the Polar apogee position sweeps through the nightside magnetotail (Figure 1, nightside opportunities). During the Southern Hemisphere Campaign, Polar's and Geotail's apogee will sample southern low-to-mid latitudes at 7-9.5 R_E while Cluster makes north/south cuts through the plasma sheet at 19 R_E. Instrumentation at geosynchronous orbits complete the array. Substorm timing and position is provided by Polar and IMAGE auroral brightenings. FAST contributes in situ observations of thermal outflows near the source and the energy flow producing the optical emissions. Because it is between 5 and 20 R_E where the geomagnetic field evolves from a dipolar to a tail-like configuration, these spacecraft have opportunities to intercept the flow of plasma energy and the violent changes in the fields which occur. Measurements accumulated over many substorms can identify instability processes and focus theoretical efforts accordingly.

A new opportunity that presents itself is Polar's perigee precession over the well instrumented northern land masses. This permits observations of flux tubes by Polar at 1.8 to 2.25 R_E to be correlated with ground-based observations. This will support studies focusing on the mechanisms of ionospheric interaction, heating, and outflow.

Our specific measurement goals with regard to the impact of the ionosphere are to:

- Determine how ionospheric core plasmas interacting at the magnetopause boundary layers impact reconnecting plasma processes.
- Identify the role of terrestrial plasmas in the formation and dynamics of the near-Earth plasma sheet during substorm dipolarizations and storms.
- Assess the importance of cross-scale coupling processes and the relative roles of solitary waves and kinetic Alfvén waves in tail dynamics.
- Resolve spiky field structures in both the perpendicular and parallel directions to understand how kinetic Alfvén waves are dissipated in the auroral acceleration region and possibly heat ionospheric plasmas.
- Understand UV and SEP effects on upper atmosphere-ionosphere coupling via load interactions.
- Quantify and analyze the terrestrial outflows supplying magnetospheric plasmas, over solar cycle variations, as boundary conditions for simulations.

Approach:

The Polar team has shown cold ionospheric plasma to be routinely present along the long duration dayside magnetopause skimming orbits [*Chandler and Moore*, 2003] and provided evidence that these plasmas are drawn rapidly toward the magnetopause as inflow into dayside magnetopause reconnection [*Chen and Moore*, 2003]. Since the amount of ionospheric plasma observed in these boundary layers varies broadly from less than 0.1 cm^{-3} to over 10 cm^{-3} at the subsolar magnetopause, this implies a similar variation of the Alfvén speed and perhaps a limit to the rate of reconnection in that region. Thus magnetospheric circulation driven by dayside reconnection could be self-limiting when it draws a substantial part of the plasmasphere out to the subsolar region, depressing the local Alfvén speed until magnetic field increases at the reconnection site are able to compensate. With Polar's ability to resolve the details of plasma distributions under 500 eV, we will pursue extensive studies of the character and distribution of these plasmas and their flows over greater portions of the dayside magnetopause. We expect to reveal new patterns of interaction among the diverse influences on the dayside magnetopause.

At the other interesting destination for ionospheric plasma outflows, the near-Earth magnetotail, global simulations have suggested that the inner plasma sheet can be dominated by ionospheric plasmas during southward IMF with strong antisunward flow over the polar caps [*Winglee et al.,* 1998]. The same result has been suggested for over a decade by investigators computing single particle trajectories [*Delcourt et al.,* 1994]. **Figure 19** is from a recent effort in this area. The top panel shows that ionospheric protons can attain ring current energies during their transit to the inner magnetosphere, where they become concentrated by convection into stronger magnetic fields. The bottom panel is a similation matched to Polar particle and field observations for the October 24, 2002 magnetic storm; nightside polar wind hydrogen ions are followed in 500 trajectories, and the resultant density distribution is plotted in the noon-midnight meridian. The pervasive features along the early portions of these paths have been well documented by Polar and others, including the oxygen-enhanced cleft plasma fountain and polar wind flows, the hot nightside auroral zone outflows, and the persistent wind within the lobes. We will just as thoroughly document the terrestrial plasmas as they encounter the neutral sheet proper, taking special care to document differences between quiescent and storm conditions. Detailed comparisons will be made between what is flowing into the plasma sheet, what is observed within the plasmasheet and what then, according to theory, the inflow can produce via neutral sheet acceleration.

These studies lead into our longstanding interest in understanding the role of solitary waves observed in the equatorial magnetotail at plasma sheet boundary crossings (that map back to the reconnection region in the geomagnetic tail) and in associated with magnetic field dipolarization and "current sheet disruptions" during geomagnetic storm and substorms [*Cattell et al.,* 2002]. A large-scale study will quantitatively investigate the importance of these cross-scale coupling processes and the associated heating and acceleration of electrons and ions by the impulsive structures. Of particular interest are the intense spiky electric fields with amplitudes ranging from tens to hundreds of mV/m observed coinciding with laminar Alfvén wave forms [*Wygant et al.,* 2002]; they appear to be small-scale kinetic Alfvén waves with perpendicular scale sizes of about 20 km. Theoretically, near 10-20 Hz, kinetic Alfvén waves transition from being predominately electromagnetic to predominately electrostatic. These spiky electric field signatures may be an intrinsic part of the electrostatic shock spatial structure or they may be due to temporal fluctuations. Thus far, it has

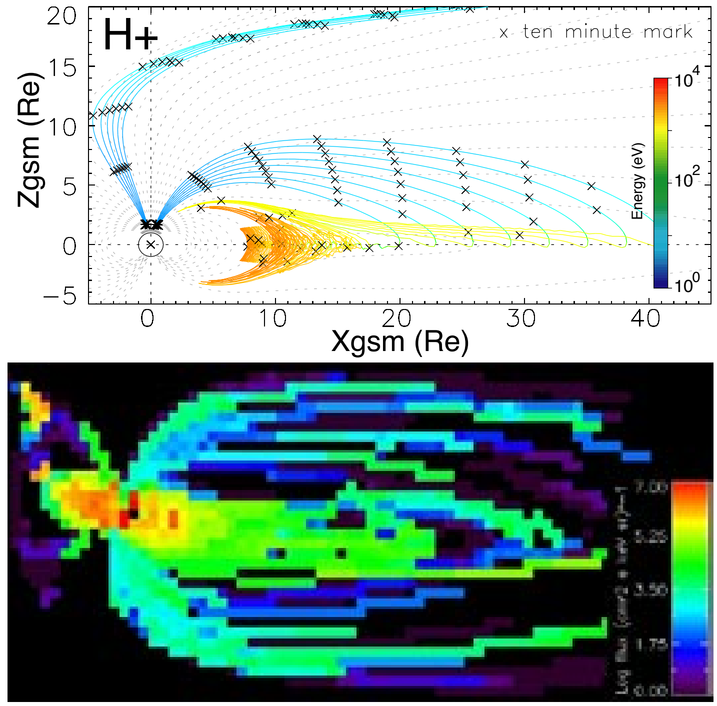

Figure 19: H^+ hot plasma flux resulting from the outflow of nightside polar wind protons and subsequent convection back into the inner magnetosphere. The downtail distance at which ionospheric plasma interacts with the plasmasheet will vary with source energy, mass and activity conditions. The consequences of this variation have only begun to be explored.

been difficult to assess the ability of these intense wave fields to energize particles because the largest spikes are not fully resolved by our instruments at their nominal data rates. Doubling the reporting rates of the EFI and MFE instrumentation will allow resolution of the waveforms to determine the spatial scale sizes and parallel potential drops as well as the efficiency of particle energization. Also, the large Polar/PWI 1996-7 dataset of very high resolution wave measurements, including Alfvén, EMIC, and impulsive solitary waveforms, will be invaluable to compare to the future EFI and MFE data.

In cooperation with NSF-GEM campaign initiatives, Polar teams are working to tie their outflow specifications to local aggregate energy fluxes into the ionosphere, including DC and AC Poynting flux over as broad a range of frequencies as possible, as well as particle precipitation fluxes as a function of energy (**Figure 20**). An important element missing in the descriptions is the connection with the basic state of the ionosphere. The heating effectiveness of solar UV radiation, the insolation, is the principal controller of ionospheric plasma although it is constantly modified through coupling to the magnetosphere and by influxes of solar energetic particles (SEP). UV insolation influences the structure of the neutral atmosphere in ways that affect auroral luminosity and ionospheric outflow [*Liou et al.,* 1997, *Shue et al.,* 2001]; and, it has recently been argued, strongly affects space weather [*Newell et al.,* 2002]. To explore how UV and SEP insolation affects auroral luminosity, ion outflow and more generally space weather, it is important to observe over as many seasonal cycles as possible. Geomagnetic disturbances maximize at equinox [*McIntosh*, 1959; *Cliver et al*. 2000], while intense aurora are most common in the winter hemisphere [*Newell et al*., 1996]. This implies that UV insolation may have some control over field-aligned electric field formation. Also, it appears that geomagnetic activity is highest when global conductivity of the nightside oval is highest [*Lyatsky et al*., 2001; *Newell et al*., 2002a]. This implies that UV and seasonal variations will themselves follow a solar cycle, matching variations in F10.7, and testable by Polar. Key to understanding these effects will be the use of gound-based assets and the AMIE model to quantify the ionospheric energy budget, its contribution to ion and electron flows, and to determine which coupling mechanisms dominate under the varying influences. Relating Polar observations at ~5000 km with ionospheric conditions below 1000 km will determine the altitude profile of energy inputs, which then determines the effect on the mass flux and energization of ionospheric outflow, which in turn controls the distribution of ionospheric material in the magnetosphere.

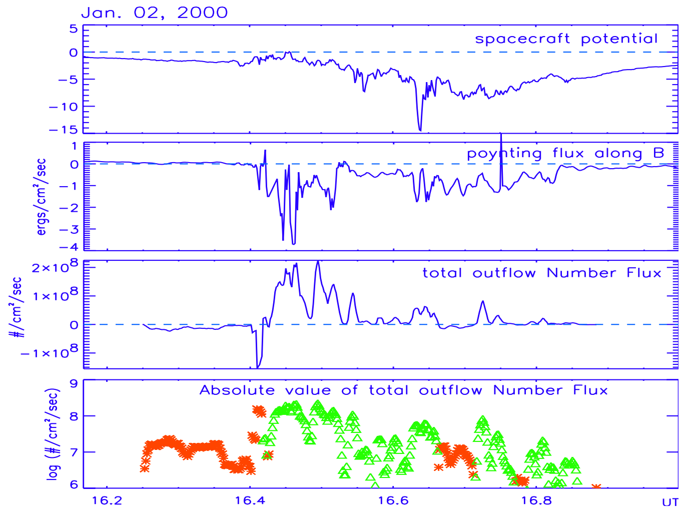

Figure 20: Increased fluxes of ion outflow, dominated by O+, have been found to be correlated with strong parallel Poynting fluxes. Simulations require specifications of the local ionospheric outflow response to magnetospheric energy inputs, including DC and AC Poynting flux, over as broad a range as possible.

Expected Results

While the results derived from new observations can rarely if ever be fully anticipated, extended Polar operations and data analysis will certainly bring new understandings in several research areas: We will probe the entire dayside magnetopause, including the southern cusp with the expanded SEC fleet and learn more about the role of plasmspheric entrainment into high latitude circulation. We will probe the ionosphere's influence on the near-Earth plasma sheet, and determine whether it is critical in the development of substorms and storms. We will revisit the auroral acceleration region with full Northern Hemisphere ground support and thereby determine its interactions with the ionosphere proper. We will also quantify the dependence of auroral processes and energy dissipation upon UV insolation over a full solar cycle.

2.5. Polar and the NASA Office of Space Science Strategic Plan

Value to the OSS Science Themes

The Polar mission has been a fundamental component of NASA's Sun-Earth Connection program for many years. The currently proposed objectives have direct impact on four of the eight SEC Research Focus Areas discussed in the Roadmap, September 2002. These are:

- Understand the response of magnetosphere and atmosphere to external and internal drivers.
- Discover how magnetic fields are created and develop and how charged particles are accelerated.
- Understand coupling across multiple scale lengths and its generality in plasma systems.
- Develop the capability to specify and predict changes to the Earth's radiation Environment, ionosphere and upper atmosphere.

Under each of the roadmap focus areas there are several SEC Investigations. The connection between those investigations and Polar's extended mission objectives is shown in the boxes below.

Science Objectives	Connection to the SEC Roadmap
1. Exploring Hemispherical Asymmetries: Identify important interhemispheric asymmetries and quantify the fundamental M-I coupling processes and parameters that influence and control them.	• Differentiate among the dynamic magnetospheric responses to steady and non-steady drivers. • Develop an understanding of the upper atmosphere and ionosphere response to solar forcing and coupling from the lower atmosphere.
2. Transport Associated with High Speed Streams: Understand inner magnetospheric particle acceleration and circulation associated with high-speed solar wind streams prevalent during the approach to solar minimum.	• Determine how charged particles are accelerated to enormous energies. • Develop the capability to specify and predict changes to the radiation environment.
3. Understanding the Microphysics of Plasmas: Obtain new understandings of the ion and electron diffusion regions, solitary wave structures and the role of small-scale field structures.	• Discover the mechanisms for creation, annihilation, and reconnection of magnetic fields. • Understand how small scale processes couple to large-scale dynamics.
4. Impact of the Ionosphere on Geospace Processes: Exploit Polar's new position in the SEC fleet to quantify the variable electromagnetic linkage between the solar wind and the ionosphere along with its reactive energy that introduces new dynamics into the system.	• Explore the chain of action/reaction processes that regulate solar energy transfer into and through the coupled system. • Develop an understanding of the upper atmosphere and ionosphere response to solar forcing and coupling from the lower atmosphere.

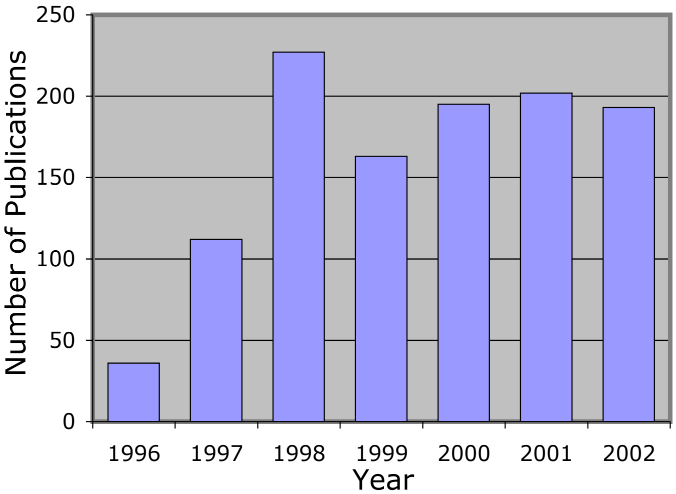

Figure 21: The number of Polar publications as a function of time is a clear indication of continuing program vitality.

Polar as an OSS Strategic Asset

The Polar mission has been in place for six years and, as a result, the science investigators have made significant impact on the space physics literature. There have been over 1000 refereed publications featuring Polar science in a primary role (see **Figure 21**). A full publication list may be found at the Polar web site (http://pwg.gsfc.nasa.gov/polar/).

The Polar PIs are internationally known leaders of the SEC science community. Three of our principal investigators, and one co-investigator, are among the most highly cited space sciences researchers [*http://isihighlycited.com*]. The PI teams supply data for collaborative studies, for image conversions, and for model boundary conditions. The imaging teams provide definitive information on the timing of substorm phases and media-ready descriptions of the magnetospheric response to solar events. Special journal issues and meeting sessions are sponsored (e.g., Causes of the Aurora, JGR special section, April, 2003) in addition to semiannual workshops often held in cooperation with other missions (*http://yosemite2003.space.swri.edu*).

The Polar payload continues to be of special value to the SEC community because it is the only mission to provide multi-spectral imaging of the ionosphere's response to energy inflow simultaneously with the phenomena the in-situ instrumentation are observing. In addition, it is the only mission to successfully observe the 3D electric and magnetic field along with full 3D ion and electron distributions. By end of mission, Polar will provide this information over the entire northern and, with this extended mission, the southern M-I coupled system under a wide variety of solar input conditions. Because future STP and LWS initiatives necessarily target different aspects of the Sun-Earth connected system, this observational database will be an important resource for decades to come.

One important example by which Polar data directly contributes to the science of other SEC missions is in the area of energetic neutral atom (ENA) image inversion. IMAGE and TWINS-1 will produce the first stereo images of the ring current early in 2004, and the duo will be joined by TWINS-2 in 2005. However, the inversion of ENA images is still far from routine. **Figure 22** depicts an early attempt at ENA validation where both ENAs and ions were measured by Polar. Also shown are the kinds of global specifications possible from ENA images and inversions, although these have yet to be validated with in situ data.

Errors in ENA image inversion can be induced by incorrectly specifying the shape of the imaged particle distributions. In situ observations through the imaged region are needed to provide information on pitch angle anisotropy, especially during dipolarization events when the magnetic field topology gives rise to very skewed distributions. A recent study by *Lui et al*. (unpublished) indicates substantial discrepancies between ENA inversions and in situ measurements, especially with regard to local-time structures in the midnight sector. Polar is currently the only mission that measures the magnetic field vector along with the full distribution function of the particles of interest. Because most of the ENA flux originates from ions near the loss cone, these measurements will be important for working out valid ENA inversion techniques.

This work also has implications for the Living with a Star program. Calculation of phase-space density in canonical adiabatic coordinates from in situ radiation belt fluxes requires frequent, detailed, global descriptions of

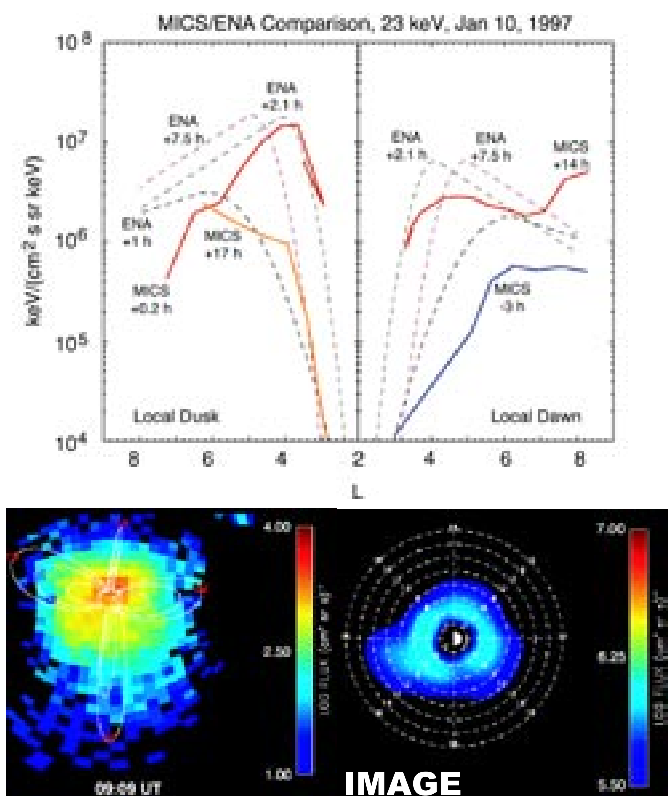

Figure 22: Example of early in-situ validation of ENA images by Polar, accompanied by examples of the global specification possible once IMAGE inversions are validated [IMAGE inserts from *Brandt et al.*, 2002].

the ring current. Since the calculation of phase-space density is so central to the diagnosis of the competing electron acceleration mechanisms, it is essential that global magnetic field specification move beyond statistical models based on Dst or tuned with on-board magnetometry. Therefore, the potential synergy between Polar and the ENA imagers holds great promise for scientific advancement now and in the future.

Another opportunity to complement the Living With a Star program is through global remote sensing of the Earth's ionosphere-thermosphere system. Polar observations of Earth's dayglow are a good opportunity to study these regions of the atmosphere as a precursor to full implementation of the LWS program. **Figure 23** shows changes in the O/N_2 total column density ratio in images acquired with the Polar/VIS Earth Camera and applying the methodology of *Strickland et al*. [1999]. The images are coded so that orange represents no change through blue which is a 45% reduction in the thermospheric O/N_2 ratio. These changes in composition appear to be due to joule heating of the upper atmosphere by auroral precipitation. Here the auroral energy input into the atmosphere occurred ~6-12 hours prior to the observation of the composition change and was transported equatorward by atmospheric winds and tides as the Earth rotated. Details of the heating and atmospheric transport can be used to validate atmospheric models such as TIMEGCM. To validate such models, two measurements are required: the global FUV dayglow on the dayside of the planet and either the northern or the southern auroral oval energy inputs. Consequently, combined observations from the Polar, TIMED, and IMAGE spacecraft represent a unique opportunity that will not be duplicated until full implementation of the LWS program.

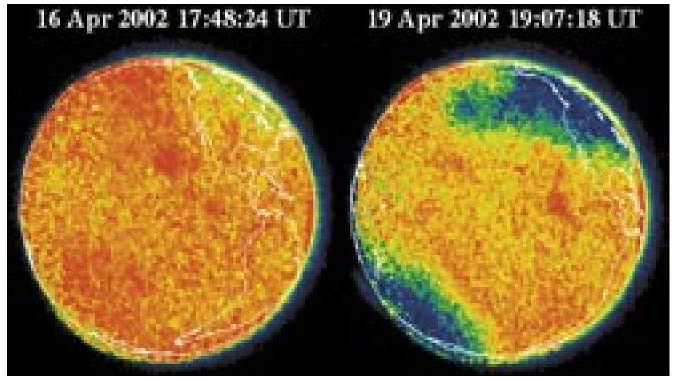

Figure 23: Images from Polar/VIS showing ~50% reductions in the O/N_2 total column density following the 17 April 2002 geomagnetic storm. This provides a clear example of solar interactions reaching deep into our atmosphere. These images were acquired while Polar was in ecliptic normal attitude.

2.6. What have we learned from Polar?

The successful operation of the Polar spacecraft has provided the SEC science community with a rich long-term database. We featured many of our more recent accomplishments in sections 2.1-2.4, herein we present a more comprehensive, although brief, overview of other Polar discoveries made to date, providing context for the science to be achieved during the continuing mission.

Causes of the Aurora

Polar started its quest toward understanding the causes of the aurora immediately after launch. One of the first discoveries was the long sought after direct experimental observation of DC, parallel electric fields [*Mozer et al*., 1997]. The large amplitude parallel electric fields were confirmed to exist both at low and high altitudes [*Mozer and Kletzing,* 1998] and along magnetic field lines linking the plasma sheet boundary layer to the auroral zone [*Cattell et al.,* 1998; 1999]. After establishing that the steady state and transient parallel electric fields existed, there remained the question as to how that power was transferred from the tail to the auroral acceleration region. The discovery of impulsive solitary wave structures was made jointly by FAST and by Polar/PWI measurements [*Franz et al.,* 1998]. The breakthrough came with the observations that polarized electric field variations associated with strong magnetic field fluctuations were found within the outer boundary of the plasmasheet at 4-6 RE near local midnight [*Ober et al.,* 2001; *Wygant et al.,* 2002]. The associated Poynting flux was directed along the average magnetic field direction towards the ionosphere and was mapped to intense auroral structures (~20-30 ergs/cm^{2}s). The energy flux in the Alfvenic structures, when mapped to ionospheric altitudes, provides sufficient power (~100 ergs/cm^{2}s) to drive all auroral processes, including acceleration of upward ion beams, electron precipitation, AKR, and Joule heating of the ionosphere [*Wygant et al.,* 2000]. Thus, for the first time, all of the contributing energy carriers could be identified [*Keiling et al.,* 2003].

Polar's original mission objectives:

"To measure the mass, momentum and energy flows through geospace and to understand their time variability;

To obtain detailed knowledge of plasma physical processes important in controlling the behavior of the major components of the geospace system;

To determine the importance of changes in energy input to the Earth's atmosphere caused by geospace processes."

We continue to identify previously unpublished auroral phenomena and to identify production mechanisms for others that had been unexplained. *Liou et al.* [2002b] recently reported a new feature named midday subauroral patches (MSPs). MSPs are sudden 5-6 min. brightenings of patchy aurora equatorward of the main auroral oval. They are concurrent with storm sudden commencements in response to shock compressions of the magnetosphere. A partial list of others includes the tracing for the first time of the 1500 UT hot-spot of auroral precipitation to the plasma sheet [*Liou et al.,* 1999b]. A "midnight void" in the nightside auroral precipitation region implied that a region of the magnetotail is inhibited from producing auroral precipitation while neighboring tail regions are quite active [*Chua et al.,* 2001]. *Anderson et al.* [2000] reported PIXIE X-ray observations of impulsive events, termed convection-driven enhancements, in the morning sector during geomagnetic storms. A new type of auroral behavior, in which a brightening occurs first near the cusp, then propagates through the dawn and dusk flanks to the nightside within 10 minutes has been shown to be the response of the magnetosphere to a large solar wind pressure discontinuity [*Spann et al.,* 1998; *Zhou et al.,* 1999*; Tsurutani,* 2000; *Sigwarth and Frank*, 2003]. And the mystery surrounding production of theta auroras was resolved [*Chang et al.,* 1998] as a response to antiparallel merging at the magnetopause. PIXIE made the first observations of the uniform, intense X-ray emissions expected from energetic solar wind "strahl" electrons streaming directly from the Sun's corona into a sunlit Polar cap [*Anderson et al,* 2000].

And finally, with our now extensive imaging database, much has been accomplished with regard to morphological characterizations (**Figure 7** is one of many examples). Polar has quantified the effects of solar UV on the aurora, with the surprising result that intense aurora are suppresssed in sunlight [*Liou et al.,* 1997, 2001a; *Shue et al.,* 2001; *Meng et al.*, 2001]. In particular, there are fewer aurora under sunlit conditions when F10.7 is higher which implies a solar cycle effect different from that commonly assumed. *Newell et al.* [2001a] determined the relationship between auroral power, polar cap size, and magnetotail stretching. The polar cap is largest at equinox, and smallest at solstice, with a combined UT and seasonal variability which is most consistent with solar illumination of the auroral ovals. [*Newell et al.*, 2001b; *Newell et al.,* 2002b] better quantified the average auroral behavior at substorm onset and showed that the aurora spends most of its time in slow decline, with the power measured from consecutive Polar UVI images typically showing a drop. Large magnitude changes are always positive, confirming there is no negative counterpart to substorm onset (no inverse substorms. Polar/UVI observations, representative of electron fluxes below 10 keV, nominally account for 80-100% of the total particle energy deposition during substorms. However, Polar/PIXIE observations show that the higher energy portions of the spectrum have greater intensity at substorm onset, are azimuthally confined during the expansive phase, and contribute significantly to Hall conductivity. This indicates that Hall conductivities derived only from UV and/or visible imaging data are routinely underestimated in models.

The Role of Magnetic Reconnection

Most recently, *Scudder et al.* [2002] provided the first documented penetration by a spacecraft of the separator of collisionless magnetic reconnection within the non-ideal MHD layers where it occurs (**Figure 13**). On April, 1, 2001 a subsolar magnetopause crossing associated with antiparallel magnetic fields provided a textbook description of the ion diffusion region. The separatrix on the magnetospheric side was shown as the boundary between turbulent and quiet electric fields containing a minimum in the plasma density, a parallel electric field and a magnetic field that reached its asymptotic value [*Mozer et al.,* 2002]. Using Polar and Cluster electric and magnetic field measurements, *Maynard et al.* [2002] established wave Poynting flux as an additional necessary, but not sufficient, discriminator for merging at the dayside magnetopause.

Polar provided the first observational evidence of northward-IMF anti-parallel reconnection [*Dempsey et al.,* 1998]. The existence of low-speed, D-shaped ion distributions mixed with cold plasmaspheric ions accelerated upon reflection from the magnetopause have been taken as evidence that low-shear, or component, merging can occur equatorward of the cusp as easily as northward-IMF anti-parallel reconnection poleward of the cusp [*Russell et al.,* 1998, *Fuselier et al.,* 1999; *Chandler et al.,* 1999]. The rate of reconnection was determined to continuously vary by ~20 percent [*Lockwood et al.,* 1998 and *Fuselier et al.,* 1999] and found to correlate with inward and outward motion (erosion and expansion) of the magnetopause [*Dempsey et al.,* 1998]. Another site experiencing significant reconnection, due to open field line creation by dayside merging, is along the high-latitude flank of the magnetopause. This magnetospheric "sash," first identified through MHD simulation [*White et al.*, 1998], is a band of low magnetic field associated with the turbulent boundary layer [*Maynard et al.,* 2001b].

Trattner et al. [1999, 2002a, 2002b] have shown that during periods of steady IMF, reconnection is steady and occurs over long X lines as suggested by Luhman and Crooker. At other times *Trattner et al.* [2002a] demonstrated significant, quantifiable, intervals of pulsed plasma entry as predicted by Lockwood and his colleagues. *Fuselier et al.* [1999, 2000a, 2000b, 2001, and 2002], *Avanov et al.* [2001], and *Topliss et al.* [2000] used particle observations to quantify reconnection stability in space during steady IMF. A survey of 13 events observed by Polar, Cluster and SuperDARN places merging at high latitudes whenever the IMF clock angle is less than ~150° [*Maynard et al.,* 2002]. While the inferred high-latitude merging sites favored antiparallel merging, this result did not specifically exclude the possible existence of guide fields.

The Nature of the Substorm Onset Region

In the past few years, substorm research has focused on two regions as candidates for the initial substorm instability: 1) the Near Earth Neutral Line (NENL) region at 20 to 30 R_E at the divide between earthward and tailward plasma flows and 2) the ring current at distances of 5 to 10 R_E which has the highest plasma and magnetic energy densities and also their steepest spatial gradients [*Frank and Sigwarth*, 2000a,b; *Frank et al.,* 2000].

There have been several studies attempting to link the injection of plasmas during the expansive phase of substorms with auroral dynamic signatures and the simultaneous dynamics observed in plasmas and magnetic fields in the plasma sheet near the magnetic equator. Earthward ion flow bursts of 200 to 400 km/s have been linked with the leading edge of the westward or eastward traveling surge during the expansive phase of the substorm [*Frank et al., 2002*]. Using more than 140 traversals of the northern plasma sheet boundary layer, *Lennartson,* [2001] showed that flows of keV-energy ions were chiefly temporal, rather than latitudinal as usually assumed, and having a duration as short as two minutes. This implies that the flows are actually bursts and cast doubts on the association between these flows and a tail neutral line.

Using high-resolution Polar images for auroral substorms when Geotail was in the nighttime sector of the magnetotail, *Frank et al*., [2000c; 2001a,b], were able to show that the merging of magnetic field lines at substorm onset occured in the plasmas with high-energy densities in the ring current but within a very restricted range of local time, several tens of minutes or less. *Frank and Sigwarth* [2000a; 2000b] determined that the auroral substorm onset occurred in the most equatorward auroral arc and that the magnetic field threading the auroral substorm onset region mapped to radial distances of 5 to 10 R_E in the magnetotail. *Liou et al*. [1999a, 2000] showed that the brightening of an equatorward auroral arc is the most reliable indicator of the onset of a magnetospheric substorm. *Lui et al*. [1998] identified 102 auroral onsets when Geotail was in the magnetotail. The onset phenomena were spatially very localized with scales of the order of 1 R_E. It has thus been proposed that an earthward directed flow from a downstream near-Earth neutral line penetrates to radial distances of 5 to 10 R_E generating field-aligned currents that cause the auroral brightening. *Liou et al*. [2002a], using geosynchronous magnetometer data and Polar/UVI auroral bulge observations directly confirmed the long hypothesized relationship between the region of dipolarization in the magnetotail and the substorm auroral bulge. *Erickson et al*. [2000] found that the energy flow was outward from an onset region at the inner edge of the plasma sheet.

Role of the Ionosphere in Magnetospheric Dynamics

One of the primary goals of Polar was to discriminate between solar wind and terrestrial sources of plasmas and understand their interactions within the system. The discovery of a significant, persistent flux of polar wind escaping to the lobes of the magnetosphere showed that the ion outflows play a more significant role than predicted [*Moore et al.,* 1997, 1999; *Lennartsson et al.,* 1998, 1999; *Su et al.,* 1998]. Polar observations make it clear that significant ion heating occurs as flux tubes flow through heating regions of the auroral zone [*Collin et al.,* 1998; *Krauklis et al.,* 1999]. At low energies, centrifugal acceleration acts as a primary energization mechanism [*Cladis et al.,* 2000]. In the inner tail current sheet, O^+ is preferentially accelerated over H^+ by increasing Bz during substorms [*Nose et al.,* 2000]. In a similar open-closed magnetic field boundary region, *Ober et al*. [2001] observed direct perpendicular acceleration of O^+ by rapidly changing electric fields. These types of non-thermal effects have rarely been incorporated into models of terrestrial plasma outflow; however, now that Polar has stressed the underlying importance of electric field structures with respect to wave-particle interactions, this area of modeling is being vigorously pursued.

Polar advanced understanding of the temporal evolution of ionospheric convection patterns in several areas. *Maynard et al*. [1998a,b] resolved a long-standing controversy and established how two-cell convection patterns evolve to four-cell patterns as the IMF clock angle decreases to near zero. The response to IMF changes is delayed by an average of eight minutes from the time an IMF change reaches the magnetopause, but occurs to some degree across the whole polar cap at once [*Ridley et al*., 1997,1998, *Ruohoniemi and Greenwald*, 1998]. MHD simulations have largely verified this work [*Maynard et al.,* 2001a].

Comparisons of Polar/UVI and TIDE observations along with data from FAST provided support for a cleft ion source for polar cap O^+ ions, by demonstrating that ion upflows are associated with auroral forms while downflows are seen in non-auroral regions, e.g. the polar cap. The flux of outflowing ions increased by over a factor of 100 as the UVI LBHL intensity increased from 0 to 4 kR. Also, a ~5-10 min delay was observed between auroral intensification and detection of O^+ at 3000 km.

The region dominated by the terrestrial outflows regularly extends well beyond the plasmasphere and, with sufficient solar wind influence, can dominate all but the far boundary layers and distant magnetotail [*Moore et al.,* 2000]. The first global simulation work to include observed ionospheric outflows [*Winglee*, 1998] reached the conclusion that the geopause expands to fill the near-Earth magnetosphere and extends to great distances down tail. A striking new result is the discovery that the geopause is often present just inside the magnetopause. That is, relatively cold but often anisotropic plasmas are routinely present just inside the magnetopause, and not only when the magnetopause is compressed [*Su et al.,* 2001; *Chandler et al.,* 2003]. These populations are often so cold that they can only be observed above spacecraft potential because of the 20-40 km/s amplitude MHD waves present most of the time at the magnetopause. The confirmation by observation of substantial densities of cold plasma at the magnetopause, means that ionospheric plasma permeates the entire magnetosphere and participates in all magnetospheric processes, even at its outermost boundaries. Assessment of impacts on reconnection and other boundary layer processes are only just beginning at this time.

Radiation Belts and Connections with Solar Variability

The results of *Green* [2002] have shown the strongest evidence to date that local electron acceleration takes place in the inner magnetosphere: evolving storm-time phase-space-density peaks are inconsistent with radial transport alone. This study showcased the kind of science that can only be done on a robust platform like Polar. [*Reeves et al.*, 2003] investigated the relativistic electron response to 276 moderate and intense geomagnetic storms. Surprisingly, only about half of all storms increased the fluxes of relativistic electrons, one quarter decreased the fluxes, and one quarter produced little or no change. Pre-storm and post-storm fluxes were highly uncorrelated suggesting that storms do not simply "pump up" the radiation belts. The conclusions were independent of the strength of the storm and L-shell. In contrast, higher solar wind velocities increased the probability of a large flux increase. The analysis suggests that the effect of geomagnetic storms on radiation belt fluxes is a delicate and complicated balance between the effects of particle acceleration and loss.

Magnetic conjunctions between Polar and SAMPEX demonstrated a close relationship between MeV microburst precipitation and VLF chorus waves and showed how VLF chorus plays a role in both the acceleration and loss of energetic electrons [*Lorentzen et al.,* 2001]. This study enables the use of MeV microbursts as a proxy for VLF chorus, which is helpful since long-term observations of chorus with high time and L-shell resolution are difficult. Polar/PWI detected VLF chorus emissions near the dawn meridian in rapid response (<60s) to magnetospheric pressure pulse events [*LeDocq et al.,* 1998, *Lauben et al.,* 1998]. VLF Chorus are the most intense, naturally occurring discrete waves, they occur regularly within the inner and outer radiation belts and appear before an injection process can take place. The emission propagates without exception away from the geomagnetic equator, the absence of a reflected component within these closed field lines regions indicates the chorus is absorbed before reflection thereby determining the lifetime of radiation belt particles and producing enhanced precipitation [*LeDocq et al.,* 1998]. The important role of whistler waves in the pitch angle scattering of plasmaspheric electrons has been directly confirmed using Polar/PWI wave and HYDRA particle data [*Bell et al.,* 2002].

Global Significance of the Cusp Energetic Particles

Extremely large diamagnetic cavities with a size as large as 6 R_E have been observed by Polar in the dayside high-altitude cusp regions. These cavities are associated with strong magnetic field turbulence and appear there day after day. Associated with these cavities are charged particles with energies from 20 keV up to 10 MeV that can have significant impact on the geospace environment when they are transported away from the cusp. Charged particles starting in the cusp have almost complete access to the equatorial plasma sheet and outer magnetosphere [*Fritz and Chen,* 1999; *Fritz et al.,* 2000]. The cusp energetic ions may drift into the nightside plasma sheet along closed field lines, populate the dayside magnetopause boundary layer along closed/open field lines, and escape into the upstream and downstream regions along open field lines [*Chen and Fritz,* 2002].

From the Sun to the Earth: Studies of the Great Storms

An important technical accomplishment of ISTP was the systematic tracking of transient events from their birth on the Sun to their effectiveness in producing magnetic storms, accelerating magnetospheric plasmas, and depositing energy into the atmosphere. The power of the combined SEC spacecraft fleet as it evolves is demonstrated as each mission adds new information toward understanding the overall system dynamics with each new storm event. For example, Polar observations during the April, 2002 event showed large depletions in the dayside low-altitude O/N_2 ratio correlated with increased geomagnetic activity and auroral brightenings (**Figure 23**). The observed changes are due to the energy of auroral precipitation and the associated Joule heating of the upper atmosphere which occurred ~6-12 hours prior to the neutral composition change.

With the May and September, 1998 magnetic cloud encounters, Polar investigators were able to separate the response of the magnetosphere to intense solar wind pressure increases as compared to extremes in the IMF direction. The Polar team found that rapid shock-like compressions shrink the magnetosphere in size, increasing the overall magnetic field strength and rapidly moving plasma downstream along the affected field lines [*Russell et al.*, 1998]. Increased plasma pressure down the throat of the cusp increases its width in local time and latitude [*Zhou et al.,* 2000]. This event also produced an immediate, intense ionospheric mass ejection with the mass flux from the Earth to northern lobe altitudes increasing by more than two orders of magnitude [*Moore et al.,* 1999]. This, combined with observations from Dynamics Explorer, indicate that fluctuations in solar wind pressure control the outflow of heavy ions from the ionosphere while the IMF more directly controls the subsequent dispersal of that flow across polar cap latitudes by controlling transport processes. Surprisingly, field aligned and region 1 currents connecting the ionosphere to the magnetopause have little reaction to pressure pulse passages, but are strongly enhanced during southward orientations of IMF [*Le et al.,* 1998]. This finding emphasizes the importance of reconnection as a driver for certain internal dynamics over the contribution due to viscous drag.

These types of analysis efforts applied to the great storms expected during solar cycle decline will further define the specific elements of geospace dynamics responsive to one type of solar input or another. In this manner, event by event, Polar, along with the other SEC missions, will build a catalogue of the magnetosphere's response to a large variety of solar input conditions.

3. Technical and Budget

3.1. Status of the Space Assets

Health of the Spacecraft

The Polar satellite, launched on February 24,1996, is in a highly elliptical orbit with a period of about 18 hours. The inclination is 82.4°, apogee is at 9.5 R_E , perigee is at 1.5 R_E geocentric, and the precession rate of the line of apside is 19°per year. Over the next few years, the Polar apogee will precess from near the equator well into southern latitudes. It will pass through midnight local times at southern hemisphere mid-latitudes in the fall of each year and noontime mid-and cusp-southern hemisphere latitudes each spring (**Figures 1 and 2**).

As the orbit evolves, so do the opportunities to acquire data appropriate for new science questions. The traversals of the radiation belts and the heart of the ring current will continuously improve as apogee moves through southern mid-latitudes. The well-instrumented spacecraft will again scan the crucial L=5 to 9 R_E nightside transition region, where the field changes from dipolar to tail-like and plasma pressure gradients are largest. The previous scan of this region occurred during solar maximum, whereas the upcoming scan will occur during the period of high speed streams from the Sun. Polar fulfills part of the role of the original "Equator" spacecraft envisaged for the "OPEN" program. Polar will continue to skim the dayside magnetopause for at least another year and will obtain excellent passes through the southern dayside cusp to complement the northern cusp work earlier in the mission. With the local time phasing of the Polar and Cluster orbits continuing, and with Cluster apogee near the equator, simultaneous cusp and magnetopause crossings will continue to occur.

The Spacecraft subsystems are operating nominally. All three batteries are very healthy, and have successfully serviced the spacecraft through the longest eclipses of the mission. Both data tape recorders are healthy. The transponder that has been used since launch has lost some output power, but the margin remains adequate without switching to the backup transponder. A nuisance operational problem seems to be an infrequent unlocking of the imaging platform. The platform recovers lock autonomously after a short period of time.

Operations After Semiannual Pointing Maneuvers

Every six months the Polar spin axis, which is oriented in orbit normal attitude, is inverted by a spin axis precession maneuver (180° flip) to keep the imaging platform in shadow for thermal and power regulation. The on-board fuel supply, sized for the 3-year design life plus a two-year extended mission phase is nearing depletion. Careful fuel expenditures, including a six-month period of operations with the spin axis oriented normal to the solar

Table 2: Status of the instrumentation onboard Polar. Extensive spacecraft subsystem and instrument subsystem redundancies have well preserved an extremely robust set of measurement capabilities.

Instrument	Capability	Status
MFE: Magnetic Fields Experiment		
	DC - 10 Hz vector magnetic field	Normal
EFI: Electric Fields Experiment		
	3D Electric field, thermal electron density	Normal
PWI: Plasma Wave Investigation		
	Spectral and wave vector characterisitics: 0.1 Hz to 800 kHz	Infrequent operations
CAMMICE: Charge & Mass Magnetospheric Ion Composition Experiment		
MICS Sensor	Energetic ion composition: 6keV/q to 400keV per ion	not operational
HIT Sensor	Energetic ion composition: 100 keV/q to 60 MeV per ion	Normal
CEPPAD - Comprehensive Energetic Particle Pitch-Angle Distribution		
IES & IPS Sensors	25 to 400 keV ions and electrons	Normal
HIST Sensor	High energy ions and electrons, E_e>350 keV and E_p>3.25 MeV	Normal
SEPS Sensor	Loss Cone measurements	partial operations
Hydra - 3D Electron and Ion Hot Plasma Instrument		
DDEIS Sensors (2)		Normal
PPA Sensors (2)	3D electron and ion distributions (2-35 keV/q)	Normal
TIMAS - Toroidal Imaging Mass-Angle Spectrograph		
	3D mass separated ions: 15 eV – 25 keV/q	Normal
TIDE - Thermal Ion Dynamics Experiment		
	2D ions: 0 to 500 eV/q	Normal, no mass separation
UVI - Ultraviolet Imager		
	far ultraviolet auroral imager: 130.4, 135.6, 140-160, 160-175, 175-190 nm	Normal
PIXIE - Polar Ionospheric X-ray Imaging Experiment		
	X-ray auroral imager: 2 to 60 keV	no images; total counts <10keV
VIS - Visible Imaging Experiment		
	3 low-light cameras: 124-149, 308.5, 391.4, 557.7, 589.0, 630.0, 656.3, 732.0 nm	Normal

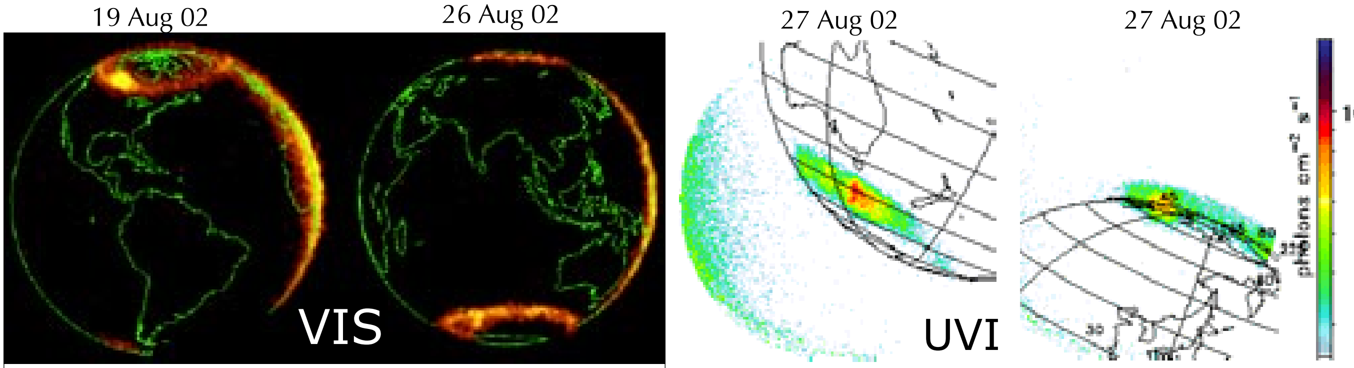

Figure 24: Auroral imaging will continue when the Polar spacecraft is re-oriented with its spin axis perpendicular to the ecliptic plane. as can be seen with these ecliptic-normal images taken during the Spring and Summer of 2002.

ecliptic, have stretched the fuel reserves to cover 7 years of flip maneuvers and preserved optimal auroral viewing through the southern hemisphere winter viewing season of this year. This fall, the spacecraft will be permanently placed in the ecliptic normal configuration.

The new orientation will have no adverse effect on our ability to address the science objectives proposed for the continuing mission as all instrumentation remains functional in this new orientation. The primary field and particle instruments are 3-dimensional and will continue to provide full spatial coverage. The despun platform imagers will provide significant Earth imaging coverage of about 4 to 6 hours during each 18-hour orbit. **Figure 24** shows examples of auroral imaging taken during the Spring, 2002 ecliptic-normal operations period. It is also worthwhile to browse the summary images on the Polar web site (*http://pwg.gsfc.nasa.gov*) for dates between March 21 and September 26 of 2002 to understand why the previous ecliptic normal operations period passed largely unnoticed by the science community.

The remaining amount of fuel is expected to be sufficient to maintain the ecliptic normal configuration into late 2005, at which time gradient drifts will turn the imaging platform towards the sun. Thermal effects are unknown but overheating of spacecraft subsystems is expected to end the mission by mid-year, 2006.

High Resolution Telemetry Operations

Polar has an alternate telemetry format, called "science mode 2", that approximately doubles the telemetry allocation for each of the fields and particles instruments at the expense of the imagers. This format was implemented and tested pre-flight as a contingency mode in the event of failure of Polar's despun platform. The mode is invoked with an onboard software command and was tested for a 12-day period in the Spring of 2003 when Polar was executing its long dayside magnetopause skimming orbits. It will be utilized in the ecliptic normal configuration, on a time-share basis with the imaging (**Figure 25**), primarily during those portions of the orbit when the imaging platform cannot achieve pointing lock on the Earth due to loss of horizon sensor coverage. The EFI, MFE and Hydra instruments will take advantage of the additional telemetry allocation by increasing the electric field sampling to 40Hz, the magnetic field sampling to 25Hz, and via Hydra, even higher sampling of the full magnetic field vector at 54Hz.

Health of the Instrumentation

Nine of Polar's 11 science experiments are operational and providing high quality science data products (see **Tables 2 and 3**). Two imagers continue to provide spectral imaging in ultraviolet and visible wavelengths; these

Figure 25: Number of hours per month during which Polar has opportunity for duty-cycling between nominal data collection, which includes imaging, and the new "Science mode 2" telemetry format in which cadences of the electric and magnetic field instruments are doubled in key regions (magnetopause boundary, auroral acceleration region and nightside plasmasheet). Conflicts between the two goals are also indicated. Through careful planning, we will take every advantage of our new high resolution operations mode while maintaining maximum imaging time.

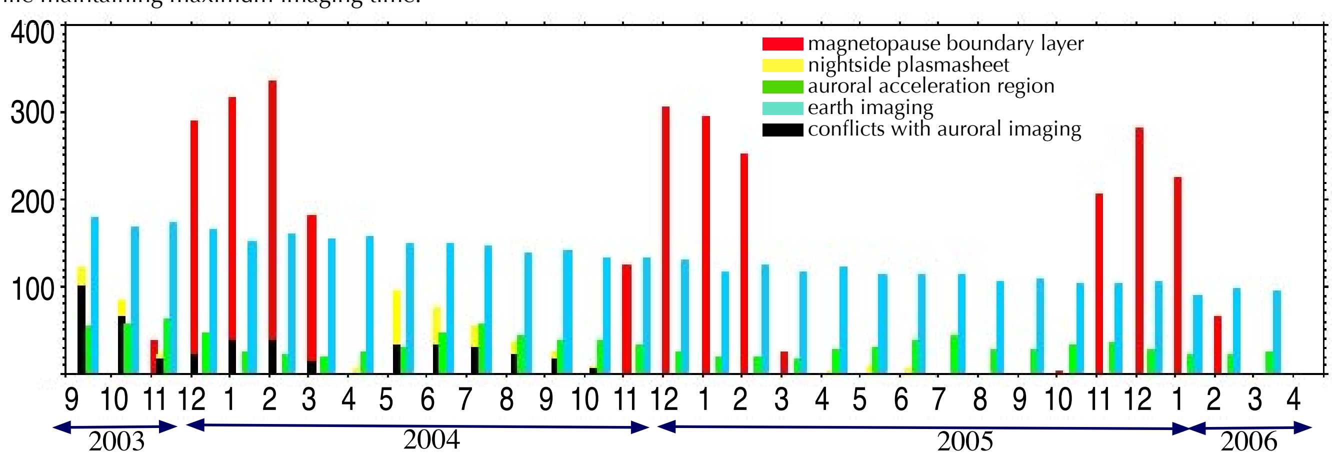

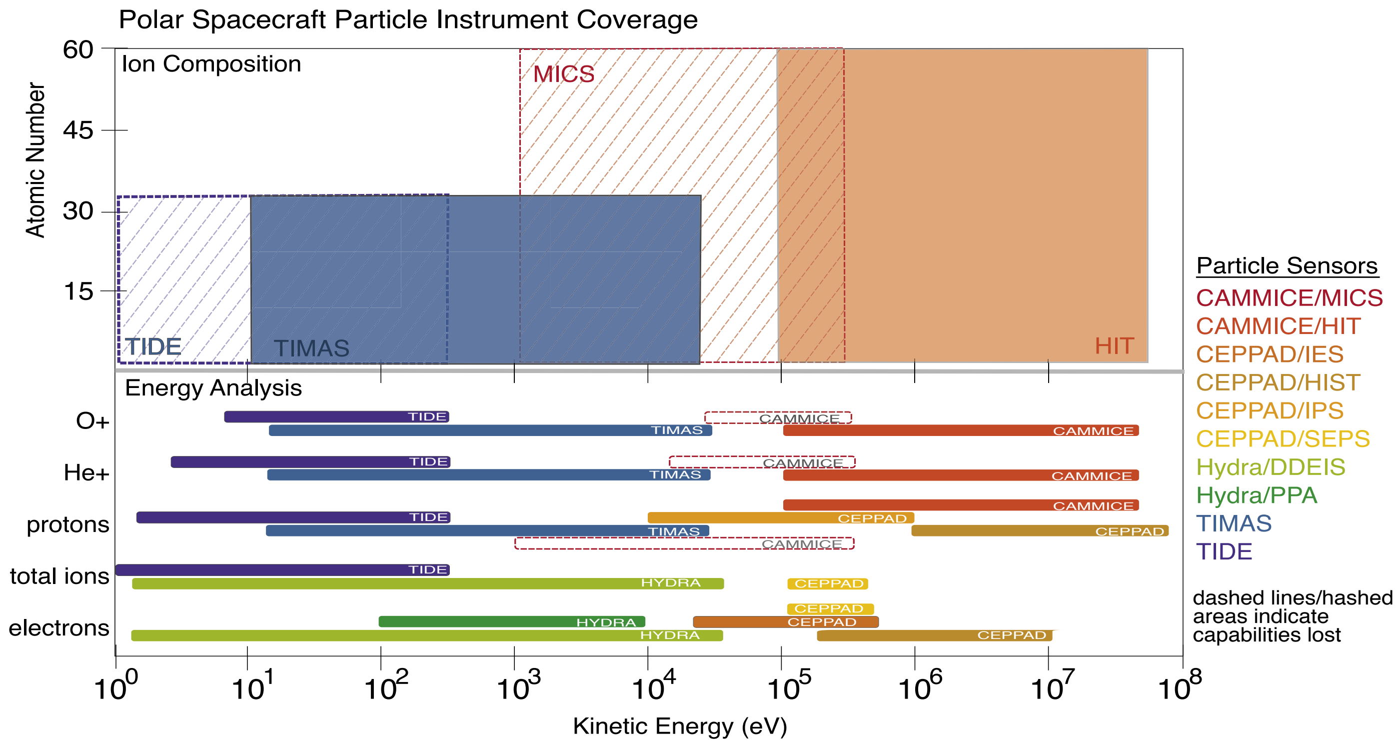

Figure 26: Energy and mass coverage for the Polar particle instrumentation suite. Being the last of the 1240 kg "gorillas", Polar's payload was designed for full angular and energy coverage with unprecedented sensitivity. There is excellent measurement overlap and sensor redundancy. Even with normal "wear and tear", Polar remains one of NASA's best instrumented assets in the magnetosphere.

are mounted on a despun platform to optimize viewing of the aurora and other targets. Polar carries five types of charged particle detectors to sample electron and ion populations and perform mass identification, from thermal to relativistic energies (**Figure 26**). Polar's electric and magnetic field instruments include dual high resolution fluxgate magnetometers, and the first successful triaxial electric field instrument with ultra-high time resolution burst-mode capability.

Two of our science investigations are only partially operational but continue to serve as valuable data resources. The PIXIE imager provided global X-ray wave-length images through November of 2002 and remains capable of providing total integrated X-ray flux measurements; the PWI Plasma Wave Instrument provided complete 0.1 Hz to 800 kHz wave vector characteristics for the first 18-months of the mission and periodically operates during thermally cold eclipse periods.

MFE Status: The Magnetic Field Experiment (MFE) continues to return precise high-resolution three-component measurements of magnetic fields. The instrument does not show any sign of aging or degradation. The magnetometer remains as a fully redundant system with duplicate processors, analog-digital converters, spacecraft interface electronics, power conversion circuits and two independent basic magnetometers. In the new Science Mode 2, the time resolution of MFE data will be enhanced to 24 Hz from the present high rate of approximately 8 Hz. MFE data also help to organize and interpret the data measured by other experiments on the Polar spacecraft, especially the energetic particles, plasmas, and electric fields experiments.

EFI Status: The three-axis Electric Field Experiment (EFI) on Polar continues to operate with no degradation or loss of function. It remains the ONLY operational three-axis electric field experiment in space. Being unique in this regard, it cannot suffer obsolescence until MMS is launched. The fixing of the Polar spin axis perpendicular to the ecliptic plane will have no impact on the EFI experiment. In fact, this configuration is an asset because the less-well-measured on-axis electric field component will point in a different direction than that covered in the first 6 years of operation; the new data will complement those previously acquired.

Hydra Status: The Hydra instrument continues to function well, with all sensors operational and all systems functioning, including the commercial burst mode memory. The inter-detector gains of the DDEIS are changing with time in an expected way with the large number of total counts these detectors have registered. The relative balancing on these detectors is accomplished by software on the ground. The absolute calibration is assisted by comparison with the ion estimates of density and intercomparison with solar wind monitors when we occasionally encounter the solar wind. The PPA sensor articulated for high resolution samples of electrons along the magnetic field direction continues to work well and is cross calibrated with the DDEIS.

TIMAS Status: The Toroidal Imaging Mass-Angle Spectrograph (TIMAS) instrument continues to return high quality three dimensionally resolved data on the energy, mass, pitch angle and composition of energetic

(15 eV < E/q < 25 keV) ions. The sensitivity in the energy range <700 eV, however was degraded by a discharge event in December, 1998. The angular bins sampled over the full three dimensional space were optimized for orbit normal operation. Data obtained during the recent season of ecliptic normal observations were nominal**.** The effective gain of the detector is showing a slow drift. While the total voltage available is fixed the effects of the gain degradation can be partially compensated by adjusting relative voltages in the detector string. The latest adjustments were made in February of 2003.

TIDE Status: The Thermal Ion Dynamics Experiment continues to return excellent quality data in an ionospheric energy range (0.3 to 450 eV) that has never before been explored from a high altitude orbit like that of Polar. It continues to provide observations of the polar wind, auroral ion outflows, and plasmaspheric material transported to the dayside magnetopause and to the nightside plasma sheet. Moreover, it provides high quality observations of low velocity magnetosheath boundary layer and cusp entry plasmas from the solar wind, allowing in one instrument the observation of the geopause region where the dominant plasma makes a transition from the former to the latter. TIDE lost its mass analysis capability in 1996 owing to loss of secondary electron yield from its carbon start foils, but has since that time served as a superb automatic-aperture electrostatic analyzer for ions. Its detector sensitivity has decayed very slowly, remaining within a factor of 3 of its original value over the seven years since launch, a negligible loss for an instrument with 1 cm^2 effective area for each of seven apertures. The plasma source neutralizer has been inoperative, apparently owing to thruster contaminaton of the cathode. Additional startup attempts are planned during the southern cap campaign, when greater benefit will be derived in very low density conditions.

CAMMICE Status: The CAMMICE [Charge and Mass Magnetospheric Ion Composition Experiment] consists of two sensor systems and two data processing units. The sensors are known as the MICS and the HIT. The HIT [Heavy Ion Telescope] is returning valuable data on the energetic total ion intensity. The MICS [Magnetospheric Ion Composition Spectrometer] was designed to use a combination of electrostatic deflection, post acceleration, time-of-flight, and a solid state detector energy measurement to determine the intensity of incident ions as a function of mass, charge-state, and energy. An interface circuit of the MICS sensor failed in 2002 ending its useful contribution to the Polar mission. By instrument command the telemetry allocated to the MICS has been reallocated to the HIT sensor.

CEPPAD Status: The CEPPAD investigation is comprised of four sensors – IPS (Imaging Proton Sensor), IES (Imaging electron Sensor), HIST (High Sensitivity Telescope), SEPS (Source/Loss Cone Energetic Particle Spectrometer) – and a DPU (Digital Processing Unit). All sensors and the DPU continue nominal operation. Over the course of the mission there have been a few Single Event Upsets in the DPU. These were expected and, in fact, the on-orbit rate is less than one third of pre-launch estimates. After an upset, power cycling restores normal operations.

The IES and HIST sensors are behaving as they did at launch; no change in performance has been observed. The IPS detectors, being openly exposed to the radiation environment, have suffered from radiation damage as expected. The damage increases the noise threshold on the silicon detectors; the DPU is commanded to raise the threshold when noise contaminates the lowest energy channel. The energy threshold has been increased from 18 keV at the time of launch to the order of 50 keV at present. The noise level is somewhat detector dependent. The rate of increase is expected to decrease with time. Although not performing as designed, the ultra high-resolution loss cone detector (SEPS) has provided useable data of high energy electrons and ions when the spacecraft has been immersed in the radiation belts. During the past couple of years the apogee location of Polar has not allowed observations of loss cone data of the radiation belts except briefly around perigee, but now as the apogee sweeps through southern latitudes the heart of the radiation belts again becomes visible.

VIS Status: The Visible Imaging System (VIS) continues to acquire images of the aurora, dayglow, and nightglow at an average rate of approximately 1 image per minute or 1400 images per day. To date, the VIS has acquired approximately 2.9 million visible and ultraviolet images. The VIS instrument continues to be healthy with no significant degradation in performance. A small decrease in sensitivity of ~10% has occurred over the life of the mission. This small decrease in sensitivity was expected prior to launch and is due to aging of the microchannel plates in the sensors as charge is drawn through them. The sensitivity has reached a plateau and only very slow sensitivity degradation is expected for the foreseeable future. All other voltages, currents, and temperatures are within expected limits. The VIS is fully capable of continuing in service for the life of the Polar spacecraft.

UVI Status: UVI is stable and fully capable of meeting its scientific mission. The backup detector, activated in December 1996 after the failure of the primary detector, shows no measurable sign of degradation. The only other failure was the microswitch used to position the filter wheel which occurred early in the mission but it has not affected operations since a backup switch was available. A light leak in the back of the housing was detected early in the mission but this is a problem only for short periods twice a year when the Sun is directly behind the UVI housing. The UVI science team is currently conducting searches of degradation by examining stars, dayglow, and searching for potential albedo features that would indicate red light leakage. In summary, UVI is healthy and obtaining high quality images.

PIXIE Status: The PIXIE instrument's capability to distribute collected X-Ray fluxes across an image plane failed in November 2002. Integrated measurements of total X-ray flux continue as before. PIXIE leaves as its legacy a 6-year database of time-tagged and energy-resolved

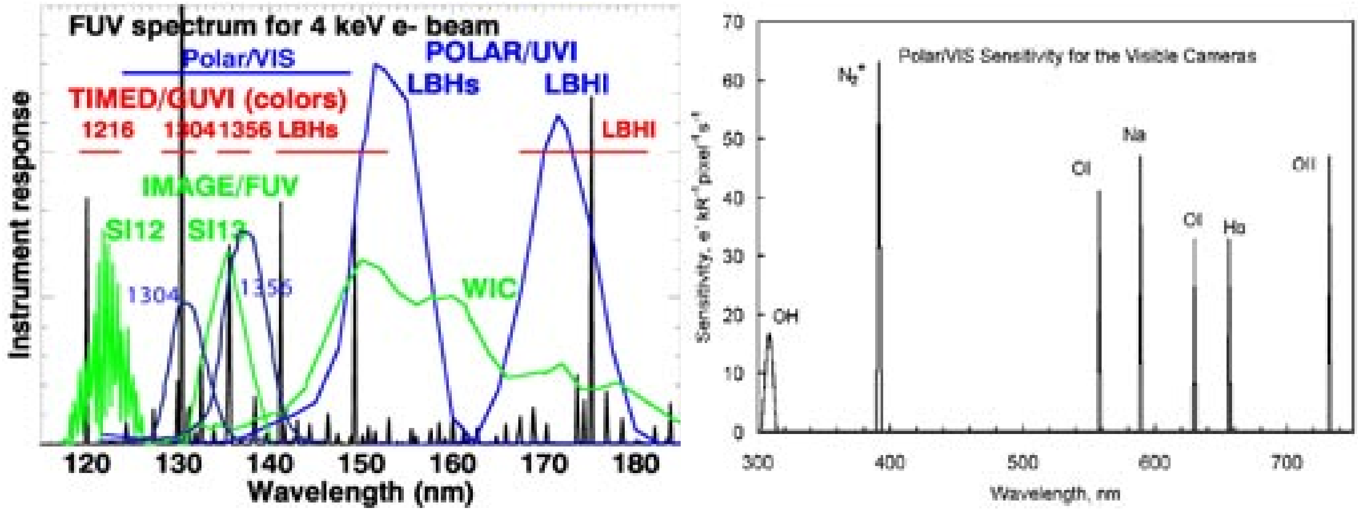

Figure 27: Responses of the SEC imagers on Polar, IMAGE, and TIMED. The UV detectors (left) make up a complimentary suite in that together they cover nearly the entire range of UV emissions between 120 and 180 nm. The narrow band filters of Polar/UVI cover both optically thin and optically thick emissions. Their ratios permit reveal the energetics of the precipitating electrons. In the visible wavelengths, which do not suffer the multiple scattering of the FUV emissions, Polar/VIS is currently the only asset. VIS's combination of high spatial resolution and high sensitivity determines the energetics of auroral arc structures and pinpoints the location of the substorm onset within the aurora.

X-ray counts (2-10 keV in 64 channels), localized in the instrument's image plane so as to permit projection back to their source points on the Earth's ionosphere. Images thus constructed, typically from exposure times ~3 min. These are publicly available in an archive at http://pixie.spasci.com. The database permits images to be constructed (even in retrospect) for chosen time intervals and energy bands within this range. PIXIE's rear chamber had failed in September 1998, leaving a 2-year database of similarly resolved X-ray counts (10-60 keV in 64 channels) from which images are likewise archived. The PIXIE data archive remains a resource for collaborative studies of past magnetospheric events. It is comprehensive enough to provide the basis for statistical analysis of geomagnetic conditions that correspond to patterns of auroral X-ray activity. The PIXIE data archive can thus facilitate the interpretation of future events that are otherwise similar (in some appropriate way) to past events.

PWI Status: The Polar Plasma Wave Instrument power supply began to exhibit an undervoltage condition on September 16, 1997. This was most likely caused by an "open" circuit at the power inductor in the power supply. This power supply is the only means of providing power to both of PWI's data processors. The low-rate processor requires less power to operate and is able to process Multichannel Analyzer (MCA) and Sweep Frequency Receiver (SFR) data during times when the power supply voltage is slightly elevated during long periods of extreme cold. These times occur twice per year during the Polar eclipse seasons. These data typically contain evidence of auroral kilometric radiation for use in substorm studies, as well as various other emissions that can be used in case studies (e.g., the SEPS/PWI study of electron precipitation coincident with electromagnetic wave bursts). The Electric Field Instrument continues to receive data from the PWI search coil antennas during its burst mode.

3.2. Status of the Combined Polar, Wind, Geotail Ground System

From ISTP to Streamlined PWG MOC

Upon completing its 2001 review of the operating Sun Earth Connection (SEC) missions, NASA's Office of Space Science (OSS) developed new guidelines for operating its fleet during the next four fiscal years (FY02 to FY05). Specifically, ISTP as a program was discontinued. The ground-based and theory portions of the GGS program were retired in FY02. The Wind mission was rephased and NASA participation in Geotail was reduced. Independent support of the ISTP Central Data Handling Facility (CDHF) was also discontinued. Funding was allocated to Polar in FY02 to develop a low cost approach to operations and data processing for Polar, Wind and Geotail.

These changes presented a special challenge because the Polar and Wind spacecraft were operated out of a combined facility. The ground data processing, command planning and command management for Polar, Wind and the Geotail spacecraft were performed in several shared facilities, some of which supported still other missions (SOHO, Cluster, IMP-8, and UARS). In addition, the FY02 and beyond MO&DA budgets for Wind and Geotail only contained some "incremental support" for a Polar project funded operations infrastructure.

Early in FY02 the Polar, Wind and Geotail projects began to define re-engineering and consolidation tasks, identified by feasibility studies, that had the most potential for substantial ground system cost savings. Several ISTP ground data processing services for the Polar, Wind and Geotail missions were immediately discontinued. The ISTP Key Parameter Integration and Testing (KITT) and Payload Assistance Center (PAC) were closed, and the services of the ISTP Science Planning and Operations Facility (SPOF) and Command Management Facility (CMF) were consolidated within the Polar/Wind Mission Operations Center (MOC) with an associated reduction in personnel. There were also immediate personnel reductions within the MOC and the ISTP CDHF. These changes reduced the combined MO&DA annual costs for GGS by approximately 3.5 million dollars.

The project identified further potential for savings by re-engineering the ISTP CDHF processes and re-engineering certain functions within the MOC. As of the end of March, 2003 the re-engineering effort has made very significant progress. Re-hosting and fully automating the data processing and distribution functions previously performed by the CDHF was successful and fully functional on schedule. The CDHF was closed in September of 2002 and resulted in an *additional* annual cost savings of approximately $1.2M over ISTP/GGS levels. The success for this project was largely based on the project's ability to perform the majority of the CDHF re-engineering work outside the confines of the Consolidated Space Operations Contract (CSOC).

The data processing environment for the Polar, Wind and Geotail spacecraft is now streamlined onto two host computers (a data server and a data processor) and fully automated to eliminate the need for data technicians (**Figure 28**). The environment is maintained, part time, by two civil servant programmers at a very low cost. Our "CDHF on a rack" serves all the functions provided by the ISTP system including the service of near-real-time data streams from Wind and Polar, processing of key parameters, and data distribution through ftp transfers or with CDs/DVDs.

A new effort to similarly streamline and automate the production of Level Zero data for Wind and Polar is underway. Level Zero data production is already efficient to the point that this task is not expected to yield significant short term cost savings. However, consolidation of this function within the "CDHF on a rack" will provide the Wind mission with a very compact and cost effective stand-alone data processing system after end-of-mission for Polar.

The greatest potential for further cost savings with the Polar, Wind and Geotail MOC lies with the implementation of unattended spacecraft contacts and data playbacks. Several studies have been completed favorably evaluating the feasibility and associated risk to the health and safety of the Polar and Wind spacecraft. Implementation remains in the development stages but schedules show a completion during the Summer of 2003. The greatest impediment for completion of the MOC re-engineering tasks lies with the requirement to perform the work within the confines of the Consolidated Space Operations Contract (CSOC). When the CSOC contract is discontinued in December of 2003, the Polar and Wind project offices are hopeful that the replacement contract mechanism will allow more freedom in the execution of re-engineering projects toward our goal of greater mission operation cost savings in the interest of preserving data analysis funds.

Figure 28: From ISTP CDHF to Polar, Wind and Geotail's "CDHF on a rack". Mission costs have been dramatically reduced over previous years by the implementation of new IT technologies, complete automation of data processing functions, and by eliminating or streamlining certain functions considered expendable, within acceptable risk levels, during our extended mission phase.

3.3. Data Availability

Polar Data as a SEC Data Resource

As part of the ISTP program, Polar's data policies were predicated on the concept of placing a constellation of satellites at key positions within the Sun-Earth connected system to obtain simultaneous, comprehensive and closely coordinated data. ISTP established an open data policy from the outset as defined by the "Data Policy for ISTP/NASA funded Missions and Instruments", approved on March 19, 1996 and revised on February 18, 1997. A copy of this data policy is available at http://pwg.gsfc.nasa.gov/rules.html.

The Polar data consists of an extensive set of high resolution particle and field measurements, covering the full energy and mass ranges of interest, and measured simultaneously with global, multi-spectral images of the aurora. Polar has one of the most complete sets of instrumentation ever flown as a package and, as such, represents a unique data source likely to be of value to the SEC science community for years to come. In particular, the Polar data set has been identified by the Living with a Star (LWS) project as a "data set required to fulfill LWS objectives". The estimated volume of mission data acquired (based on average bits per orbit, an 18 hour orbit, and Level-1 &2 data products, which are estimated at 20% of the Level-0 volume) to be archived at the NSSDC will be approximately 2.4 TB over the 10-year lifetime of the mission.

Polar End-to-End Data Flow

The Polar mission maintains a series of World Wide Web (WWW) pages which provide the latest information about all aspects of Polar, including the type and accessibility of Polar data. These pages are located at the following URL: *http://pwg.gsfc.nasa.gov/*.

Data are downlinked three to five times per day using the Deep Space Network (DSN) subnet and forwarded to the Mission Operations Center (MOC) located at GSFC. Once the data from an orbital segment have been delivered to the MOC, Level-0 and Level-1 science data processing are automatically initiated. The resulting products are made available on completion of the processing cycle to anyone via an anonymous ftp site maintained at GSFC. The ftp site is accessible from the Polar web site (URL noted above) or can be accessed directly at *ftp://pwgdata.gsfc.nasa.gov/pub/*. Access is fully open, there are no accounts, passwords, or registration procedures to complete before gaining access to the complete set of data products. The products are also immediately forwarded to the NSSDC for permanent archiving and open public distribution via CDAWeb.

In addition, all of the instrument teams have Remote Data Analysis Facilities (RDAFs) and maintain open access WWW servers at their institutions that are used in processing, analyzing, disseminating and correlating Polar data. Investigators with the appropriate data types routinely generate additional data products which are posted at their web sites.

Polar's Data Policy:

The Polar data are open to all scientists and the public.

There are no proprietary periods associated with any of the Polar data products.

All Polar data (including Level-0), associated documentation and generation software, are archived at the NSSDC.

Browse Data Products

The ability to quickly survey the vast array of data being generated by each instrument is essential to broader community use of the Polar data set. Level-1 data processing is performed at GSFC and, in select cases, at the instrument RDAFs. Level-1 products include images, spectrograms, and data files of varying resolution referred to as Key Parameter files (KP). All KP data sets are created as Common Data Format (CDF) files using the ISTP Guidelines (*Kessel et al.* [1993,1995]) for Key Parameter Data. The project office, and instrument teams processing level-1 data, provide the files directly to the NSSDC for distribution by CDAWeb. The site *http://pwg.gsfc.nasa.gov/data_products.shtml* provides an overview of the Level-1 data products that are currently available at CDAWeb and elsewhere.

Full Science Data Products

Several forms of calibrated higher level Polar data products are produced and made available for science analysis. For the most part, binary higher level data products are also in the ISTP/Common Data Format although the imaging teams provide single images and movies in the more common JPG and MPG formats. These products are routinely delivered to the NSSDC for long-term archiving and community-wide distribution. They are also available from the individual instrument team's web sites. The associated documentation and generation software will be delivered to the NSSDC at end-of-mission for long-term archiving. The site *http://pwg.gsfc.nasa.gov/data_products.shtml* provides an overview of the higher Level data products currently being archived.

Science Analysis Tools

Several of the Polar instrument teams have been at the forefront of efforts to provide device-independent data analysis tools. The most well-known and utilized of these is the PAnel Plot COmposer (PAPCO). PAPCO is a free, IDL-based, open source software package that allows the interactive processing and plotting of data from a variety of instrument sources on the same time base (http://leadbelly.lanl.gov/ccr/software/papco/papco.html). There are PAPCO modules for the eight Polar in-situ observation instruments. The calibrated data files in each case are available from the instrument web servers and have been archived to the NSSDC for distribution by CDAWeb.

Other Polar teams have exploited the power of the World Wide Web and its ability to provide an interface for data analysis that is also free of installation procedures. The best example of this capability was implemented for TIDE data analysis (see **Figure 29** and the site *http://tide.gsfc.nasa.gov/*). Access to a web browser is the only prerequisite for full and open access to the data. Given resources to do so, we plan to implement similar interfaces to the analysis software for other Polar data sets.

Plan for Enabling Increased Use

The Living with a Star project will enact fundamental changes in the way researchers access data from multiple-spacecraft missions. Based on the SEC emphasis of "virtual observatories", the database for any given LWS mission will be loosely linked with the data for other LWS missions via a series of metadata agents that interface with an LWS metadata broker.

The Polar, Wind and Geotail project offices have partnered with LWS to use the Polar, Wind and Geotail PWG data in prototyping efforts for an operational LWS ground data system. The Polar, Wind and Geotail data sets are housed together in a compact system easily accessible to the LWS project. The instrument teams already have metadata descriptions (via the ISTP CDF standards) for their data products which are well established, verified and mature. Our data processing personnel are poised to take advantage and adopt any methods and software useful toward positioning the Polar, Wind and Geotail data system as a fully functional data provider within the broader community Virtual Observatory efforts.

Detailed plans for the LWS prototype system are under study. We believe that beginning the LWS Program's Data System with fully functioning access to Polar, Wind and Geotail data will benefit both projects.

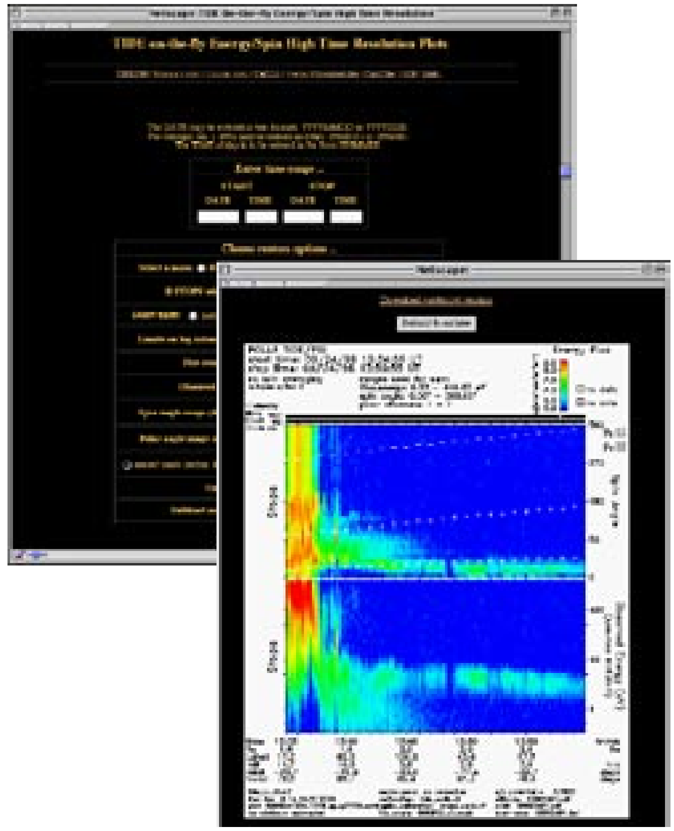

Figure 29: All Polar/TIDE software analysis tools are available through open access web interfaces. Custom spectrograms, calculation of the plasma moments (even over portions of the particle distribution function) may be executed through simple forms. PWI, MFE and PIXIE have also implemented interactive data analysis tools. All teams have browse data interfaces.

Table 3: Instrument-by-instrument availability of data products. Note that full science analysis products are available in every case. In the future, Polar will partner with the LWS project in prototyping a "Virtual Observatory" data system that will enable increased use of the Polar, Wind and Geotail data sets by the SEC science community.

Instrument	Browse Products/ Key Parameters	Open access to High Resolution Calibrated Data	Summary Plot Web Interfaces	Custom Plot Interfaces
MFE	via CDAWeb KP is high res product	via CDAWeb KP is high res product	on PI server, several resolutions	via PAPCO
EFI	via CDAWeb KP is high res product	via CDAWeb, & PI server KP is high res product	KP only	via PAPCO
PWI	via CDAWeb	via CDAWeb many high res products	many products at various resolutions	create many types of spectrograms via PAPCO, or web interface
CAMMICE	via CDAWeb	via CDAWeb PAPCO compatible	many types of summary plots	via PAPCO
CEPPAD	via CDAWeb	via CDAWeb PAPCO compatible	many types of summary plots	via PAPCO
Hydra	via CDAWeb	via CDAWeb PAPCO compatible	DDEIS spectrograms	create many types of spectrograms, moments and distribution plots via PAPCO
TIMAS	via CDAWeb	via CDAWeb PAPCO compatible	Summary spectrograms on PI server, high resolution spectrograms via CDAWeb	via PAPCO
TIDE	via CDAWeb	via CDAWeb PAPCO compatible	Several types of summary spectrograms, high resolution spectrograms via CDAWeb	create many types of spectrograms, moments and distribution plots via web or PAPCO
UVI	via CDAWeb	via CDAWeb	full sets of images on line	
PIXIE	via CDAWeb	via CDAWeb	full sets of images and movies on line	custom auroral movies via web
VIS	via CDAWeb	via CDAWeb	full sets of images on line	

3.4. Polar Budget

The Polar funding history and future funding guidelines are consistent with the Office of Space Science published guidance on the conditions for mission extensions. We request a modest increase over planning guidelines during the mission extension to maintain a level amount of support to our bare-bones mission and science operations. A mission extension budget including this increase would still remain well within the mission extension paradigm.

In evaluating the Polar budget it should be noted that although mission operations are conducted in a shared facility with the Wind spacecraft, and the data processing is performed with equipment and personnel shared with the Wind and Geotail spacecraft, joint cost accounting has not been applied. Rather, the Polar mission bears the entire infrastructure cost after receiving a contribution from the Wind and Geotail missions equal to the estimated "incremental" cost of supporting the Wind operations, and the incremental cost of supporting Wind and Geotail data processing. For FY03, the Wind and Geotail contribution is 18% of the combined Polar, Wind and Geotail "Mission Services".

Tables in Appendix C list the Polar guideline and optimal/requested funding levels following the categories and instructions applicable to this Senior Review. The FY03-FY07 "in-guidelines" budget supports a bare-bones mission operation and science operations mission. Compared to the prime mission phase, a significantly higher risk and lower data collection efficiency have been implemented and fewer services are provided to science investigators (section 3.2). There is minimal support for the science analysis required to understand and maintain optimal performance of the instrumentation.

FY03-FY07 In Guidelines Scenario

Table I provides the In-Guidelines scenario, which includes Flight Dynamics support, Flight Operations Team (FOT) support, Level Zero (LZ) processing, and CSOC Customer Service Support. Flight Dynamics is supported by one FTE through the life of the mission. FOT and LZ support includes 13.5 FTEs, the result of staff reductions in FY03. The staff reductions (17.5 to 13.5 FTEs) were enabled by operations concept changes (re-allocation of staff duties, cross-training of personnel, utilization of stored commands for tape recorder dumps, more efficient use of stored command tables for instrument commanding, etc) and the implementation of automation. These changes will allow for half of the mission operations to be performed unattended. This staffing level is the minimum required to sustain the mission, ensuring the health and safety of the mission assets. Further reductions in science data capture requirements will not impact the staffing level.

FY03 – FY07 Requested/Optimal Scenario

Table II shows the Requested/Optimal scenario. Costs for FY04 and beyond are based on 3% inflation per year over the current year's PSLA Estimate at Completion plus projected FY04 SODA costs. FY04 also includes a one-time $206k request for contract transition from CSOC to MOMS and four weeks carryover to cover the new contract into the next fiscal year FY05. The number of FTEs for Flight Dynamics and FOT support remains unchanged from the In-Guidelines scenario. This scenario ensures the health and safety of mission assets in an environment of increased costs (due to the change in contract) and inflation.

FY03 – FY07 Requested/Optimal Scenario (in-kind)

Table III provides the in-kind NASA costs. "Data Services" encompasses the cost of Deep Space Network (DSN) support, mission critical routed data lines, and dedicated voice communications. DSN support costs are based on the User Loading Profile, which is provided by the project to the Deep Space Mission System's (DSMS) Resource Allocation Planning Group. The costs were provided by JPL and are based on the most recent DSN pricing. "Mission Services" includes hardware maintenance and sustaining engineering services. The elevated "Mission Services" costs for FY04 include 5% for CSOC to MOMS contract transition and four weeks carryover. The "Other Mission Operations" cost is comprised of the Multiple Program Support (MPS) assessment. "Science Data Analysis" includes full-cost civil servant salaries associated with the TIDE and EFI instrument teams and for maintenance of the combined Polar, Wind and Geotail ground data processing system.

FY03 – FY07 Instrument team breakdown

Level support for the science teams represents an effective funding decrease per year equal to the cost of inflation and personnel performance increases. Funding to the teams is intended to cover the cost of the facilities, materials, services and personnel required to operate the instruments. This includes but is not limited to: commanding the flight hardware and monitoring instrument health; tuning instrument response and processing procedures to accommodate the changing orbit or spacecraft operations; routine processing of data products; maintenance of RDAF and web servers; and, most important, the supply of processed science data, graphics, analyses and interpretation in support of science studies. Funding differences between teams reflect special challenges or advantages in their individual environments. For example, teams with some civil servant support require less direct MO&DA funding while teams challenged with additional commanding or higher overhead rates require slightly more. Sensors no longer collecting science data must still be commanded in support of other instrumentation or to maintain thermal balance (i.e., PWI search coil data supplied through EFI). With this Requested/Optimal scenario, we have requested a small amount of additional support for the dissemination and analysis of the new high resolution and burst mode data. Additional science investigators supported to exploit this dataset would have immediate pay-off in the area of understanding the meso- and microscale processes operating in boundary layers.

4. Education and Outreach

Introduction

Building on the foundation of the ISTP E/PO program, Polar has continued to commit significant time, energy, and funding into a wide-ranging program. The goal of our program is to excite and inspire the next generation of space explorers and enhance science understanding by creating personal learning experiences for students, educators, and the public.

Linkage to national education standards increases the value of a product to classroom teachers. The Polar mission provides exciting real-world examples for curriculums in physical science, Earth and space science, and the history and nature of science, as well as technology, math, and geography. All of our products developed since 2002 directly address education standards.

We maximize our impact through partnerships, often with the SOHO project, the SEC Education Forum (SECEF), and now with the "Living with a Star" (LWS) program. These partnerships help us share resources such as education expertise and funding, create better products and programs based on previous evaluations, utilize proven successful distribution channels, evaluate our projects, and report our work through EDCATS.

Dr. Nicola Fox leads the Polar E/PO program. Ms. Kerri Beisser cultivates opportunities for new partnerships, and Ms. Beth Jacob leads the effort to produce E/PO products. Dr. R.A. Hoffman is responsible for scientific accuracy. All four are exceptionally experienced and committed to NASA E/PO. A number of our instrument teams pursue their own E/PO programs but also contribute concepts and material for Project activities.

Accomplishments

Polar scientists have been enthusiastic participants in a range of formal and informal education programs. We have been able to reach the Hispanic and African-American communities, females, Native Americans, professional societies for underserved and underrepresented populations, and rural and inner-city communities.

Shaping Education for the Future: Several Polar team members represent the SEC community in national and regional educational committees. The Polar E/PO Lead is a member of the AGU Space Physics and Aeronomy Education & Public Outreach committee (both formal and information education) and the NASA GSFC Visitor Center Advisory Group (informal education). Dr. Donald Gurnett spoke on space research to the Iowa Senate Education Committee last year.

Sun-Earth Day: The Sun-Earth Day program was developed by SECEF, with Polar as a co-leader, to bring together education communities around the world. Sun-Earth Day focuses on a different topic each year and includes classroom and museum events around the country leading up to live television and web broadcasts. SECEF assembles educator kits with teacher-tested activities, web and print resources connecting real science to national education standards. Polar provided the 2001 and 2002 (which had a Native American emphasis) programs with presentations at the Maryland Science Center (MSC), the Cedar Rapids Science Station in Iowa, and the *Celebrate the Equinox* teacher workshop in Washington, D.C. *Sun-Earth Day 2003: Live From the Aurora* included a series of live TV interactive experiences for students. Dr. Fox hosted the live show and Polar scientists answered student questions on air. Polar provided live auroral images via the website, which allowed students in southerly regions to view an aurora for themselves, and students in the north to compare them with auroras they actually saw. The Polar-developed products, *What Causes the Northern Lights?* flyer and the *Aurora* poster

Education and Outreach Implementation Approach

Use Polar real-world examples to develop high quality, standards-based activities and materials based on educational need.

Support educator workshops that best match our science.

Promote SEC science, not the Polar mission, to complement and enhance science curricula and inspire the public.

Expand our base of Información en Español enabling SEC science to reach a large audience often left out of science education materials.

Encourage and assist team scientists in participation and initiation of E/PO activities.

Ensure that our products are evaluated, catalogued, and appropriately disseminated.

Optimize the use of our extended mission resources by channeling efforts into highly leveraged partnerships to reach a large audience, including the underserved.

(see E/PO Products), along with Polar auroral imagery, went into the 2003 educator kits.

Polar scientists also presented a high-school student workshop in Baltimore as part of the 2003 Maryland Pre-College Fair held in conjunction with the Black Engineer of the Year awards. Students learned to use real scientific data, observe the Sun, make predictions, conduct online collaborations and track solar storms. Dr. John Sigwarth also gave public lectures at the Cedar Rapids Science Station for *Sun-Earth Day 2003*.

Other Educator Workshops and Support: Over the last two years, the Polar team presented science content at many educator workshops. High profile events took place each year at the National Science Teachers Association, National Council of the Teachers of Mathematics, and Maryland State Teachers Association national meetings. Our scientists gave talks on space weather and aurora at seven SECEF teacher workshops, and at the annual Maryland State Teachers Association meetings. Dr. Hospodarsky spoke at a Korean teachers' workshop in 2001, and at a high school physics teachers' QuarkNet class in 2002. The TIDE team conducted two K-12 teacher workshops in 2002 at Vanderbilt University. Polar team members have made themselves available for long-term support by email and phone to teachers as well as former student interns.

Student Events: Providing students an opportunity to interact directly with a scientist is often the spark that leads to a career in space, and the Polar team reaches out to many. For example, Dr. Sigwarth and Dr. Hospodarsky regularly give on-site tours of their facilities to K-12 student groups and prospective graduate students. They, and other team members, also give classroom talks to elementary and middle school students about space physics and life as a space scientist. During the two-week Maryland Summer Center for Space Science Education camp for talented 6th and 7th graders run by the Maryland State Department of Education, Dr. Fox introduced students to the excitement of designing their own missions and the opportunities to study space weather. Several Polar scientists went into K-16 classrooms, giving talks on topics such as states of matter, space weather, and the magnetosphere.

Museums around the Globe: Polar has played a leading role in bringing the topics of space weather and the aurora to the informal education community. Our team members provided science content and auroral movies for the MSC *Raging Sun* planetarium show. Dr. Fox participated in three "Scientist in Residence" days at MSC's SpaceLink exhibit, answering questions from the public in person. She also hosted MSC's Live from the Sun planetarium show, narrating the live show with taped planetarium segments, and identifying interesting features on observatory Sun images in real time. The MSC's *Teachers' Thursdays* program brings local teachers together with scientists. Polar was well represented providing movies on the aurora and Sun-Earth connections. In 2001, a Polar *Teachers' Thursdays* presentation on Sun-Earth Connections was broadcast throughout the state by the Maryland Interactive Distance Learning Network. At the GSFC Visitor's Center, Dr. Fox gave several presentations for school groups and the general public in a 2-month long program in summer 2002 designed by the NASA Education Programs Office, Visitor Center staff, and GSFC E/PO mission representatives.

A University of Iowa exhibit kiosk with Polar auroral videos, images, and text traveled throughout Iowa from 1998 to 2002. Polar/PWI information and photos

were included in an exhibit at the Sanford Museum and Planetarium in Cherokee, IA. The Polar/VIS team also provided auroral images for a planetarium show at the Yamanashi Prefectural Science Center in Japan.

The *Space Weather Center* museum exhibit continues to travel. It has been at ten locations to date, including the Lawrence Hall of Science in Berkeley, CA, the Adler Planetarium in Chicago, Insights El Paso Science Museum, Wayne County Community College in Detroit, and Kitt Peak National Observatory, reaching several large underserved communities in the process. Polar acquired, built, maintained, and organized programs for the exhibit during its 2001 stay at the GSFC Visitor Center, and the team assisted in the generation of education programs to complement the exhibit at other locations. This year, it will be at the Arizona Challenger Learning Center.

E/PO Products:

Print products: All of our print products were developed with national education standards in mind, and all have been named exemplary NASA OSS E/PO products, having undergone comprehensive evaluation by scientists and educators. As such they are listed in the NASA Space Science Educator Resource Directory (SSERD). The popular 1998 *Storms from the Sun* poster explores the science of coronal mass ejections and space weather. Spanish-language translations of both the print and online versions of the poster, *Tormentas Solares*, were released in 1999. These are in wide use by teachers in U.S. Hispanic communities and South and Central America. The comparable *Aurora* poster, released in 2002, tells a more detailed story of the aurora with pictures, history, myths, resources, and a lesson plan that addresses science, math, and geography standards. A companion to the *Aurora* poster, the colorful tri-fold *What Causes the Northern Lights?* covers common questions and myths surrounding the aurora. A second flyer, *What Causes Storms from the Sun?*, is in development.

On the World Wide Web: The *Mission to Geospace* web site, also in the SSERD, continues as a portal for journalists, teachers, and space aficionados to find easy-to-read and engaging materials related to SEC science. The site averages 1000 accesses per day. It contains publicly accessible articles, news releases, and space weather imagery; the images and movies are by far the most popular section. The *Conexión Sol-Tierra* web site, based on *Mission to Geospace*, provides links to many Spanish language Sun-Earth connections resources, including *Tormentas Solares*. The Polar team also contributes to other well-visited sites. VIS, for example, provides real-time auroral images to the award-winning *Windows To The Universe* site, which serves over 4 million users per year and is used extensively in K-12 classrooms.

Polar in the Public Eye:

Movies: The Core, in theaters around the country this year, has Polar auroral images, which were also featured in the opening sequence of the IMAX *Solarmax* movie.

Press: The Polar team contributed to the development of the June 2000 press release on reconnection and the December 2000 Space Science Update on solar maximum. The October 2001 story on conjugate auroras prompted a press release and the development of a NASA GSFC web article.

Print: National Geographic consulted the Polar team and used Polar images for the "Auroras: Earth's Grand Show of Lights" article in its November 2001 edition. The team also worked closely with *Nature* on an aurora article and *Discover* magazine used a Polar image on its cover in 1998.

TV: Dr. Fox was interviewed for the BBC program *Blackout*, and VIS supplied auroral movie footage. VIS also provided science content for the Einstein Channel (European television) program, *Causes of the Aurora*.

Music: Composer Terry Riley developed *Sun Rings* for the Kronos Quartet based on sounds of space collected by Polar PI Dr. Donald Gurnett over the course of 30 years. The NASA Arts Program Office commissioned the composition. It premiered in Iowa City in October 2002, played in London, and continues to tour the U.S.

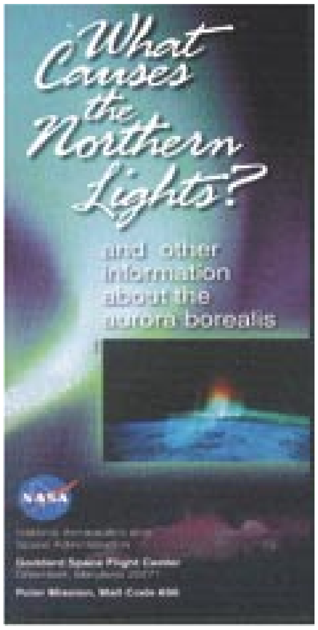

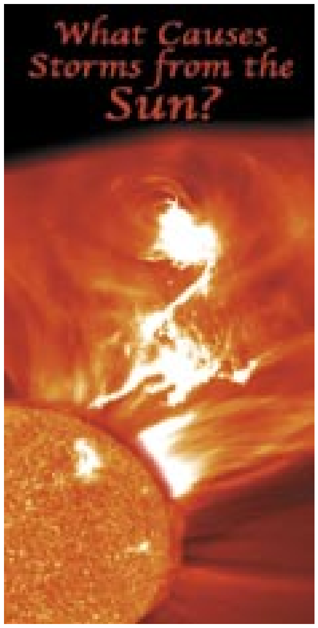

Dr. Gurnett gave pre-performance presentations at each of the Iowa presentations. AGU's Eos publication included an article about *Sun Rings* in February 2003. Polar team members also gave the opening presentation for *Dance of the Auroras*, a ballet themed on solar and magnetospheric science. Conducted by the Maida Withers Dance Construction Co. at Washington's Lisner Auditorium, the music included sounds derived from Polar/PWI data. The dancers performed in front of ever-changing pictures of science-inspired graphics, as well as auroral images from Polar VIS and PIXIE.

Community outreach: Polar scientists took advantage of every opportunity to share with their communities. Among others, these activities included Dr. Fox as a keynote SEC speaker at GSFC's 2001 Community Day. Dr. Hospodarsky spoke to the Burlington, Iowa Kiwanis and Dr. Robinson gave a tour of the University labs for the Iowa City Amateur Radio Club. At the 2002 Iowa State Fair, Dr. William Kurth spoke with WSUI *Iowa Talks* in a live radio broadcast and gave presentations at the University of Iowa exhibit booth. Polar hosted a display at *Fly Iowa 2001*, an aviation fair and Dr. Kurth presented Songs of the Aurora at one of the University of Iowa weekly "Family Adventures in Science" programs.

New E/PO Efforts

Polar expects to continue pursuing a vigorous and challenging E/PO program. Past activities have shown that we maintain our long-term partnerships and continuously search out new partnerships and opportunities to present exciting SEC science to the public. The team will continue to provide scientist time and E/PO materials for Sun-Earth Day, educator workshops, community and student events, and museums, and will take advantage of other appropriate opportunities as they arise.

Teacher Training: NASA's highly successful Solar System Ambassador program, serving all 50 states, has trained volunteer educators to organize and conduct public events that communicate exciting space science. Polar will provide the support for training one Ambassador each year.

Plans are in place to host a workshop for selected middle- and high-school educators. These educators will be responsible for training other educators in their own area, resulting in a long-term impact on teachers and students. Also, working with our partners, Polar will search for the appropriate role to take in NASA's new Explorer Schools program.

Información en Español: With the past successes of the *Tormentas Solares* poster and the *Conexión Sol-Tierra* web site, Polar has taken full advantage of opportunities to translate our E/PO materials into Spanish, reaching a large audience often lacking in good science education materials. Our new partnership with the LWS E/PO team is facilitating translation and printing of the *Aurora* poster, as well as the brochures on the northern lights, storms from the Sun, and "killer" electrons (see Print section below). Polar is making all of the Spanish E/PO materials available to the LWS K-14 educator summer workshops at the University of Puerto Rico.

Space Place: We will work with the Space Place program to either convert the information in our two posters, Storms from the Sun and Aurora, into the correct format for their library and small museum display series or create new activities, as appropriate for the audience. These displays remain on the website indefinitely and have the potential to reach an audience of 27 million, primarily in rural and inner-city locations. The Space Place will also distribute our materials to their subscribing museum and astronomy club network.

We will also pursue the possibility of converting our flyers into newspaper columns. Currently the Space Place column is published monthly in seven English language papers and several Spanish language papers in major U.S. cities.

Print: Our collaboration with the LWS E/PO office and SECEF allows us to continue development of additional brochures on topics covering the span of key topics in SEC science. Each will be aligned with national education standards, and they and will fill gaps in the developing NASA "Curriculum Quilt" whenever possible. We will develop the third in the series of tri-fold flyers, Killer Electrons and You, with the potential to be followed by three more brochures over the course of the next two years. Along with these new products, our Aurora poster and *What Causes the Northern Lights?* flyers will continue to be distributed by SECEF at major educator venues.

Appendices

A. References

Anderson, P. C., D. L. McKenzie, D. W. Datlowe, J. D. Hawley, S. M. Petrinec, M. Schulz, and D. E. Larson, Polar Cap X-rays and Electrons under Low Density Solar Wind Conditions: Coordinated PIXIE and DMSP Observations on 11 May 1999, Geophys. Res. Lett.., 27, 40214024, 2000.
Avanov, L. A., V.N. Smirnov, J.H. Waite Jr., S.A. Fuselier, O.L. Vaisberg,High-latitude magnetic reconnection in sub-Alfvnic flow: Interball Tail observations on May 29, 1996, J. Geophys. Res., 106, 29491, 2001.
Bale, S. D., F. S. Mozer, and T. Phan, Observation of low hybrid drift instability in the diffusion region at a reconnecting magnetopause, Geophys. Res., Lett., 29(24), 2180, 2002.
Bell, T. F., U. S. Inan, J. Bortinik, and J. D. Scudder, The Landau damping of magnetospherically reflected whistlers within the plasmasphere, Geophys. Res. Lett., 107, 1150, 2002.
Brandt, C:son, P. R. Demaistre, E.C. Roelof, D.G. Mitchell, and S. Mende, IMAGE/HENA: Global ENA imaging of the plasmasheet and ring current during substorms, J. Geophys. Res., in press, 2002.
Cattell, C., J., et al., Observations of Large Amplitude Parallel Electric Field Wave ackets at the Plasma Sheet Boundary, Geophys. Res. Lett., 25,857-860, 1998
Cattell, C.A., et al., Comparisons of Polar satellite observations of solitary wave velocities in the plasma sheet boundary and the high altitude cusp to those in the auroral zone, Geophys. Res. Lett., 26, 425-428, 1999.
Cattell, C., J. Crumley, J. Dombech, J. Wygant and F. S. Mozer, Polar observations of solitary waves at the Earth's magnetopause, Geophys. Res. Lett., 29, 2001GL0140046, 2002.
Cattell, C., J. Dombeck, J. Wygant, F. S. Mozer and M. Andre, The role of waves in magnetotail dynamics, Proceedings of the International Conference on Substorms, 2002.
Cattell, C., C. Neiman, J. Dombeck, J. Crumley, J. Wygant, C. A. Kletzing, W. K. Peterson, F. S. Mozer, and M. Andre, Large amplitude solitary waves in and near the Earths magnetosphere, magnetopause and bow shock: Polar and Cluster observations, Nonlinear Proc. Geophysics, 10(1), 3-11, 2003.
Chandler, M O, and T E Moore, Observations of the geopause at the magnetopause: Quantification of density and temperature, Geophys. Res. Lett.., in review, 2003.
Chandler, M. O, S. A. Fuselier, M. Lockwood, and T. E. Moore, Evidence for component merging equatorward of the cusp, J. Geophys. Res., 104(A10), p.22623, 1999.
Chang, W. W., et al., Cusp energetic ions: A bow shock source, Geophys. Res. Lett., 8, 1193, 1998.
Chen, J. , and T. A. Fritz, The global significance of the CEP events in Solar-Terrestrial Magnetic Activity and Space Environment, edited by H. N. Wang and R. L. Xu, COSPAR Colloquia Series, 14, 239-249, 2002.
Chen, S.-H., and T.E. Moore, Dayside flow bursts in the Earth's outer magnetosphere, J. Geophys. Res., in review, 2003.
Chua, D., G. Parks, M. Brittnacher, W. Peria, G. Germany, J. Spann and C. Carlson, Energy characteristics of auroral electron precipitation: A comparison of substorms and pressure pulse related auroral activity, J Geophys. Res., 106, 5,945-5,056, 2001.
Cladis, J.B., H. L. Collin H.L. Collin, O.W. Lennartsson, T.E. Moore, and C.T. Russell, Observations of centrifugal Acceleration of ions during compression of the magnetosphere, Geophysical Research Letters, 27, 615, 2000
Cliver, E. W., Y. Kamide, and A. G. Ling, Mountains versus valleys: Semiannual variation of geomagnetic activity, J. Geophys. Res., 105, 2413-2424, 2000.
Collin, H. L., W. K. Peterson, O. W. Lennartsson, and J. F. Drake, The seasonal variation of auroral ion beams, Geophys. Res. Lett., 25, 4071, 1998.
Crooker, N. U., Dayside merging and cusp geometry, J. Geophys. Res., 84, 951, 1979.
Dempsey, D. L., et al., Reflected solar wind ions and downward accelerated ionospheric ions during the January 1997 magnetic cloud event, Geophys. Res. Lett., 25 (15), 2979, 1998.
Drake, J. F., M. Swisdak, C. Cattell, M. A. Shay, B. N. Rogers, and A. Zeiler, Formation of electron holes and particle energization during magnetic reconnection, Science, Feb. 7, 2003.
Elliott, H. A.,, R. H. Comfort, P. D. Craven, M. O. Chandler, and T. E. Moore; Solar wind influence on the oxygen content of ion outflow in the high-altitude polar cap during solar minimum conditions; J. Geophys. Res., 106, 6067-5084, 2001.
Erickson, G. M., N. C. Maynard, W. J. Burke, G. R. Wilson, and M. A. Heinemann, Electromagnetics of substorm onset in the near-geosynchronous plasma sheet, J. Geophys. Res., 105, 25,265-25,290, 2000.
Frank, L. A., W. R Paterson and J. B. Sigwarth, Observations of plasma sheet dynamics earthward of the onset region with the Geotail spacecraft, J. Geophys. Res., 106, 18,823 - 18, 841, 2001b.
Frank, L.A. and J.B. Sigwarth, Findings concerning the positions of substorm onsets with auroral images from the Polar spacecraft, J. Geophys. Res., 105, 12,747-12,761, 2000a
Frank, L. A. and J. B. Sigwarth, Findings concerning the positions of substorm onsets with auroral images from the Polar spacecraft (correction due to publisher's error), J. Geophys. Res., 105, 18,919-18,920, 2000b.
Frank, L.A., J. B Sigwarth, W. R. Paterson and S. Kokubun, Two encounters of the substorm onset region with the Geotail spacecraft, J. Geophys. Res., 106, 5811-5831, 2001a.
Frank, L.A., W.R. Paterson, J.B. Sigwarth, and S. Kokubun, Magnetic field dipolarization during auroral substorm onset, J. Geophys. Res., 105, 15,897-15,912, 2000c.
Frank, L. A., W. R. Paterson and J. B. Sigwarth, Observations of plasma injection into the ring current during substorm expansive phase, J. Geophys. Res., 107(A11), 1343, DOI 10.1029/2001JA000169, 2002.
Frank, L. A. and J. B. Sigwarth, Simultaneous images of the northern and southern auroras from the Polar spacecraft: An auroral substorm, J. Geophys. Res., 108(A4), 8015, DOI 10.1029/2002JA009356, 2003.
Franz, J. R., P. M. Kintner and J. S. Pickett, Polar observations of coherent electric field structures, Geophys. Res. Lett., 25, 1277-1280, 1998.
Fritz, T. A. , and J. Chen, The Cusp as a Source of Magnetospheric Particle, Proceeding of the Workshop on "Space Radiation Radiation Modeling: New Phenomena and Approaches" published in Radiation Measurements., Vol 30, No 5, 599-608, 1999
Fritz, T. A., J. Chen, and R. B. Sheldon, The role of the cusp as a source for magnetospheric particles: A new paradigm? Adv. Space Res., 25(7-8), 1445-1457, 2000.
Fuselier, S. A., K.J. Trattner, and S.M. Petrinec, Cusp Observations of High- and Low- Latitude Reconnection for Northward IMF, , J. Geophys. Res. 105, 253, 2000a.

Fuselier, S. A., M. Lockwood, T.G. Onsager, and W.K. Peterson, The Source Population for the Cusp and the Cleft/LLBL for Southward IMF, Geophys Res. Lett., 12, 1665, 1999.
Fuselier, S. A., S. M. Petrinec, and K. J. Trattner, Stability of the high-latitude reconnection site for steady northward IMF, Geophys. Res., Lett., 27, 473, 2000b.
Fuselier, S. A., S.M. Petrinec, K.J. Trattner, and W.K. Peterson, O+ Observations in the Cusp: Implications for Dayside Magnetic Field Topology, J. Geophys. Res., 106, 5977, 2001.
Fuselier, S.A., H.U. Frey, K.J. Trattner, S.B. Mende, and J.L. Burch, Cusp aurora dependence on interplanetary magnetic field Bz, J. Geophys. Res., 107(A7), doi:10.1029/2001JA000165, 2002.
Green and Kivelson, A tale of two theories: How the adiabatic response of ULF waves affect relativistic electrons, J. Geophys. Res., 106, 25,777, 2001.
Green, J., Testing Relativistic Electron Acceleration Mechanisms, Ph.D. thesis, UCLA, 2002.
Horne, R. B., and R.M. Thorne, Relativistic electron acceleration and precipitation during resonant interactions with whistler-mode chorus, submitted to GRL, 2003, in review.
Keiling, A., J. R. Wygant, C. A. Cattell, F. S. Mozer and C. T. Russell, The global morphology of wave poynting flux: Powering the Aurora, Science, 299, 383-386, 2003.
Kessel, R. L., R. E. McGuire, H. K. Hill, N. J. Schofield, Jr., and J. Love, "ISTP Guidelines for CDF," in International Solar-Terrestrial Physics (ISTP) Key Parameter Generation Software (KPGS) Standards and Conventions, Version 1.2, W. H. Mish, NASA, 1993.
Kessel, M, and R. Candey, "Visualization of International Solar-Terrestrial Physics Program (ISTP) Data," Visualization Techniques in Space and Atmospheric Sciences, NASA SP-519, December 1995.
Krauklis, I., A.D. Johnstone, and W.K. Peterson, The acceleration of ionospheric O+ ions on open field lines in the LLBL and cusp region, J. Geophys. Res., submitted, 1999.
Lauben, D. S., et al, VLF Chorus Emissions Observed by Polar During the January 10, 1997 Magnetic Storm, Geophys. Res. Lett., 25, 2995-2998, 1998.
Le, G., et al., Initial Polar magnetic field experiment observations of the low-altitude polar magnetosphere: Monitoring the ring current with polar orbiting spacecraft, J. Geophys. Res., A8, 17,345, 1998.
Le, G., C. T. Russell and K. Takahashi, Morphology of the ring current derived from magnetic field observations, sub. Annales Geophysicae, 2003.
LeDocq , M. J., D. A. Gurnett, and G. B. Hospodarsky, Chorus Source Locations From VLF Poynting Flux Measurements With the Polar Spacecraft, Geophys. Res. Lett., 25, 4063-4066, 1998.
Lennartsson, O.W. et al, A statistical comparions of the outflow of N2+, No+, and O2+ molecular ions with that of atomic O+ ions using Polar/TIMAS observations, Journal of Atmospheric and Solar Terrestrial Physics (JASTP), submitted, 1999.
Lennartsson, O.W. et al, POLAR/TIMAS statistical results on the outflow of molecular ions from Earth at solar mimimum, Advances in Space Research, submitted, 1998.
Lennartsson, O. W., Ion composition aspects of magnetotail plasma flows,, J. Geophys. Res., 106, p.15,635, 2001.
Lennartsson, O.W., K.J. Trattner, H.L. Collin, and W.K Peterson, Polar/TIMAS Survey of Earthward Field-Aligned Proton Flows From the Near-Midnight Tail, J. Geophys Research, 106, 5859, 2001.
Li, X., I. Roth, M. Temerin, J. Wygant, M. Hudson, and J. Blake, Simulations of the prompt energization and transport of radiation belt particles during the March 24, 1991 SSC., Geophys. Res. Lett., 20, 2423-2426, 1993.
Liou, K., C.-C. Wu, R. P. Lepping, P. T. Newell, and C.-I. Meng, Midday sub-auroral patches (MSPs) associated with interplanetary shocks, Geophys. Res. Lett., 29, 10.1029/2001GL014182, 2002b.
Liou, K., C.-I. Meng, A. T. Y. Lui, P. T. Newell, and S. Wing, Magnetic dipolarization with substorm expansion onset, J. Geophys. Res., 107, 10.1029/2001JA00179, 2002a.
Liou, K., et al., On relative timing in substrom onset signatures, J. Geophys. Res., A10, 22,807, 1999a.
Liou, K., P. T. Newell, and C.-I. Meng, Seasonal effects on auroral particle acceleration and precipitation, J. Geophys. Res., 106, 5531-5542, 2001a.
Liou, K., P. T. Newell, C.-I. Meng, M. Brittnacher, and G. Parks, Synoptic auroral distribution: A survey using Polar ultraviolet imagery, J. Geophys. Res., 102, 27197-27205, 1997.
Liou, K., P. T. Newell, C.-I. Meng, T. Sotirelis, M. Brittnacher, and G. Parks, The source region of 1500 MLT auroral bright spots: Simultaneous Polar UV-images and DMSP particle data, J. Geophys. Res., 104, 24587-24602 1999b.
Liou, K., P. T. Newell, D. G. Sibeck, C.-I. Meng, M. Brittnacher, and G. K. Parks, Observation of IMF and seasonal effects in the location of auroral substorm onset, J. Geophys. Res., 106, 5799-5810, 2001b.
Lockwood, M., C.J. Davis, T.G. Onsager, J.D. Scudder, Modelling signatures of pulsed magnetopause reconnection in cusp ion dispersion signatures seen at middle altitudes, Geophys. Res. Lett., 25, 591-594, 1998.
Lorentzen et al., Observations of relativistic electron microbursts in association with VLF chorus, J. Geophys. Res., 106, 6017, 2001.
Lui, A. T. Y., et al., Plasma and magnetic flux transport associated with auroral breakups, Geophys. Res. Lett., 21, 4059, 1998.
Lyatsky, W., P.T. Newell and A. Hamza, Solar illumination as cause of the equinoctial preference for geomagnetic activity, Geophys. Res. Lett., 28, 2,353 - 2,356, 2001.
Ma., Z. W., and A. Bhattacharjee, Fast impulsive reconnection and current sheet intensification due to electron pressure gradients in semi-collisional plasmas, Geophys. Res. Lett., 23, 1673-1676, 1996.
Maynard, N. C., Coupling the solar-wind/IMF to the ionosphere through the high latitude cusps, submitted to a compendium on the cusp edited by T. Fritz, Klewer, 2003.
Maynard, N. C., D. M. Ober, W. J. Burke, J. D. Scudder, M. Lester, M. Dunlop. J. A. Wild, A. Grocott, C. J. Farrugia, E. J. Lund, C. T. Russell, D. R. Weimer, K. D. Siebert, A. Balogh, M. Andre, and H. Reme, Polar, Cluster and SuperDARN evidence for high latitude merging during southward IMF: Temporal/spatial evolution, submitted to Annales Geophysicae, 2002.
Maynard, N. C., G. L. Siscoe, B. U. Ö. Sonnerup, W. W. White, K. D. Siebert, D. R. Weimer, G. M. Erickson, J. A. Schoendorf, D. M. Ober, and G. R. Wilson, The response of ionospheric convection to changes in the IMF: Lessons from a MHD simulation, in press J. Geophys. Res., 2001a.
Maynard, N. C., S. Savin, G. M. Erickson, H. Kawano, Z. Nemecek, W. K. Peterson, J. Safranokova, I. Sandahl, J. D. Scudder, G. L. Siscoe, B. U. Ö. Sonnerup, D. R. Weimer, W. W. White, and G. R. Wilson, Observation of the magnetospheric "sash" and its implications relative to solar-wind/magnetosphere coupling: A multisatellite event analysis, J. Geophys. Res., 106, 6097-6122, 2001b.
Maynard, N.C., W.J. Burke, E.M. Basinska, G.M. Erickson, W.J. Hughes, H.J. Singer, A.G. Yahnin, D.A. Hardy and F.S. Mozer, Dynamics of the inner magnetosphere near times of substorm onsets, J. Geophys. Res., 101, 7,705, 1996.
Maynard, N. C., W. J. Burke, D. R. Weimer, F. S. Mozer, J. D. Scudder, C. T. Russell, W. K. Peterson, and R. P. Lepping, Polar observations of

convection with northward IMF at dayside high latitudes, J. Geophys. Res., 103, 29-45, 1998a.
Maynard, N. C., W. J. Burke, D. R. Weimer, F. S. Mozer, J. D. Scudder, W. K. Peterson, R. L. Lepping, and C. T. Russell, Polar observations of cusp electrodynamics: Evolution from 2- to 4-cell convection patterns, in Polar Cap Boundary Phenomena, edited by A. Egeland, J. Moen and M. Lockwood, pp. 157-172, Klewer, Dordrecht, 1998b.
McIntosh, D. H., On the annual variation of magnetic disturbances, Phil. Trans. Roy. Soc. London, Ser. A, 251, 525, 1959.
Meng, C.-I., K. Liou, and P. T. Newell, Asymmetric sunlight effect on dayside/nightside auroral precipitation, Phys. Chem. Earth (C) 26, 43-47, 2001.
Menietti, J. D., R. R. Anderson, J. S. Pickett, D. A. Gurnett, and H. Matsumoto, Near-source and remote observations of kilometric continuum radiation from multi-spacecraft observations, J. Geophys. Res., in review, 2003.
Meredith et al., Evidence for acceleration of outer zone electrons to relativistic energies by whistler mode chorus, Ann. Geophys., 20, 967-979, 2002.
Moore, T. E., B. L. Giles, D. C. Delcourt, and M.-C. Fok, The plasma sheet source groove, J. Atmos. Solar Terr. Phys., 62(6), p.505, 2000.
Moore, T. E., et al, High altitude observations of the polar wind, Science, 277, p.349, 1997
Moore, T.E., et al, Ionospheric mass ejection in response to a coronal mass ejection, Geophys. Res. Let, 26, 15, 1999.
Moore, T. E., M.-C. Fok, and M. O. Chandler, The dayside reconnection X line, J. Geophys. Res., 107(A10), 10.1029/2002JA009381, 2002.
Mozer, F. S., et aL, New features of time domain electric field structures in the auroral acceleration region, Phys. Rev. Lett., 79, 1281, 1997
Mozer, F.S., and C. A. Kletzing, Direct observation of large, quasi-static, parallel electric fields in the auroral acceleration region, Geophys. Res. Lett., 25, 1629, 1998
Mozer, F.S., S. D. Bale, and T.D.Phan, Evidence of diffusion regions at a subsolar magnetopause crossing, Phys. Rev. Lett., 89(1), pp.015002-1-4, 2002.
Newell, P. T., C.-I. Meng, and K. M. Lyons, Discrete aurorae are suppressed in sunlight, Nature, 381, 766-767, 1996.
Newell, P. T., C.-I. Meng, T. Sotirelis, and K. Liou, Polar Ultraviolet Imager observations of global auroral power as a function of polar cap size and magnetotail stretching, J. Geophys. Res., 106, 5895-5905, 2001a.
Newell, P.T., K. Liou, F.P. Skura, nd C.-I. Meng, Auroral power during substorms: A Polar UVI based superposed epoch analysis, J. Geophys. Res., 106, 28,885-28,896, 2001b.
Newell, P. T., K. Liou, J. P. Skura, and C.-I. Meng, The distribution of auroral power increases and decreases, Geophys. Res. Lett. 29, 10.1029/2002GL016288, 2002b.
Newell, P. T., T. Sotirelis, J. P. Skura, C.-I. Meng, and W. Lyatsky, Ultraviolet insolation drives seasonal and diurnal space weather variations, 10.1029/2001JA00029610 J. Geophys. Res., 2002a.
Nose, M., A. T. Y. Lui, S. Ohtani, B. H. Mauk, R. W. McEntire, D. J. Williams, T. Mukai, Y. Saito, and K. Yumoto, Acceleration of oxygen ions of ionospheric origin in the near-Earth magnetotail during substorms, J. Geophys. Res., 105, 7669, 2000.
O'Brien et al., Energization of Relativistic Electrons in the Presence of ULF Power and MeV Microbursts: Evidence for Dual ULF and VLF Acceleration, JGR, 2003, in review
O'Brien, T.P. Empirical Analysis of Storm-Time Energetic Electron Enhancements, Ph.D. thesis, UCLA, 2001.
Ober, D. M., N. C. Maynard, W. J. Burke, W. K. Peterson, J. B. Sigwarth, L. A. Frank, J. D. Scudder, W. J. Hughes, and C. T. Russell, Electrodynamics of the poleward auroral border observed by Polar during a substorm on April 22, 1998, J. Geophys. Res., 106, 5927-5943, 2001.
Peterson, W. K., Ionospheric Influence on Substorm Development, Proceedings of the Sixth International Conference on Substorms, University of Washington, ISBN 0-9711740-3-2, p. 143. 2002.
Peterson, W. K., H.L. Collin, A.W. Yau, and O.W. Lennartsson,Polar/TIMAS Observations of Suprathermal Ion Outflow During Solar Minimum Conditions, J. Geophys. Res., 106, 6059, 2001.
Raeder, J., R.L. McPherron, L.A. Frank, S. Dodubun, G. Lu, T. Mukai, W.R. Paterson, J.B. Sigwarth, H.J. Singer and J.A. Slavin, Global simulation of the Geospace Environment Modeling substorm challenge event, J. Geophys. Res., 106, 381-395, 2001.
Reeves et al., Acceleration and loss of relativistic electrons during geomagnetic storms, GRL, 2003, in press.
Ridley, A. J., G. Lu, C. R. Clauer, and V. O. Papitashvili, A statistical study of the ionospheric convection response to changing interplanetary magnetic field conditions using the assimilative mapping of ionospheric electrodynamics technique, J. Geophys. Res., 103, 4023, 1998.
Ridley, A. J., G. Lu, C. R. Clauer, and V. O. Papitashvili, Ionospheric convection during nonsteady interplanetary magnetic field conditions, J. Geophys. Res., 102, 14,563, 1997.
Rodger, Alan S., Iain J. Coleman and Mike Pinnock, Some comments on transient and steady-state reconnection at the dayside magnetopause, Geophys. Res. Lett., 27, 1,359 – 1,362, 2000.
Ruohoniemi, J. M., and R. A. Greenwald, The response of high-latitude convection to a sudden southward IMF turning, Geophys. Res. Lett., 25, 2913, 1998.
Russell, C. T., et al, Entry of the POLAR spacecraft into the polar cusp under northward IMF conditions, Geophys. Res. Lett., 25, 3015-3018, 1998.
Sandel, B. R., et al., Initial Results from the IMAGE Extreme Ultraviolet Imager, Geophys. Res. Lett., 28(8), p. 1439, April 2001.
Scudder, J.D., F.S. Mozer, N.C. Maynard, and C.T. Russell, Fingerprints of Collisionless Reconnection at the Separator, I: Ambipolar Hall Signatures, J.Geophys. Res., 107(A10), 1294, doi:10.1029/2001JA000126,2002.
Selesnick et al., Atmospheric losses of radiation belt electrons, J. Geophys. Res., in press, 2002.
Shue, J.-H., P. T. Newell, K. Liou, and C.-I. Meng, Influence of interplanetary magnetic field on global auroral patterns, J. Geophys. Res., 106, 5913-5926, 2001a.
Shue, J.-H., P. T. Newell, K. Liou, C.-I. Meng, and S. W. H. Cowley, Interplanetary magnetic field Bx asymmetry effect on auroral brightness, J. Geophys. Res. 107, 10.1029/2001JA000229, 2002.
Sigwarth, J. B., and L. A. Frank, Global auroral response to dynamic pressure impulses in the solar wind, submitted to J. Geophys. Res., 2003.
Siscoe, G. L., G. M. Erickson, B. U. Ö. Sonnerup, N. C. Maynard, K. D. Siebert, D. R. Weimer, and W. W. White, Global role of E in magnetopause reconnection, J. Geophys. Res., 106, 13,015-13,022, 2001.
Slinker, S. P., J.A. Fedder, J.M. Ruohoniemi and J.G. Lyon, Global MHD simulation of the magnetosphere for November 24, 1996, J. Geophys. Res., 106, 2001
Slocum, P.L, et al., Observations of Ion Injections During Large Solar Energetic Particle Events, Eos Trans. AGU, 83(47), Fall Meet. Suppl., Abstract SM51A-0501, 2002.
Smith, M.F., and M. Lockwood, The pulsating cusp, Geophysical Research Letters, vol. 17, 1069-1072, 1990.
Spann, J. F., G. A. Germany, R. Elsen, M. J. Brittnacher, G. K. Parks, Initial response of the aurora to the January 10, 1997 magnetic cloud, Geophysical Research Letters, 25, 2577-2580, 1998.
Strickland, D. J., R. J. Cox, R.R. Meier and D.P. Drob, Global O/N2 derived from DE 1 FUV dayglow data: Technique and examples from two storm periods, J. Geophys. Res., 104, 4251-4266, 1998.

Su, Y.-J.,J. L. Horwitz, T. E., Moore, B. L. Giles, M. O. Chandler, P. D. Craven, M. Hirahara, C. J. Pollock, Polar wind survey with TIDE/PSI suite aboard POLAR, J. Geophys. Res. 103(A12), 29305, 1998
Su, Yi-Jiun, J. E. Borovsky, M. F. Thomsen, N. Dubouloz, M. O. Chandler, and T. E. Moore, Plasmaspheric material on high-latitude open field lines, J. Geophys. Res., 106(A4), p.6085, 2001.
Summers, D., R. M. Thorne, and F. Xiao, Relativistic theory of wave-particle resonant diffusion with applicaton to electron acceleration in the magnetosphere, J. Geophys. Res., 103, 20,487-20,500, 1998.
Terasawa,, T., et al., On the determination of a moving MHD structure: Minimization of the residue of integrated Faraday's equation, J. Geom. and Geo., 48, 603-614, 1996.
Toivanen, P. K., D.N. Baker, W.K. Peterson, X. Li, E.F. Donovan, A. Viljanen, A. Keiling, and J.R. Wygant,Plasma Sheet Dynamics Observed by the Polar Spacecraft in Association with Substorm Onsets, J. Geophys. Res., 106, 19117, 2001.
Topliss, S. M., C.J. Owen, and W.K. Peterson, A simple model of complex cusp ion dispersions during prolonged intervals of northward interplanetary magnetic field, , Geophys. Res. Lett. 27. 3587, 2000.
Trattner, K. J., S.A. Fuselier, W.K. Peterson, J.A. Sauvaud, H. Stenuit, N. Dubouloz, and R.A. Kovrazhkin On spatial and temporal structures in the cusp,, J. Geophys. Res. 104, 28411, 1999.
Trattner, K. J., S.A. Fuselier, W.K. Peterson, M. Boehm, D. Klumpar, C.W. Carlson, and T.K. Yeoman, Temporal versus spatial interpretation of cusp ion structures observed by two spacecraft, J. Geophys. Res., 107(A10), 1287, doi: 10.1029/2001JA000181, 2002a.
Trattner, K. J., S. A. Fuselier, W. K. Peterson, and C. W. Carlson, Spatial features observed in the cusp under steady solar wind conditions, J. Geophys. Res., 107(A10), 1288, doi: 10.1029/2001JA000262, 2002b.
Tsurutani, B.T, Solar/Interplanetary Plasma Phenomena Causing Geomagnetic Activity at Earth, in Proceedings of the International School of Physics "Enrico Fermi," ed. by B. Coppi, A. Ferrari, and E. Sindoni, IOS Press, Amsterdam, 2000
Valek, P. W., J. D. Perez, J.-M Jahn, C. J. Pollock, M. P. Wuest, r. H. Friedel, t. E. Moore, W. K. Peterson, Outflow from the ionosphere in the vicinity of the cusp, J. Geosphys. Res., 107(A8), doi: 10.1029/2001JA000108, 2002.
Vasyliunas, V. M., Theoretical models of magnetic field line merging, 1, Rev. Geophys., 13, 303-336, 1975.
Weimer, D.R., An improved model of ionospheric electric potentials including substorm perturbations and application to the Geospace Environment Modeling November 24, 1996, event, J. Geophys. Res., 106, 407-416, 2001.
Weimer, D.R., D. Ober, N. C. Maynard, W. J. Burke, M. R. Collier, D. J. McComas, N. F. Ness, and C. W. Smith, Variable time delays in the propagation of the interplanetary magnetic field, J. Geophys. Res., 107(A8), 10.1029/2001JA009102, 2002.
White, W. W., G. L. Siscoe, G. M. Erickson, Z. Kaymaz, N. C. Maynard, K. D. Siebert, B. U. Ö. Sonnerup, and D. R. Weimer, The magnetospheric sash and cross-tail S, Geophys. Res. Lett., 25, 1605-1608, 1998.
Winglee, R. M., Multi-fluid simulations of the magnetosphere: the identification of the geopause and its variation with IMF, Geophys. Res. Lett., 25 (24), 4441-4444, 1998.
Wygant, et al., Polar spacecraft based comparisons of intense electric fields and Poynting flux near and within the plasma sheet-tail lobe boundary to UVI images: An energy source for the aurora, JGR, 105 (A8), 18,675, 2000
Wygant, J.R., A. Keiling, C. A. Cattell, R. Lysak, M. Temerin, F. S. Mozer, C. A. Kletzing, J. D. Scudder, V. Streltsov, W. Lotko, and C. T. Russell, Evidence for kinetic Alfven waves and parallel electron energization at 4-6 RE altitudes in the plasma sheet boundary layer, J. Geophy. Res., 107(A8), 10.1029/2001JA900113, 2002.
Zhou, X, and B. Tsurutani, Rapid intensification and propagation of the dayside aurora: Large scale interplanetary pressure pulses (fast shocks), Geophys. Res. Lett, 26, 1097-1100, 1999.
Zhou, X. W., et al., Solar wind control of the polar cusp at high altitude, J. Geophys. Res., A1, 245, 2000.

B. Acronym List

3D - three dimensional
AC - alternating current
ACE - Advanced Composition Explorer
AGU - American Geophysical Union
AKR - auroral kilometric radiation
AMIE - Assimilative Mapping of Ionospheric Electrodynamics
CAMMICE - Charge and Mass Magnetospheric Ion Composition Experiment (Polar experiment)
CEPPAD - Comprehensive Energetic Particle Pitch-angle Distribution (Polar experiment)
CANOPUS - Canadian Auroral Network for the Open Program Unified Study
CD - compact disk
CDAWeb - Coordinated Data Analysis Web (NSSDC)
CDHF - Central Data Handling Facility (part of ISTP)
CIR - corotating interaction region
CME - coronal mass ejection
CRRES - Combined Release and Radiation Effects Satellite
CSOC - Consolidated Space Operations Contract
DC - direct current
DDEIS - Duo-Deca-Electron-Ion-Spectrometer (Polar/Hydra)
DMSP - Defense Meteorologial Satellites Program
DSMS - Deep Space Mission System
DSN - Deep Space Network
DVD - digital versitile disk
EDCATS - NASA's E/PO reporting database
EFI - Electric Field Instrument (on Polar)
EMIC - Electromagnetic ion cyclotron
EMF - electromotive force
EOM - end of mission
E/PO - Education/Public Outreach
ENA - energetic neutral atoms
eV - electron volt
DPU - Data Processing Unit
FAST - Fast Auroral Snapshot Explorer
FOT - Flight Operations Team
FTE - Full Time Equivalent
GEM - Gepsapce Environment Modeling
GGS - Global Geospace Science
GOES - Geostationary Operational Environment Satellite
GPS - global positioning system
GSE - Geocentric Solar Ecliptic
GSFC - Goddard Space Flight Center
HEO - High Earth Orbit
HIST - High Sensitivity Telescope (part of Polar/CEPPAD)
HIT - Heavy Ion Telescope (part of Polar/CAMMICE)
Hydra - not an acronym - 3D electron and ion hot plasma instrument
IDL - Interactive Data Language
IMAGE - Imager for Magnetopause to Auroral Global Exploration
IES - Imaging Electron Sensor (part of Polar/CEPPAD)
IMF - interplanetary magnetic field
IPS - Imaging Proton Sensor (part of Polar/CEPPAD)
ISTP - International Solar-Terrestrial Physics program
JGR - Journal of Geophysical Research
JPG/JPEG - Joint Photographic Experts Group (file standard)
keV - kilo electron volt (unit of measure)
KITT - Key Parameter Integration and Testing
km - kilometer
KP - Key Parameter
L - L-shell (nominally the McIllwain L-shell)
LANL - Los Alamos National Laboratory
LBHL - Lyman-Birge-Hopfield (FUV emissions)
LLBL - low latitude boundary layer
LWS - Living with a Star
MeV - mega electron volt (unit of measure)
MFE - Magnetic Field Experiment (Polar experiment)
MDI - Magnetospheric Dynamics Investigation (investigation on Polar)
MHD - magnetohydrodynamics
MI - magnetosphere-ionosphere
MICS - Magnetospheric Ion Composition Sensor (part of Polar/CAMMICE)
MMS - Magnetosphere Multiscale (a SEC STP mission)
MO&DA Mission Operations and Data Analysis
MOC - Mission Operations Center
MOMS - Mission Operations and Mission Services
MPG/MPEG - Moving Pictures Experts Group (file standard)
MSC - Maryland Science Center
MSP - midday subauroral patches
NASA - National Aeronautics and Space Administration
NENL - near earth neutral line
NSF - National Science Foundation
NSSDC - National Space Science Data Center
OPEN - Origin of Plasmas in Earth's Neighborhood
OSS - Office of Space Science
PAC - Payload Assistance Center
PAPCO - Panel Plot Composer
PI - Principal Investigator
PIXIE - Polar Ionospheric X-ray Imaging Experiment
PPS - Parallel Plate Analyzer (part of Polar/Hydra)
PSI - Plasma Source Instrument (part of Polar/TIDE)
PSLA - project service level agreement
PWI - Plasma Wave Instrument (Polar experiment)
RDAF - Remote Data Analysis Facility
RE - earth radii (unit of measure)
RHS - right hand side
SAMPEX - Solar Anomalous and Magnetospheric Particle Explorer
SEC - Sun-Earth Connections
SECEF - Sun-Earth Connections Education Forum
SEP - solar energetic particles
SEPS - Source/Loss-Cone Energetic Particle Spectrometer (on Polar)
SFR - Stepped Frequency Radar
SODA - Space Operations Directive Agreement
SOHO - Sola and Heliospheric Observatory
SSERD - Space Science Education Resource Director
STP - Solar Terrestrial Probes
SuperDARN - Super Dual Auroral Radar Network
TIDE - Thermal Ion Dynamics Experiment
TIMAS - Toroidal Imaging Mass-Angle Spectrograph (Polar)
TIMED - Thermosphere, Ionosphere, Mesosphere, Energetics and Dynamics (a SEC STP mission)
TIMEGCM - Thermosphere Ionosphere Mesosphere Electrodynamics General Circulation Model
TWINS - Two Wide-Angle Imaging Neutral-Atom Spectrometers
ULF - ultra-low frequency (waves)
UV - ultraviolet
UVI - Ultraviolet Imager
VIS - Visible Imaging System
VLF - very low frequency (waves)
WIC - Wideband Imaging Camera (on IMAGE)

C. Required Budget Forms

	FY03 Budget ($k)	FY04 Budget ($k)	FY05 Budget ($k)	FY06 Budget ($k)	FY07 Budget ($k)
In-Guide (I) or Minimal (M)*?	I	I	I	M	M
1. Development	0.0	0.0	0.0	0.0	0.0
2.a Data Services	0.0	0.0	0.0	0.0	0.0
2.b Mission Services	1,564.0	1,364.0	1,364.0	1,023.0	0.0
2.c Other Mission Operations					
Science Operations	198.0	85.0	85.0	30.0	0.0
E/PO	73.0	65.0	63.0	30.0	30.0
3. Science Center Functions					
4. Science Data Analysis	5,194.0	5,015.0	4,552.0	4,940.0	2,595.0
Total	7,029.0	6,529.0	6,064.0	6,023.0	2,625.0

* Supply Minimal budget figures only if the NASA budget guideline is zero for the FY.

II. FY03 - FY07 Requested/Optimal Scenario:

	FY03 Budget ($k)	FY04 Budget ($k)	FY05 Budget ($k)	FY06 Budget ($k)	FY07 Budget ($k)
1. Development	0.0	0.0	0.0	0.0	0.0
2.a Data Services					
2.b Mission Services	1,564.0	1,492.0	1,537.0	1,187.0	0.0
2.c Other Mission Operations (Note 1)		206.0			
Science Operations	198.0	85.0	85.0	37.0	0.0
E/PO	73.0	65.0	65.0	60.0	20.0
3. Science Center Functions					
4. Science Data Analysis	5,194.0	5,135.0	5,066.0	5,110.0	2,595.0
Total	7,029.0	6,983.0	6,753.0	6,394.0	2,615.0

III. FY03 - FY07 Requested/Optimal Scenario (in-Kind NASA cost attributions):

H/W & Sustaining Engineering captured in Multi-mission,UPN470-90

	FY03 Budget ($k)	FY04 Budget ($k)	FY05 Budget ($k)	FY06 Budget ($k)	FY07 Budget ($k)
1. Development	0.0	0.0	0.0	0.0	0.0
2.a Data Services	550.1	550.0	501.6	489.3	0.0
2.b Mission Services	708.0	830.0	751.0	774.0	0.0
2.c Other Mission Operations (MPS)	143.2	143.2	143.2	143.2	0.0
3. Science Center Functions					
4. Science Data Analysis (Note 2)	770.0	779.0	724.0	714.0	357.0
Total	2,171.3	2,302.2	2,119.8	2,120.5	357.0

IV. FY03 - FY07 Instrument team breakdown for the Requested/Optimal Scenario:

	FY03 Budget ($k)	FY04 Budget ($k)	FY05 Budget ($k)	FY06 Budget ($k)	FY07 Budget ($k)
1. CAMMICE	366.0	358.0	353.0	353.0	176.5
2. CEPPAD	425.0	425.0	419.0	425.0	212.5
3. EFI (Note 3)	388.0	428.0	422.0	428.0	214.0
4. HYDRA (Note 3)	400.0	440.0	434.0	440.0	220.0
5. MFE (Note 3)	440.0	480.0	473.0	480.0	240.0
6. PIXIE	437.0	285.0	281.0	281.0	140.5
7. PWI	232.0	232.0	229.0	229.0	114.5
8. SEPS	50.0	50.0	50.0	50.0	25.0
9. TIMAS	675.0	675.0	666.0	675.0	337.5
10. TIDE	452.0	452.0	446.0	452.0	226.0
11. UVI	450.0	450.0	444.0	450.0	225.0
12. VIS	560.0	560.0	552.0	560.0	280.0
Other Science Teams					
MDI, science principal investigator	219.0	210.0	207.0	207.0	103.5
other funded investigators	55.0	55.0	55.0	50.0	50.0
Other mission expenses					
Project Scientist Office	45.0	35.0	35.0	30.0	30.0
Total	5,194.0	5,135.0	5,066.0	5,110.0	2,595.0

Note 1: 5% CSOC to MOMS contract transition + 4wks carryover
Note 2: Reflects adjusted POP 02-1 full cost data to better represent current workforce plan, residual ISTP FTEs were applied at recast.
Note 3: Requested/Optimal funds over guidelines are for additional MFE, EFI, HYDRA analysis of high resolution Science Mode 2 data

On the covers:

Front Cover Top, left to right:

a) Model of the radiation belts based on Polar energetic electron fluxes [*Reeves, G. D., AGU press conference on radiation belt science*]

b) Frame from animation for press conference on ionospheric outflow [Moore et al., *Science*, 1997]

c) High resolution, full-color image of the visible nighttime auroral oval acquired in red, green, and blue emission lines by the Polar/VIS. Note the color variation at the limb due to the altitude separation of the neutral atmospheric species.

d) Dayside O/N_2 ratio before and after a magnetospheric storm showing a 50% decrease in the mid-latitude atmospheric neutral density ratio.

Front Cover Left, top to bottom:

e) Typical auroral oval from late in the expansive phase of a substorm observed with the Polar/VIS.

f) A number of striking auroral arcs observed at the visible wavelength of 557.7 nm with ~10 km resolution in this high resolution Polar/VIS image of a portion of the nighttime auroral oval during a substorm.

g) Superposed epoch picture of electron diffusion region captured by Polar [*Scudder et al.,* 2002]

h) A conjugate pseudo onset acquired with the Polar/VIS Earth Camera is observed simultaneously in both hemispheres with the southern hemisphere pseudo onset brighter than its northern conjugate counterpart.

i) Recent observations by UVI shows the increasingly good imaging aspect angle as the Polar orbit precesses through southern latitudes.

Back Cover Top, left to right:

j) TIDE co-investigator Craig Pollock after successful calibration of the instrument.

k) The *Space Weather Center* museum exhibit continues to travel. This year, it will be at the Arizona Challenger Learning Center.

l) Polar's latest E/PO product, the *Aurora* poster. All E/PO products adhere to National Education Standards. A Spanish language edition is in development.

Back Cover Left, top to bottom:

m) Animation showing change in electron access at magnetic reconnection site: red electrons from solar wind field lines and blue ones from the magnetosphere, initially separated are permitted joint access to reconnected field lines [based on fluid code of Ma and Bhattacharjee, 1996].

n) MHD simulation of solar wind interaction with the magnetosphere showing density (in color, red being densest) and magnetic field lines in the noon-midnight meridian.

o) Simultaneous image of northern (left) and southern (right) X-ray aurora from PIXIE, 24 March 2002.

p) Typical observation of a substorm onset in the northern auroral oval when the Polar spacecraft was oriented with its spin vector perpendicular to the ecliptic plane.

q) The fully integrated Polar spacecraft during thermal-vacuum testing.

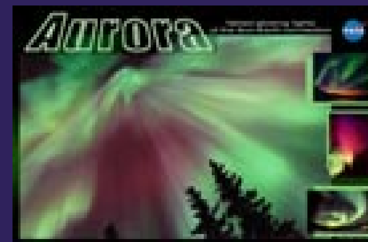

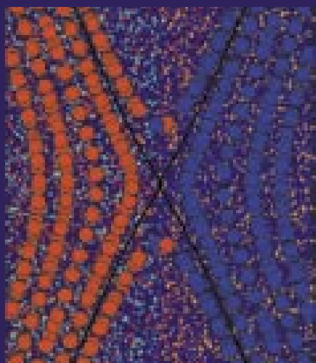

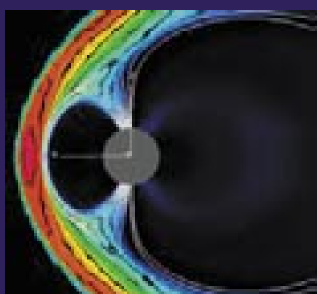

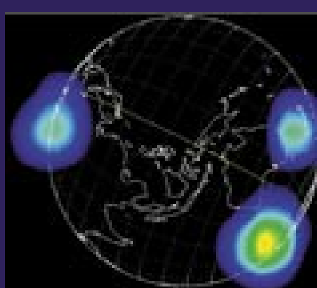

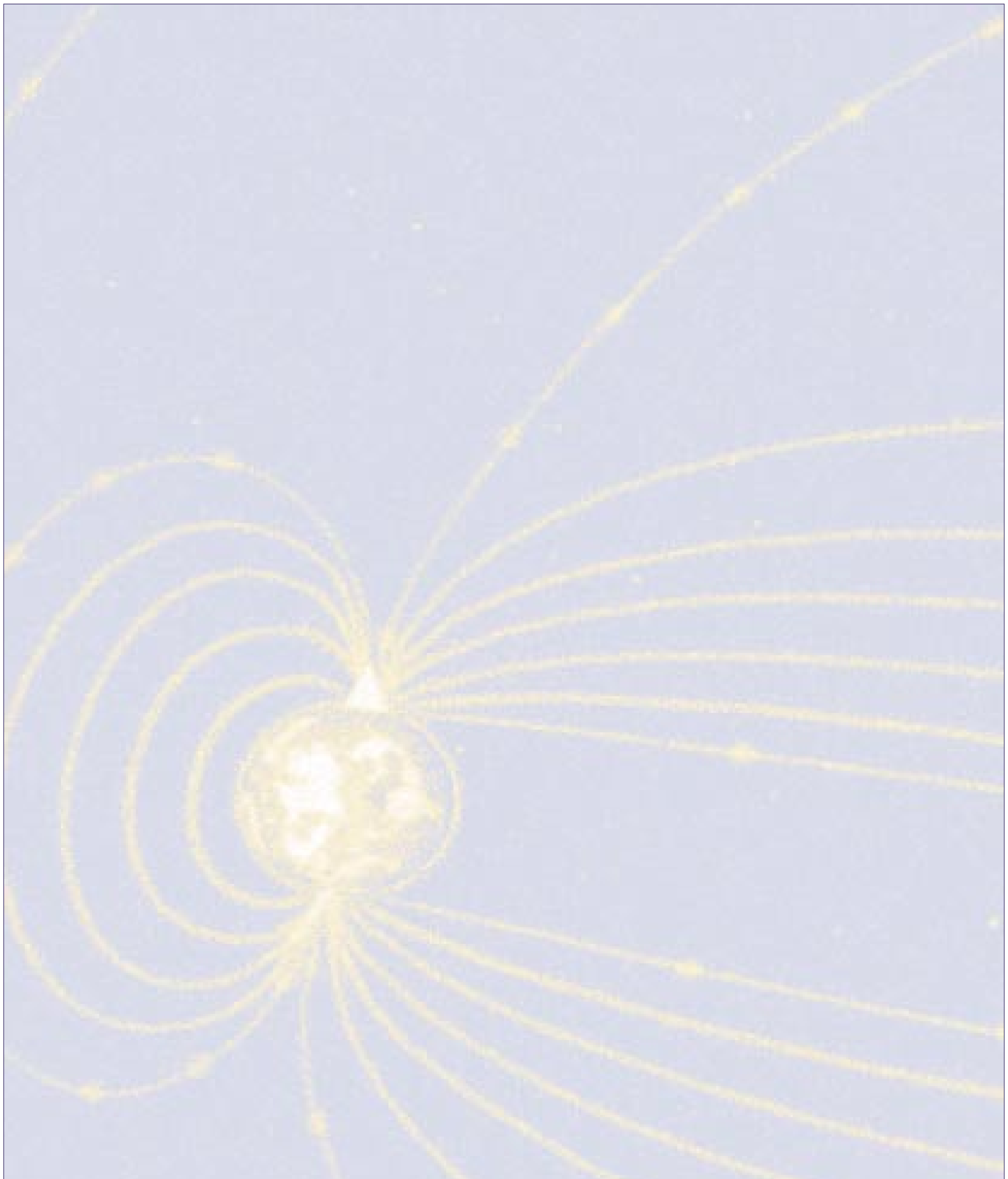

National Aeronautics and
Space Administration

Goddard Space Flight Center
Greenbelt, Maryland 20771